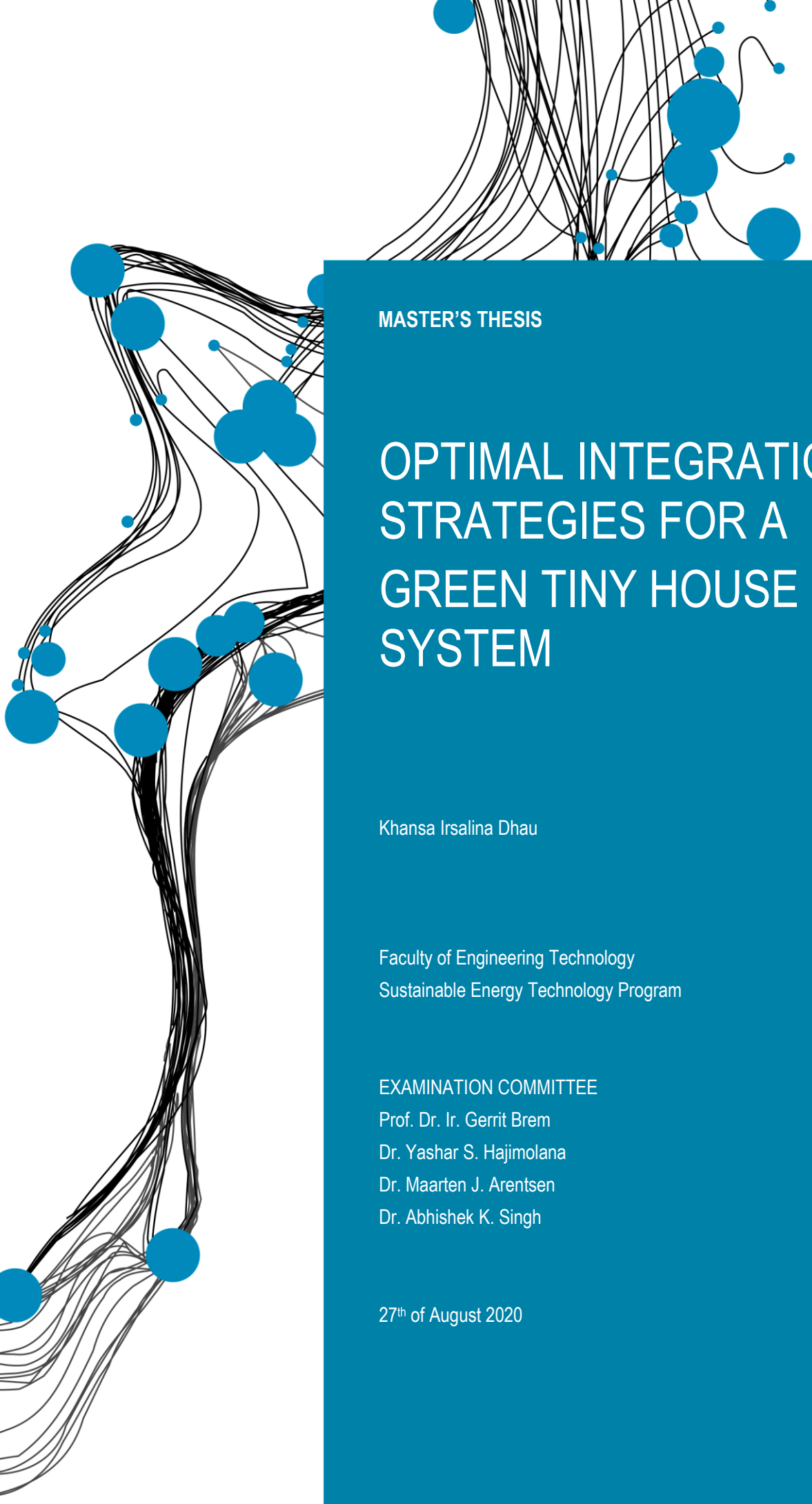

MASTER'S THESIS

OPTIMAL INTEGRATION STRATEGIES FOR A GREEN TINY HOUSE ENERGY SYSTEM

Khansa Irsalina Dhau

Faculty of Engineering Technology
Sustainable Energy Technology Program

EXAMINATION COMMITTEE
Prof. Dr. Ir. Gerrit Brem
Dr. Yashar S. Hajimolana
Dr. Maarten J. Arentsen
Dr. Abhishek K. Singh

27th of August 2020

Acknowledgement

This master's thesis is the primary last step towards achieving my Master of Science (M.Sc.) degree in Sustainable Energy Technology. Working on this thesis has helped me to extend my knowledge, my skills (especially in using MATLAB and Simulink), and to further understand the challenges of implementing sustainable energy.

I would like to thank my supervisor, Dr. Yashar S. Hajimolana, for being a great mentor, for guiding me in every weekly online meeting, and for always taking the time to give me valuable feedback regarding the work that I have done. I would also like to acknowledge all committee members, Prof. Dr. Ir. Gerrit Brem, Dr. Maarten J. Arentsen, and Dr. Abhishek K. Singh for their time to assess my thesis work.

Moreover, I would like to express my gratitude to all the donors of the Kipaji Scholarship and the donors of the Prof. De Winter Scholarship, [redacted] and [redacted]; as well as the people who introduced me to them, [redacted] and [redacted]. I am happy to have met such generous and wonderful people.

Finally, this journey would not have been possible if it were not for the unconditional love and support from my close ones; Mamah, Papap, Dek Sissy, Dek Hanif, and Rasyid (my unofficial advisor).

Enschede, August 2020

Khansa Irsalina Dhau

Abstract

In this study, three self-sufficient energy system configurations for six tiny houses with eight inhabitants were evaluated:

- **Configuration 1**: solar photovoltaic (PV), Li-ion battery, ground source heat pump (GSHP)
- **Configuration 2**: solar photovoltaic-thermal (PV/T), solar thermal collectors (STC), Li-ion battery, latent heat storage (LHS)
- **Configuration 3**: PV, Li-ion battery, GSHP, hydrogen storage (electrolyzer, compressor, hydrogen tank, fuel cell)

These configurations were compared according to seven factors: (1) area and volume, (2) reliability, (3) energy loss, (4) energy excess, (5) battery capacity utilization, (6) technology complexity, and (7) cost. The houses were evaluated as one whole system; thus, the energy components sizes are expressed for a total of six houses.

The energy demand was modelled by dividing them into heat and electricity. The heat demand profile is built according to the houses' heat balance, based on the Netherland's climate. The heat demand profile affects electricity demand by 33% when electric-based heater (e.g. heat pump) is used. The energy component sizing optimization was done by varying energy storage size and obtaining the minimum energy generator (PV, PV/T, STC) size to fulfil 100% of the demand.

It was found that the third configuration shows the best performance because it requires the smallest PV size (54 kWp), smallest battery size (75 kWh), it is the most reliable, it produces the least amount of unused energy (50%), and it shows the best battery capacity utilization amongst the other two. This is mainly because the third configuration has a seasonal energy storage. Consequently, the technology is more complex, and the cost is higher. Its levelized cost of energy (LCOE) is the highest compared to other configurations, €2.3/kWh for electricity and €0.1/kWh for heat. Those are ten times higher than the price of electricity from the main grid and 1.4 times higher than the price of gas.

If the parameter of choice is only focused on economic feasibility, then the first configuration is recommended because it shows the lowest LCOE amongst all configurations (€1.4/kWh for electricity and €0.2/kWh for heat), although it still costs 1.7-6.5 times more than buying energy from utility companies. The first configuration requires the largest PV size (117 kWp), largest battery size (248 kWh), and it produces a large amount of unused energy (349%). This unused energy could be sold back to the grid if the houses are grid-connected. However, the technologies in this configuration are not as advanced as the second and third configuration; hence, the lower LCOE. Overall, the study sees that new technologies like LHS and hydrogen storage are technically feasible when aiming for 100% self-sufficiency, but are not currently economically viable in this scale (six tiny houses). Possible solutions include making the system scale larger to achieve the economy of scale, technology advancement that could drive the cost down and improve the roundtrip efficiency, or increasing the price of fossil fuel so that clean technologies become competitive.

Contents

List of Figures

List of Tables

Nomenclature

Abbreviations

ASHP	Air source heat pump
CAES	Compressed air energy storage
CHP	Combined heat and power
COP	Coefficient of performance
DoD	Depth of discharge
EES	Electrical energy storage
EU	European Union
GSHP	Ground source heat pump
HP	Heat pump
HWTS	Hot water tank storage
IEA	International Energy Agency
LHS	Latent heat storage
O&M	Operation and maintenance
PCM	Phase-changing material
PHES	Pumped hydro energy storage
PV	Photovoltaic
PV/T	Photovoltaic-thermal
SAT	Sodium Acetate Trihydrate
SDG	Sustainable Development Goals
SDS	Sustainable Development Scenario
SES	Supercapacitor energy storage
SHS	Sensible heat storage
SMES	Superconducting magnetic energy storage
STC	Solar thermal collector
TCM	Thermochemical material
TRL	Technology readiness level
UN	United Nations

List of symbols

A_{PV}	PV panel area
$C_{p,s}$	Heat capacity of PCM (solid)
$C_{p,l}$	Heat capacity of PCM (liquid)
D_{excess}	amount of excess electricity
D_{grid}	Amount of electricity drawn from grid
D_{waste}	Amount of heat wasted
E^{i}_{PV}	Electricity produced by PV module at hour-i
E^{i}_{bat}	Energy stored in battery at hour-i
$E^{max/min}_{bat}$	Maximum/minimum energy stored in battery
$Elec_{heat}$	Amount of energy required by electric immersion heater
e_{cap}	Rated capacity of electrolyzer
fc_{cap}	Rated capacity of fuel cell

h^{i}_{LHS}	Enthalpy of latent heat storage at hour-i
$h^{max/min}_{LHS}$	Maximum/minimum enthalpy of latent heat storage
I^{i}_{T}	Solar irradiance at hour-i
I_{ref}	Reference irradiation at nominal condition
m^{i}_{H2}	Amount (mass) of hydrogen inside hydrogen tank at hour-i
E^{max}_{bat}	Maximum amount (mass) of hydrogen inside hydrogen tank
m_{PCM}	Mass of PCM
N_{PV}	Number of PV panels
P_{prod}/Q_{prod}	Electricity/heat produced
P_{cons}/Q_{cons}	Electricity/heat consumed
PR	PV system performance ratio
PV_{cap}	Rated capacity of PV
T^{i}_{amb}	Ambient temperature at hour-i
T^{i}	Temperature of PCM at hour-i
T_{melt}	Melting temperature of PCM
T_{NOC}	PV cell temperature at nominal operating conditions
$T_{ref,NOC}$	Reference PV module temperature at nominal operating conditions
$T_{ref,STC}$	Reference PV module temperature at standard condition
β_{ref}	PV temperature coefficient
η_{bat}	Li-ion battery charging and discharging efficiency
$\eta_{charger}$	PV efficiency due to charger losses
η_{fc}	Fuel cell efficiency or conversion factor
η_{e}	Electrolyzer efficiency or conversion factor
η_{inv}	PV efficiency due to inverter losses
η_{mis}	PV efficiency due to mismatch losses
η^{i}_{PV}	PV module efficiency at hour-i
$\eta_{PV,ref}$	PV module reference efficiency
η_{soil}	PV efficiency due to soiling losses
η_{th}	Thermal efficiency of PV/T or STC
η_{wire}	PV efficiency due to wiring losses
λ	Latent heat capacity
$\rho_{SAT,l}$	Liquid density of sodium acetate
$\rho_{SAT,s}$	Solid density of sodium acetate trihydrate

Chapter 1

Introduction

1.1. Background

The European Union (EU) aims to have a net-zero greenhouse gas (GHG) emission by 2050, which is in line with the European Green Deal; a roadmap to make EU's economy sustainable [17]. This 2050 objective is also in line with the Paris Agreement, which aims to limit global warming to well below 2°C [1]. Concrete actions need to be taken to realize this goal, and one of the opportunities to apply this action is in the buildings sector.

The global buildings sector is growing rapidly, but not without consequences. The sector accounts for 36% of global final energy consumption in 2018 and 39% of energy-related GHG emissions [2]. The residential sector of buildings, specifically, accounts for 61% of the buildings sector's final energy consumption and 44% of GHG emissions, as depicted in Figure 1. In EU-28, particularly, households are the second-highest contributors to final energy consumption in 2017 [3].

Buildings emissions have increased by 7% from 2010 to 2018 [2]. Indirect emission in the residential sector is the highest contributor among building emissions because energy consumption has increased in the last few years. The energy is used for various purposes, including space heating and cooling, hot water provision, and appliances. Most of the energy is generated from fossil fuel, such as coal, oil and natural gas, which indicates how crucial it is to deploy energy-efficient and green solutions for this sector.

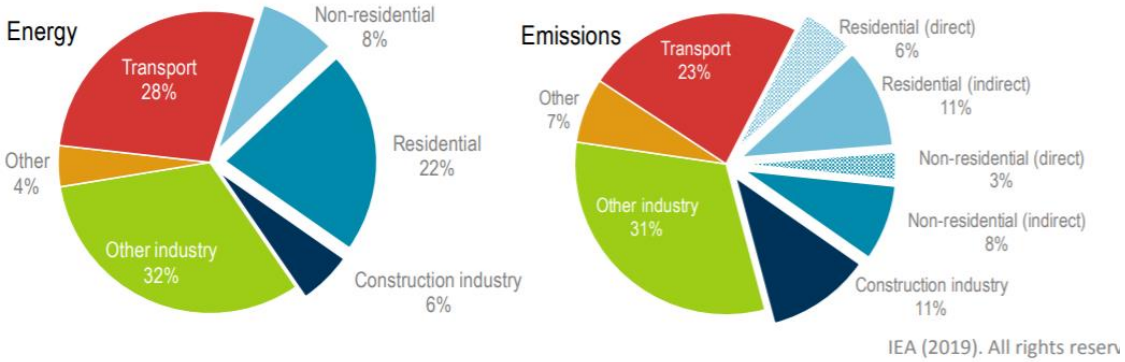

Figure 1. Sector share of final energy consumption and emissions globally [5]

Renewable energy is the key for this energy transition. The importance of renewables has been recognized globally, shown by the 21% global increase of renewable energy source for buildings from 2010 to 2018 (Figure 2). The use of coal, on the other hand, has reduced by 10%. This shows a positive development of energy transition, but there is still a long way to go to achieve the 2050 target. However, renewable energy has its benefits and drawbacks.

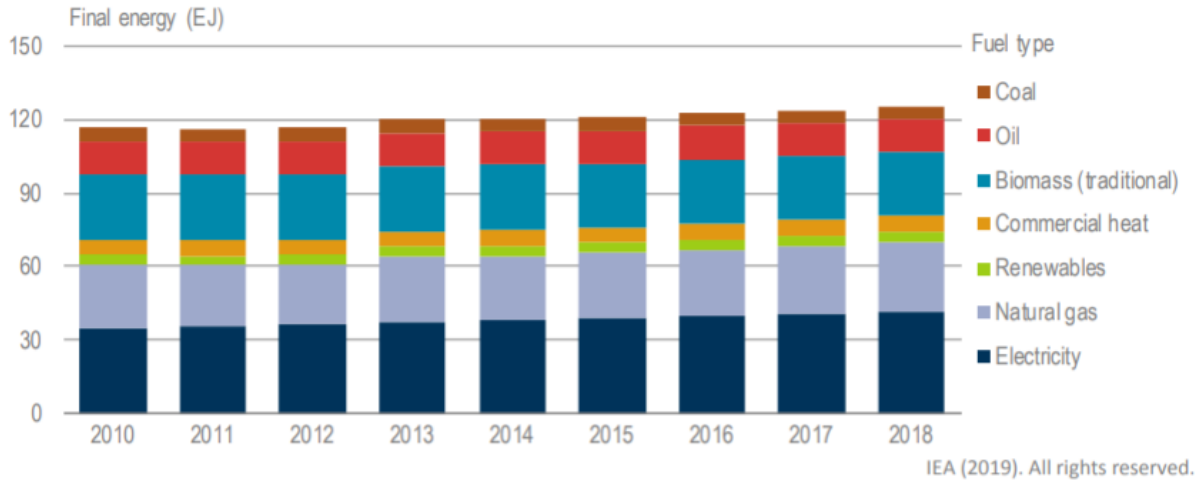

Figure 2. Energy source of global building final energy consumption

One of the benefits of renewable energy sources, besides their sustainability, is the fact that they require no fuel cost, such as solar and wind energy [4]. However, the challenge is the fact that renewables are often intermittent; their availability is dependent on uncontrolled conditions such as the weather. It might be possible to adjust the energy consumption based on the energy's availability, but this is difficult to do, especially when there are many consumers. Moreover, in a non-hybrid system, adjusting energy consumption is not a robust solution. For instance, solar energy is only available during the day, so it is not practical for consumers to not have any energy during the night.

One of the most sensible solution to resolve this energy supply and demand mismatch is to install an energy storage system. The renewable energy generation units must be well-integrated with these storage systems to achieve their optimal performance. A large variety of technologies are available with different characteristics; hence, they must be properly selected for every setup. To understand the energy system integration in buildings, a case study was conducted for the Living Project for Future Innovative Environment or abbreviated into LIFE.

LIFE is an experimental living environment consisting of six inhabited tiny houses, that is planned to be located at the University of Twente (UT), Netherlands (see Figure 3). The term "tiny house" here means that the floor area is smaller than regular houses (25-40 m^2); hence, each house is only occupied by one to two persons. The technical specifications of these houses will be explained later in this report. LIFE is a cooperation between UT, Saxion, small-medium enterprises (SME), and large corporations, with the aim of developing technologically advanced water and energy system [5]. The tiny house system shall have an (almost) autarkic nature, meaning that it can independently supply its own renewable energy and water throughout the year. This objective shall be achieved by integrating different technologies, such as renewable energy generation, energy storage, smart grid, and water recycling. This report, however, only focuses on the energy system of LIFE. It does not discuss the water system, power electronics in the electrical system, or smart grid.

Several energy system setups will be created. The different setups will not only be evaluated based on their technical performance, but also based on their cost. Cost is one of the main considerations in a project, especially because green technologies often have higher investment cost compared to conventional ones. By addressing both technical and economic aspect of the energy system, it is expected that this study could give an overview of the energy system performance in a group of tiny houses. Lastly, it needs to be highlighted that all energy system

configurations considered in this study shall be 100% self-sufficient, meaning that they can independently supply for their own energy demand throughout the whole year.

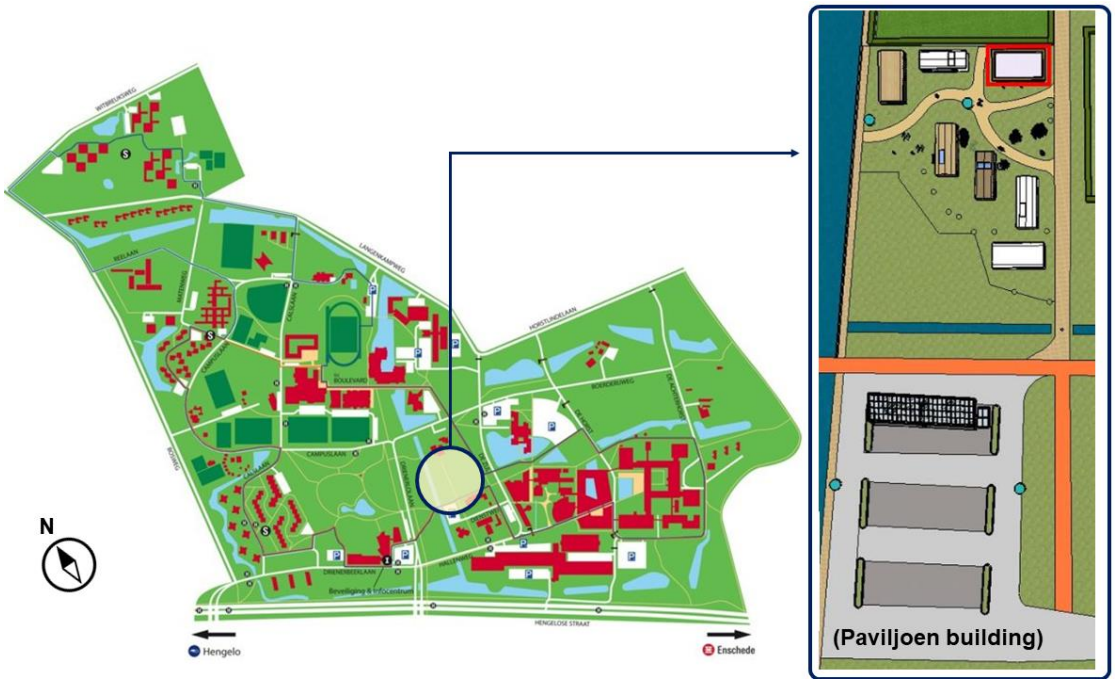

Figure 3. The map of UT campus and the location of LIFE project's tiny houses

1.2. Problem Statement

Energy systems integration in the built environment is discussed separately in many previous studies, based on heat-only or electricity-only. There is an excellent opportunity to integrate both systems to achieve higher efficiency. Therefore, this study shall address the energy system as a whole. In addition, many studies that aim to compare different energy system configurations are mostly focused on the cost. In this study, both technical and economic aspects shall be addressed proportionally using weight factors.

Lastly, according to previous studies, there are mainly two heating options for buildings, which are electric-based (e.g. electric boiler, heat pump) and purely thermal-based (e.g. solar thermal collectors, heat storage). There has not been a comprehensive comparison between the two options; therefore, this study shall evaluate the performance of both system for residential purposes.

1.3. Research Objective

The objective of this research is to gain insights about energy system integration for self-sufficient tiny houses. This objective shall be achieved by establishing several different energy system configurations and modelling them, to assess their characteristics and performances.

1.4. Research Questions

To achieve the previously mentioned objective, the following research questions are created:

1. What are the energy system components that will be considered and filtered for the energy system configurations?
2. What is the method of optimization in sizing energy system components?

3. What are the established energy system configurations to be modelled and evaluated?
4. How is the energy system configuration for self-sufficient tiny houses that would be the most optimum in terms of its technical performance and cost?
5. How does the integration between heat and electricity system affect the overall performance of the system?
6. What are the recommendations for an innovative building energy system?

1.5. Research Approach

The research questions will be answered by creating **three different energy system configurations** for the tiny houses. Each configuration's energy, both heat and electricity, will be evaluated individually and then compared. The evaluation is conducted through a theoretical study consisting of literature review/desk research and creating simulations. It includes building models and simulating them using a combination of tools, namely MS Excel, MATLAB, and Simulink. The main steps taken to achieve the objective of this study are best explained by the following table.

Table 1. Main steps taken in the thesis

No.	Steps	Literature study	MS Excel/MATLAB/Simulink	Chapter in report
1.	Selection of energy technology	Yes	-	2
2.	Defining three energy system configurations to be evaluated	Yes	-	3
3.	Modelling of energy demand	Yes	Yes	3
4.	Modelling and sizing of energy components	Yes	Yes	3
5.	Analysis of energy flow and system operation	Yes	Yes	4
6.	Economic analysis	Yes	Yes	4
7.	Conclusion		Based on the result	5

Chapter 2

Literature Review

The study of energy systems integration using renewable energy sources has previously been conducted for different conditions (location, scale, etc.). These studies are discussed in section 2.1. After reviewing the studies, one could then understand the current development of the topic. Therefore, in section 2.2, different energy technologies will be considered and selected for further analysis.

2.1 Energy systems integration for the built environment

Energy systems can be divided into electricity and heat. In the case of electricity, the evaluation between a system with just a battery versus a system with a hybrid battery and hydrogen storage were extensively studied. Das et al. [6] compared the feasibility of PV-battery, PV-battery-hydrogen storage (using fuel cell), and diesel generator to fulfil the demand of 50 families in a Malaysian village (51 MWh/year). In the PV-battery system, the electricity load is fulfiled directly by PV panels during the day and by batteries during the night. Besides supplying the load, PV panels would also charge batteries during the day. A similar principle applies to the PV-battery-fuel cell system, but in this case, hydrogen storage is also present. Lastly, in the diesel generator system, electricity load is always fulfiled by operating the generator; thus, an energy storage system is not required. The energy system layout is shown in Figure 4.

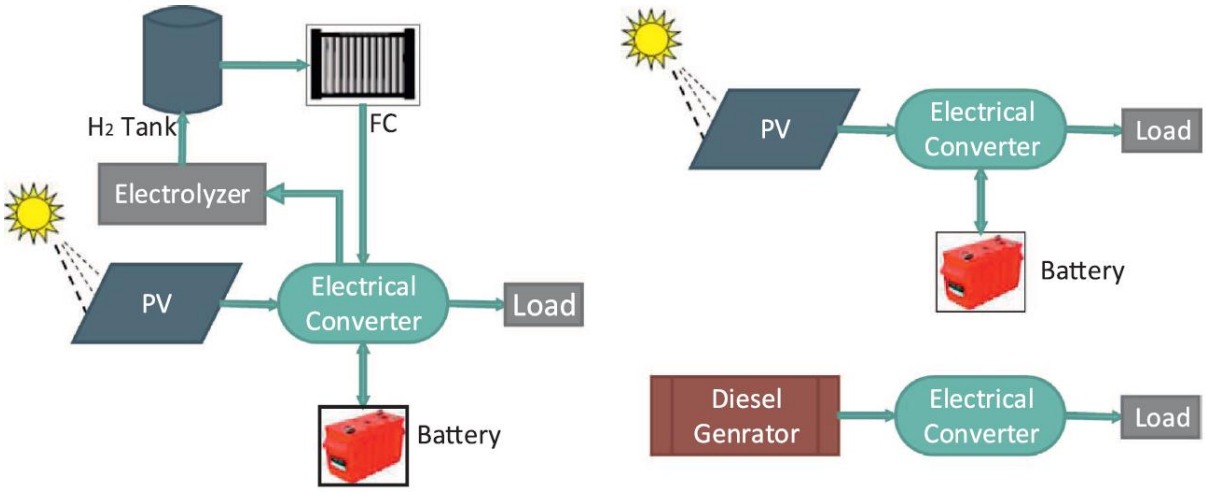

Figure 4. Energy system configuration evaluated by Das et al. in Malaysia [6]

Based on the net present cost (NPC) and the cost of energy (COE), it was concluded that a PV-battery system is the best option with a COE of 0.36 €/kWh. The COE of diesel generator system is higher than the PV-battery and PV-battery-fuel cell system due to its fuel cost over the evaluated period, while PV requires no fuel cost. The PV-battery-fuel cell system results in higher COE compared to PV-battery due to the expensive fuel cell technology. Nelson's et

al. [7] and Bezmalinović's et al. [8] study also agrees with Das' et al. [6] result about PV-battery having a lower COE than PV-battery-fuel cell system. It needs to be highlighted that the main advantage of systems with a fuel cell is it can store energy in a long-term (seasonally).

Furthermore, both scenarios can fulfil almost all electricity demand (98.2% in PV-battery, 98.3% in PV-battery-fuel cell) in the area. However, in both cases, the excess energy generation is quite high (37.5% in PV-battery, 31.3% in PV-battery-fuel cell) because the required size of PV is large but the load during the day is low. If the PV size is reduced, there are days when sun irradiation is low and there is insufficient energy produced to charge the energy storage system, which would result in energy shortage during the night or when solar energy is completely unavailable.

On the contrary, Kharel & Shabani [9] found that in South Australia, a hybrid battery-hydrogen storage system has a COE of 0.74 €/kWh, much lower compared to a battery-only system which has a COE of 3.16 €/kWh. However, in this case, the scale is much larger, as it fulfils the demand of the whole state (15,859 MWh/year). In addition, the energy source is not only PV, but also wind energy. This indicates that the scale of system might significantly affect its cost-competitiveness. Moreover, with South Australia's current energy generation mix and demand, the energy system would produce excess hydrogen. This hydrogen has the potential to be utilized for other purposes, such as fuel cell electric vehicles (FCEV). If the excess hydrogen can be utilized, the COE would further decrease 0.58 €/kWh. Lastly, if the fuel cell acts as a combined heat and power (CHP) unit, then the COE could be further reduced. A PV-hydrogen storage system without any battery was also concluded to be feasible in France, according to Mohammed et al. [10], resulting in a COE of 0.16 €/kWh.

Comparisons between different renewable energy sources were also studied by various groups. Luta & Raji's [11] research showed that a wind-hydrogen storage system (using fuel cell) is less cost-competitive than a hybrid PV-wind-fuel cell system in South Africa with a demand of 394 MWh/year. However, both scenarios are not economically feasible in the rural area of South Africa because high-cost hydrogen storage technology results in a high COE, and the inhabitants do not have the financial capacity to pay for the bills. They concluded that grid extension is a better option compared to the installation of PV-wind-fuel cell energy system, but only if the grid extension distance is under 4,728 km. The disadvantage, however, is the probable use of non-renewable energy source from the main grid, which would not help the environment.

Mudgal et al. [12] evaluated the combination of PV, wind, and biogas to fulfil electricity demand of 64.4 MWh/year in India. The most optimum system comprises of 12-kW PV system, 3-kW wind turbine, and 15-kW biogas generator. With this size, the energy excess generated is only 10%, which is two-thirds less than in Das' et al. [6] system. The presence of energy storage is not mandatory in this case due to the use of biogas. The system results in a relatively low COE of 0.10 €/kWh. However, the article did not state whether the cost of organic material fed into the anaerobic digester is considered in the economic evaluation.

In the case of heat provision for residential purposes, there are three main technologies that are frequently discussed, namely heat pump, solar thermal energy, and heat storage. Ramos et al. [13] analyzed PV/T panels that are coupled with heat pumps and absorption refrigeration (AR) system to provide both heating and cooling demand for urban environments, depicted by Figure 5. They evaluated four scenarios by varying the task of PV/T, heat pump, and AR system for various cities in Europe. The most promising scenario was shown by the one which uses thermal output of PV/T to provide DHW demand, while the heating and cooling demand

are fulfiled by a water-to-water heat pump. The heat pump itself is powered by the electricity output of PV/T. This setup is best implemented in Seville, Rome, Madrid, and Bucharest due to their location and climate condition. However, the system size studied was only able to supply 60% of the space heating and DHW demand.

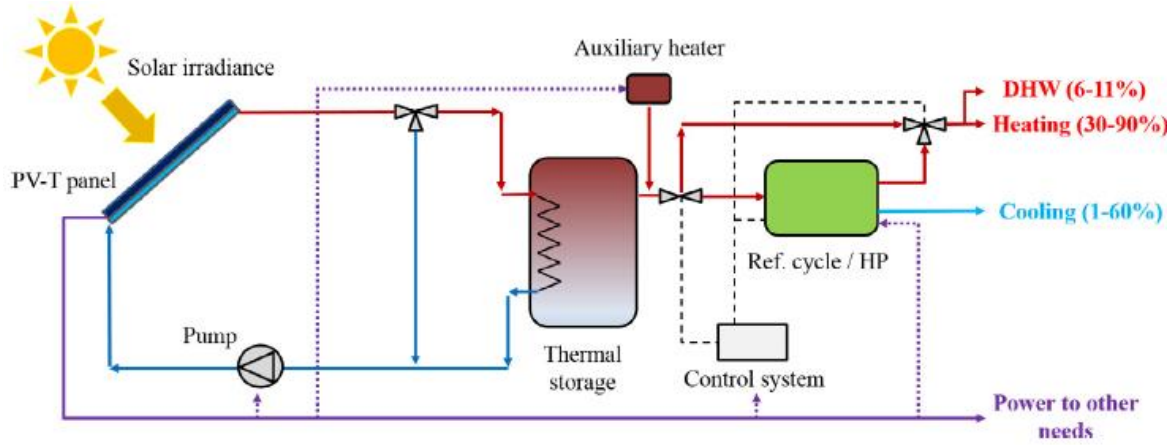

Figure 5. PV/T heating and cooling system [15]

Hesaraki et al. [14] discussed combining solar thermal collectors with heat pump and different seasonal heat storage technologies to provide domestic hot water (DHW), space heating, and space cooling. A system that provides both space heating and DHW is commonly called a solar combi system [15]. The heat storage technologies discussed were underground hot water, water-gravel pit storage, borehole thermal energy storage (BTES), and aquifer thermal energy storage (ATES). The presence of a heat pump is necessary because heat losses from the storage results in lower stored temperature, and heat pump has the ability to increase it. The most suitable heat storage technology depends on various factors, namely, cost, heat demand, and geological conditions. They concluded that these seasonal heat storage technologies are more efficient and economically feasible for community-level instead of individual housings.

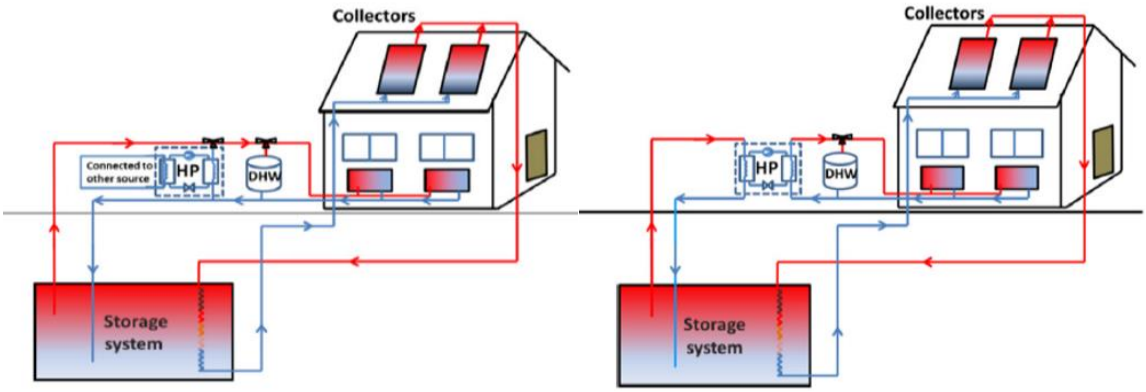

Figure 6. Solar combi system with heat pump and underground heat storage [13]

The heat storage technologies studied by Hesaraki et al. [14] were all based on sensible heat, but there are actually other existing technologies; they are latent heat storage (LHS) and thermochemical storage (TCS). Dannemand et al. [10] studied the provision of DHW and space heating using solar thermal collectors combined with LHS technology for long-term energy storage, shown in Figure 7. In this case, no heat pump is present. They used the supercooling nature of a phase-changing material (PCM) called sodium acetate trihydrate (SAT) to store heat for a long period of time. The study showed that a house in Danish climate could achieve

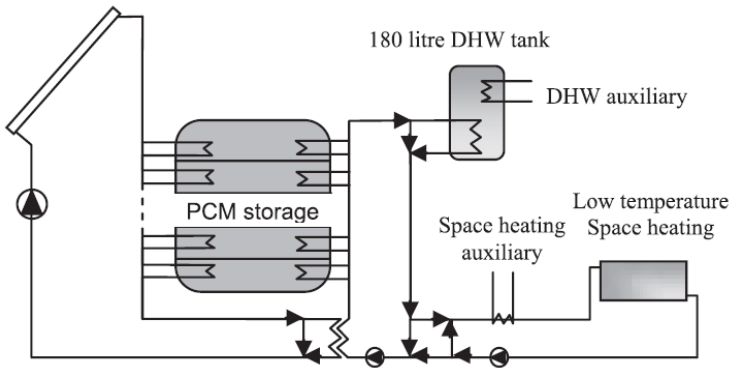

Figure 7. Solar heating combi system with PCM storage [10]

80% of solar fraction due to the help of this heat storage and a high heat exchange rate. Nevertheless, there are still a lot of technical challenges in controlling the SAT's supercooling character, despite its high potential to act as seasonal heat storage.

Leonhardt and Müller [16] also used PCM storage, but in their case, a heat pump is present, and the system is only used for space heating, shown in Figure 8. The conclusion of this study was that PCM storage improved the solar thermal and heat pump system efficiency, which was shown by the reduction of primary energy consumed. Other studies involving PCM storage for home heating was also performed by Zhao et al. [17], Lin et al. [18], and the EU-funded TESSE2B Project [19].

Other possibilities of solar energy heating system for homes include direct and indirect solar DHW system [20], various configurations of solar-assisted heat pump for space heating and DHW [20], indirect solar heating system with PCM-integrated water tank for space heating and DHW [21] [22].

Most of the studies discussed a heat-only or electricity-only system when it comes to built environment. There is actually an excellent opportunity to integrate both systems to achieve higher efficiency, for instance by operating fuel cell as a CHP unit or by integrating PV with solar thermal collectors (STC) to become PV/T. Therefore, this study shall address the energy system as a whole.

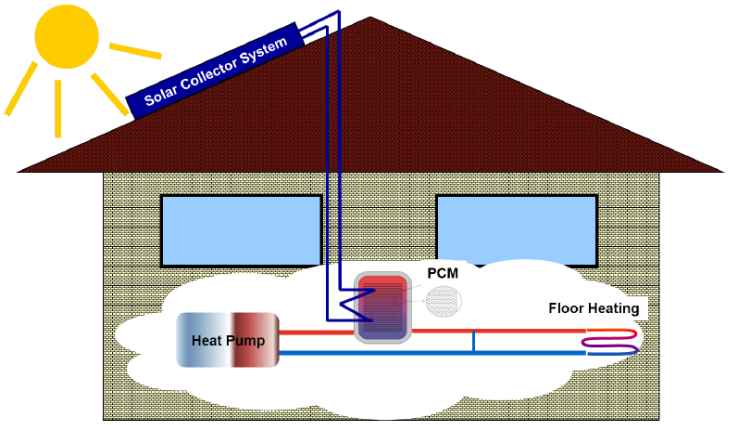

Figure 8. Solar heating system with heat pump and PCM storage [16]

Based on previous studies, heat can either be supplied by an electric-based system such as electric boiler and heat pump, or a purely heat-based system such as STC or the thermal output of PV/T. It is necessary to evaluate these two heating options in order to understand the benefits and drawbacks of it. Departing from these points, this study will evaluate three different energy system configurations, mainly in terms of their operation, system size, and cost.

2.2 Justification of Technology Selection

The design of energy system configurations starts with reviewing existing technologies and selecting them. In this study, only renewable energy would be considered because the use of fossil fuel is not aligned with the Paris Agreement's objective of keeping the increase in global

average temperature to well 2°C above pre-industrial levels [23]. Therefore, coal and diesel generators are eliminated.

Renewable energy sources are mainly divided into solar energy, wind energy, biomass energy, and hydropower energy. In this study, nuclear energy is not considered as a renewable energy source because the material used (e.g. uranium) is finite. In addition, it produces harmful radioactive waste, which opposes the whole idea of clean and renewable energy.

In the case of renewable energy such as solar and wind energy, their availability fluctuates, and they are considered intermittent. Therefore, an energy storage system is necessary to achieve 100% self-sufficiency. The Netherlands has a temperate climate; thus, it requires heat during the winter and cooling during the summer. The energy storage system shall then be capable of fulfilling both electricity and heat demand.

For a clear general overview, the energy components are divided into their energy types: heat and electricity. Both heat and electricity are further divided into generator and storage. Once the technologies are selected, three different energy system configurations will be developed, which will be explained in section 3.1.

2.2.1 Renewable Electricity Generator

According to a report by Frontier Economics for the Dutch Ministry of Economic Affairs, more than 50% of Dutch electricity will be produced from renewable sources by 2035 [24]. Figure 9 shows the projected mix of electricity generation in the Netherlands. In 2035, the majority of renewable energy source comprises of wind energy, followed by solar energy. Hydropower only makes a small percentage in the mix because the Netherlands' geographical condition does not support the utilization of this energy. Biomass energy is part of the "other renewable sources" category; thus, it is assumed that the percentage is lower than wind and solar energy. This leaves us with two options: wind and solar energy.

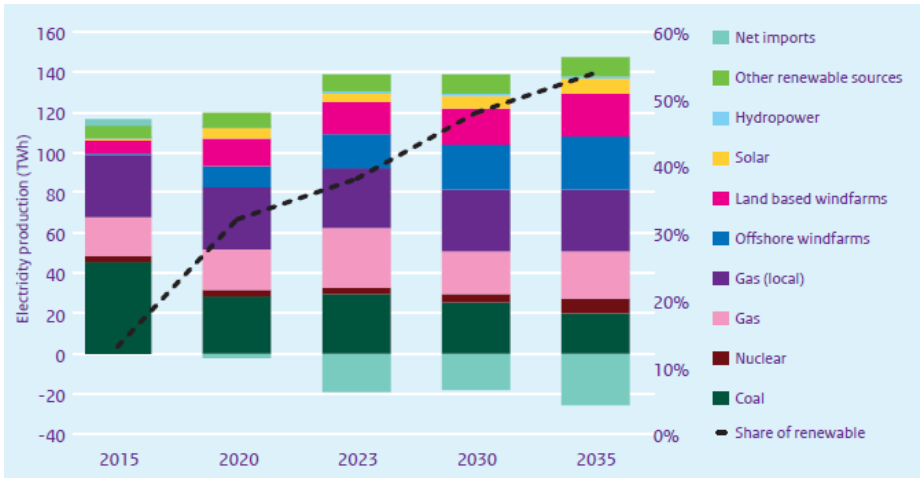

Figure 9. Past (2015) and expected (2020-2035) electricity production in the Netherlands [2]

Wind energy is not suited for small scale energy system such as the six tiny houses in this study. Moreover, the presence of a large wind turbine on the campus is not viable, as the noise disturbs people surrounding it, and it disturbs the landscape. A PV system, on the other hand, is well-suited in residential areas because the size can be adjusted according to the inhabitants' requirement, it does not significantly disturb the landscape, and it operates silently. Therefore, electricity generation technology being considered in this study is the PV system. A PV panel

converts solar radiation into electricity, with an efficiency ranging from 5-20% for commercial panels [25].

2.2.2 Energy storage for electricity

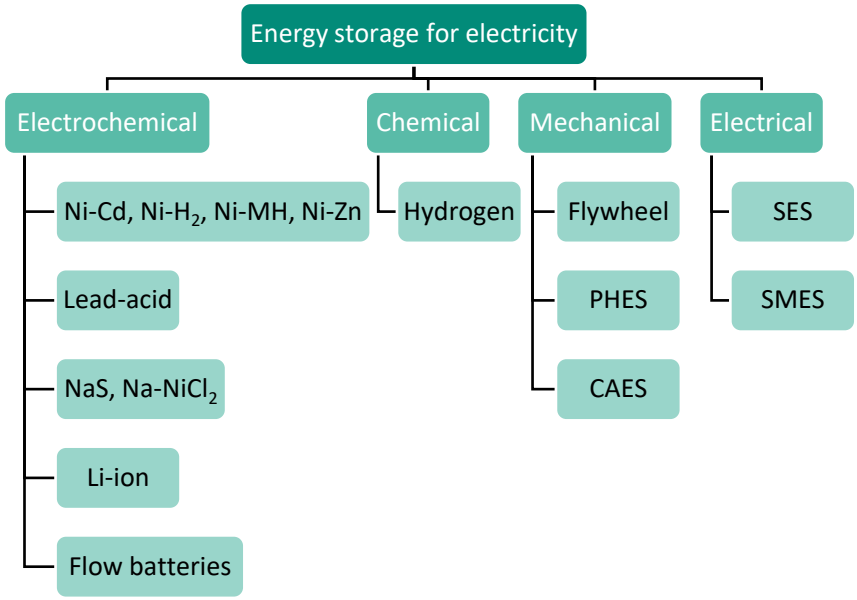

Figure 10. Classification of energy storage technology for electricity [11]

The classification of energy storage for electricity is shown in Figure 10. Mechanical storage like flywheels, pumped hydro energy storage (PHES), and compressed air energy storage (CAES) have high rated power (100kW – 1 GW); thus, they are usually employed to manage power quality in the grid or ancillary services [26] [27]. In addition, PHES is only built for large-scale energy storage plants. These high rated power and capacity are not necessary for just six tiny houses. The same goes to electrical storage like supercapacitor energy storage (SES) and superconducting magnetic energy storage (SMES), which are often used for power quality. This leaves us with just two types of energy storage, which are electrochemical (battery) and chemical (hydrogen).

Like heat storage, two types of energy storage for electricity are considered in this study according to their storage period, which are daily and seasonal. The suitable option for seasonal storage is hydrogen because it is in the form of gas; hence, it can be compressed or liquefied to give a high energy density. In addition, there is no self-discharge over the storage period, provided that the hydrogen storage does not have any leaks. Batteries, on the other hand, have losses due to their self-discharge.

In a hydrogen storage system, electricity is stored in the form of chemical (hydrogen), through the help of electrolyzer and fuel cell as energy converters [26]. Electrolyzer uses electricity to convert deionized water into hydrogen and oxygen, according to the following reaction [27]:

$$2H_2O \leftrightarrow 2H_2 + O_2 \quad (1)$$

The hydrogen is then compressed and stored inside tanks. When the electricity generation is not sufficient to fulfil the demand, energy would be discharged from the hydrogen storage by passing it through a fuel cell. Air enters the fuel cell, allowing hydrogen to react with oxygen to produce water. The water is pushed out of the cell with excess flow of oxygen [28]. This electrochemical reaction produces electricity, which could then fulfil the houses' demand.

During the operation of a fuel cell, it produces heat as a byproduct; thus, it can act as a combined heat and power (CHP) system. Because heat is considered as a byproduct, the fuel cell in a hydrogen storage system is designed according to the required electric energy supply instead of thermal [4].

Commercially, there are two types of fuel cell that currently exist; alkaline fuel cell (AFC) and proton-exchange membrane (PEM) fuel cell [27]. In this study, PEM fuel cell is chosen because it can operate with oxygen from the air, while an AFC requires pure oxygen [29]. Additional oxygen purification system installation for six tiny houses' is considered to be too sophisticated. Hydrogen storage technology for households is commercially available; for instance, the Picea system from a German company called Home Power Solutions (HPS) [30].

For daily storage, electrochemical energy storage (battery) is considered. The two most common battery technologies used at homes with PV system are Lead-acid and Li-ion. In this study, Li-ion is chosen as short-term storage because it has higher energy density, more cycle life, and higher efficiency. The downside of Li-ion is the higher cost, but it has been reducing and will be reduced even more in the future [1]. Examples of popular Li-ion battery brands include Tesla Powerwall & LG Chem RESU, both using the Li-ion NMC technology.

2.2.3 Renewable Heat Generator

As mentioned at the beginning of section 2.2, the Netherlands require heating due to its temperate climate. The average temperature in the winter is 3°C [31], which is much lower than the comfort room temperature (20-23°C [32]). Hence, space heating is essential. In addition, heat is also needed for the provision of DHW. The amount of heat required for the tiny house energy system will be discussed later in section 3.5.1.

The main options for a renewable heat generator according to previous studies are solar thermal energy, biomass energy, conventional electric boilers, and heat pump. To select between these four technologies, we refer to the International Energy Agency's (IEA) Sustainable Development Scenario (SDS). It outlines a major transformation of the global energy system to deliver energy-related United Nations' (UN) Sustainable Development Goals (SDG). The SDS is also fully aligned with the Paris Agreement's objective [23]. One of the sectors that are considered in IEA's SDS is the buildings sector.

In EU households, space heating and DHW account for 79% of total final energy use [33]. Therefore, the implementation of clean heating technologies in households must increase in the future. This is the reason behind the targeted reduction of fossil-fuel-based equipment for household heating in 2030, as depicted in Figure 11. The use of conventional electric equipment such as electric boilers shall also be reduced and replaced by heat pumps because heat

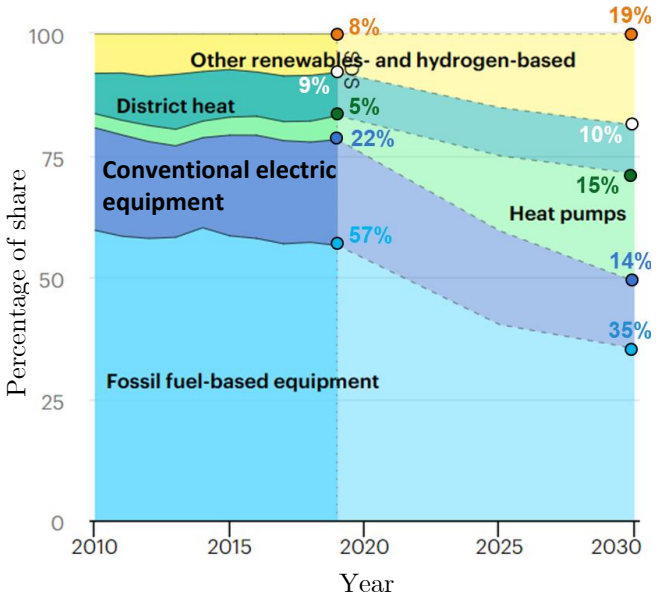

Figure 11. Global household heating technology share in the SDS 2010-2030 [4]

pump's efficiency is about three times higher than conventional electric equipment. A heat pump transfers heat from a low-temperature source to a high-temperature sink by using the principle of Carnot cycle [34] [35]. It can operate reversibly, as a heater and a cooler. Its efficiency is defined as the coefficient of performance (COP), which is typically three times higher than that of a conventional electric heater.

The share of heat pump used as household heating technologies was 5% in 2019, and this number needs to triple by 2030 to be in line with SDS [36]. Furthermore, the Dutch government states that homeowners are encouraged to install new systems such as hybrid heat pumps to become energy neutral homes [24]. Lastly, the International Renewable Energy Agency's (IRENA) Renewable Energy Roadmaps (REmap) analysis shows significant potential to accelerate the implementation of heat pumps as well as solar water heaters in industry and buildings [37].

District heating refers to a centralized large-scale heat generation system for households, and the source varies from power plants, biomass/biogas, industrial heat waste, waste incinerator, etc. [38]. Because the studied energy system is small (six tiny houses), district heating will not be considered here.

Lastly, solar thermal energy and biomass energy are categorized into "other renewables", and the number must double in 2030. Biomass energy, however, is mostly used in an industrial scale, rather than household-scale [39]. This might be due to the local pollution that it would cause around the residential area, or because building-owners prefer technologies with no fuel cost. Departing from these facts, the heating technologies being considered in this study are the heat pump and solar thermal energy.

Air source heat pump (ASHP) and ground source heat pump (GSHP) are the two most used types of heat pump for home heating. At the end of 2017, 394,000 ASHP & 55,000 GSHP were in use in the Netherlands [40]. In cold climates and during the winter, GSHP generally has a better energy performance than ASHP because the ambient air temperature is lower than the soil or ground temperature [41]. A lower supply temperature causes the heat pump's heating COP to be lower. Conversely, during the summer when cooling demand is present, the ambient air temperature is higher than the soil or ground temperature, which causes the ASHP's cooling COP to be lower than that of GHSP's. In addition, when ambient temperature drops around 0°C, moisture from the air could condensate and freeze on the outdoor unit of ASHP, which causes the heat pump's COP to be lower than one or less efficient than ordinary electric heaters. Table 2 shows how most of the time, ASHP does not achieve a COP above 3, which is the typical COP of a heat pump. It will only happen if the air is at or above 0°C and the sink temperature is 35°C. This is not the case for GSHP.

The consequence of the higher GSHP efficiency is the larger investment cost compared to ASHP, as presented in Table 2. However, if GSHP is installed for a new house, where holes are being dug anyway, then the cost can be reduced [41]. In this study, GSHP is chosen because it has higher efficiency and the energy system is installed for six new tiny houses. By installing the ground coils/collectors collectively, it is estimated that the total investment cost per kW_{th} could be reduced.

Solar thermal energy can be harvested either using a solar thermal collector (STC) or PV-integrated solar thermal collector called PV/T. STC absorbs solar energy and converts it into heat using a stream of liquid or gas [43]. For residential purposes, there are two main types of STC: flat-plate collector (FPC) and evacuated tube collector (ETC). The efficiency of different STCs changes according to their working temperature, as shown in Figure 12. In this study,

the required temperature for space heating is about 35°C because the houses will be newly built, so they are well-insulated, and they do not use old radiators. The highest temperature required is around 60°C, used for DHW. Figure 12 shows that at a temperature of 10-60°C above ambient, FPC has the highest efficiency. In addition, Table 3 shows that FPC fulfils the heat requirement and has a lower cost compared to ETC. Therefore, FPC is selected in the case of STC.

Table 2. Variation of heat pump COP with different source and sink temperatures, as well as the installation cost [41]

Heat pump type	**Installation cost (€/kW$_{th}$)** [42]	**Source**	**COP variation with sink temperature**			
			35°C	**45°C**	**55°C**	**65°C**
ASHP	542 – 2,845	Air at -20°C	2.2	2.0	-	-
ASHP		Air at 0°C	3.8	2.8	2.2	2.0
GSHP	1,044 - 2,024	Water at 0°C	5.0	3.7	2.9	2.4
GSHP		Ground at 10°C	7.2	5.0	3.7	2.9

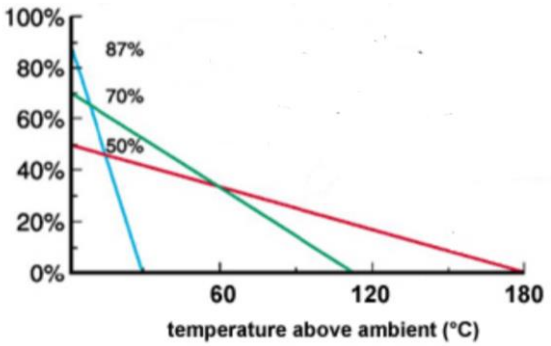

Figure 12. Efficiency of different types of STC [44]

Table 3. Comparison between FPC and ETC [43]

Parameter	**FPC**	**ETC**
Temperature range	30-80	50-200
Major applications	Water heating, space heating, air conditioning, industrial process heat	Water heating, space heating,
Cost	€370.74/panel (1.81 m^2) [45]	€754.8/panel (2.83 m^2) [45]

The second way of harvesting solar thermal energy is through PV/T panels. When PV panels absorb solar radiation, its temperature increases because the energy is not completely converted into electricity. The efficiency of solar cells reduces with increasing module temperature [27]. This performance deterioration can be prevented by circulating a heat transfer fluid under the PV modules. In addition, this fluid can be utilized for heating purposes, such as DHW and space heating. As a result, the overall efficiency of PV would be improved, and the required area to produce electricity and heat is reduced. However, it needs to be noted that PV/T's thermal efficiency is lower than that of regular STCs because there is a higher emissivity from PV laminate and a lower absorption factor due to the withdrawal of electrical energy in PV/T [46]. In summary, the selected heat generation technologies to evaluate are as follows.

Table 4. Selected heat generation technologies

Technology	**Type**

Heat pump	Ground source heat pump
Solar thermal collector (STC)	Flat-plate collectors (FPC)
PV/T	-

2.2.4 Heat Storage

There are three main heat storage technologies existing today, which are sensible heat storage (SHS), latent heat storage (LHS), and storage using thermochemical material (TCM). Generally, the capacity and energy density increase respectively from SHS, LHS, to TCS, as shown in Table 5. Consequently, the cost of TCM is the highest, while SHS is the lowest. Based on the key parameters of these technologies presented in Table 5, a matrix of choice is created, as shown in Table 24 (Appendix A.4). Cost is an important factor for a small system such the tiny houses, so the weight factor is 5. Storage period is also important because the aim of this study is to have a self-sufficient energy system. As the highest point is shown by LHS, it is the chosen technology for this study. LHS technology for households is commercially available; for instance, the UniQ device from a Scottish company called Sunamp [47]. However, the commercial option is very limited, and the technology is still developing, unlike the mature SHS technology.

Table 5. Typical parameters of heat storage technology [48]

Parameter	**Heat storage technology**		
	SHS (water)	**LHS**	**TCM**
Capacity (kWh/t) [48]	10-50	50-150	120-250
Energy density (GJ/m^3) [49]	0.2	0.3-0.5	0.5-3
Power (MW) [48]	0.001-10	0.001-1	0.01-1
Efficiency (%) [48]	50-90	75-90	75-100
Storage period [48]	Hours/days*	Hours/days*	Days/months
Cost (€/kWh) [48]	0.1-10	10-50	8-100
Technology readiness level (TRL) [50]	9	7	7
Heat loss [49]	Significant, but depends on insulation	Significant, but depends on insulation	Low or absent

**depends on the insulation as well*

Paraffin, fatty acid, salt hydrate, and metallic materials are several types of phase-changing material (PCM) used for LHS. Metallic materials are a good candidate for temperatures above 550°C [51], so this material is eliminated from this study. Fatty acids have the advantage of high heat of fusion and no supercooling, but they are unstable at high temperature, more costly than paraffin, and most importantly, toxic [51]. Fatty acids are therefore eliminated as well. This leaves paraffin and salt hydrate as the last options.

In this study, the LHS shall provide both space heating and domestic hot water (DHW) [52], so the PCM must have a higher temperature than that of DHW (50-60°C). According to Figure 13, there are five prospective materials that fulfil this criterion, which are the sodium acetate trihydrate (SAT), paraffin (1), paraffin 6035, paraffin 6403, and paraffin 6499. As the six houses are self-sufficient, LHS shall be able to cover the energy mismatch throughout the year. Hence, high energy density is an important factor in ensuring that the storage size is not too large. Based on this consideration, the chosen PCM is SAT.

Based on the period of storage, heat storage is divided into long-term (seasonal) storage and short-term (daily/weekly) storage. A PCM can become seasonal heat storage in two ways: (1) by the application of excellent thermal insulation, and (2) by stable supercooling [53]. The first

principle is not specific for PCM because one can apply it to any other material, such as water. On the other hand, the second principle is specific for some PCM, and SAT is one of them.

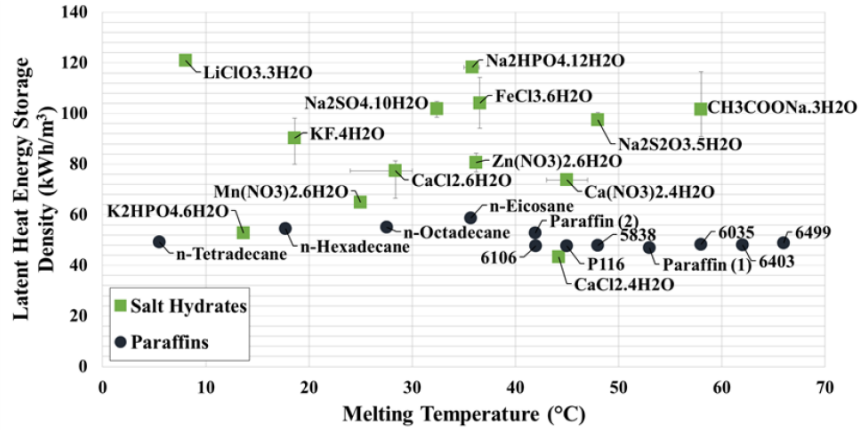

Figure 13. Thermal energy storage density of salt hydrates and paraffins [81]

A material that experiences supercooling would solidify at a temperature below its melting point [54], as shown in Figure 14. This character is undesirable in short-term storage because the latent heat is not released when the PCM cools down, so a trigger is required for the PCM to solidify, such as introducing the liquid PCM to its crystal form. However, in long-term storage, the supercooling nature of salt hydrate (including SAT) is desirable because one can store a PCM's latent heat for a long period of time at ambient temperature (20°C) [55], and then release its contained latent heat at a specified time. The challenge is to keep the PCM at its stable supercooled state throughout the season because it is affected by pressure changes and rapid temperature changes to below its minimum level of supercooling. The density difference between the material's solid and liquid state, small cracks and deformations on the internal surface of the heat storage (e.g. welding), could cause pressure change, so those factors must be taken into account as well. In summary, the selected heat storage is as follows.

Table 6. Selected heat storage

Type	Latent heat storage (PCM storage)
Material	Sodium Acetate Trihydrate (SAT)
Duration of storage	Both daily and seasonal will be evaluated

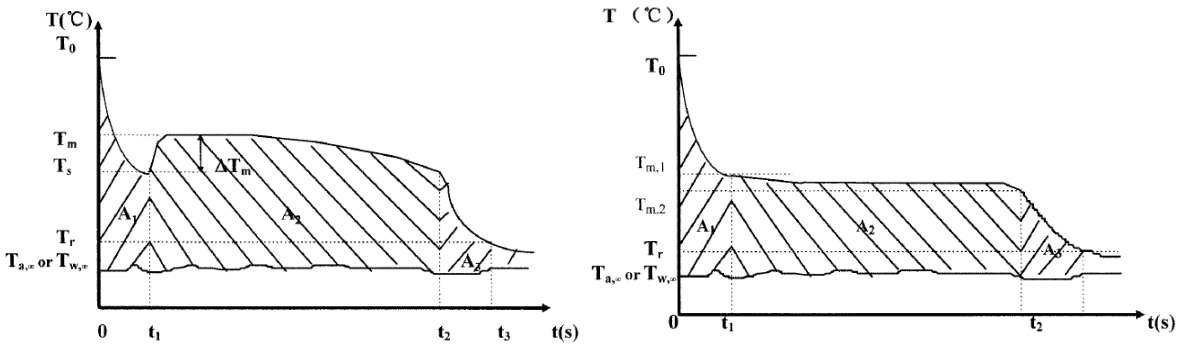

Figure 14. Temperature of a PCM during cooling process, with (left) and without (right) supercooling [14]

Chapter 3

Design and Modelling

This chapter discussed the three energy system configurations that will be evaluated (section 3.1) as well as the houses' design (section 3.2). Next, the method to analyze each energy components is discussed in section 3.3, followed by the optimization method of sizing in section 3.4. After understanding the whole setup, section 3.5 explains the derivation of energy demand by analyzing the energy balance, and section 3.6 uses the energy balance to build a temperature control system. Lastly, section 3.7 describes the cost model used in this study.

3.1 Energy System Configuration

There are three tiny house energy system configurations considered in this study. Each configuration contains different components and technology, as well as different ways of operations. However, there are several assumptions that apply to all three configurations, as follows:

- The system must be powered solely by renewable energy and must be 100% self-sufficient. It means that they do not require any electricity from the main grid or gas from the main network.
- Although the systems are self-sufficient, they are assumed to be connected to the grid so that excess electricity can be injected to the grid.
- The heating system provides for both space heating and DHW.
- The heating system is centralized because the houses are located close to each other, and the cost of a collective system would be less expensive than individual ones.
- Space heating in all configurations is delivered by heat convectors. They are similar to radiators because they also use convection heat transfer to increase room temperature, but they use small fan coils to speed up the heating cycle [56]. Due to its way of operation, it can provide comfort with a lower heating medium temperature (35-45°C), as opposed to radiators (±60°C). This feature is beneficial, especially for an energy system with heat pump (first and third configuration), because its efficiency increases with lower sink temperature. Lastly, convector can operate in both heating mode in the winter and cooling mode in the summer.
- In configurations with heat pump (first and third configuration), space cooling cannot be provided while there is a need to provide DHW because the heat pump operates in a different mode (heating vs cooling). Therefore, it is assumed that the DHW requirement is prioritized over space cooling.
- All configurations have DHW tanks, or commonly referred to as hot water cylinders, to ensure that systems with a centralized heat pump can provide hot water to the six houses at the desired temperature, whenever needed. A system with DHW tanks can cope with a high demand of hot water [57], which is the case for six houses. The DHW tanks are insulated to reduce heat loss to the environment. A system control simulation

was generated to ensure that the room still receives enough cooling and room temperature is still comfortable for the inhabitants.

- All systems fulfil the same amount of heat and cooling demand.
- All systems fulfil the base electricity demand (for lighting, appliances, and cooking) and EV demand. On top of that, there are other electricity demands that are specific for each configuration.
- All systems experience the same external conditions, such as solar irradiance and outside temperature. They are based on the conditions in Enschede, Netherlands.
- The electricity system has a DC bus because most of the energy components operate on DC, such as PV, Li-ion battery, as well as electrolyzer and fuel cell (for the third configuration). AC loads thus require an inverter, which is assumed to have a 95% efficiency [58]. In actual, DC-DC converters are also required for some components, but its efficiency is neglected in this study.
- The system sizing and simulations are evaluated on an hourly basis for a one-year period.

3.1.1 Configuration 1: PV - Li-ion - GSHP

Figure 15 shows the layout of the first energy system configuration. In the first configuration, PV provides electricity for base demand (lighting, appliances, cooking), EV demand, and heat pump. The PV system is equipped with Li-ion batteries to cover the energy demand during the night or during days where there is a lot of overcasts, especially in the winter. Li-ion battery usually acts as a daily or short-term energy storage, but in this study, various sizes of Li-ion battery is simulated to see if it is feasible to act as seasonal storage.

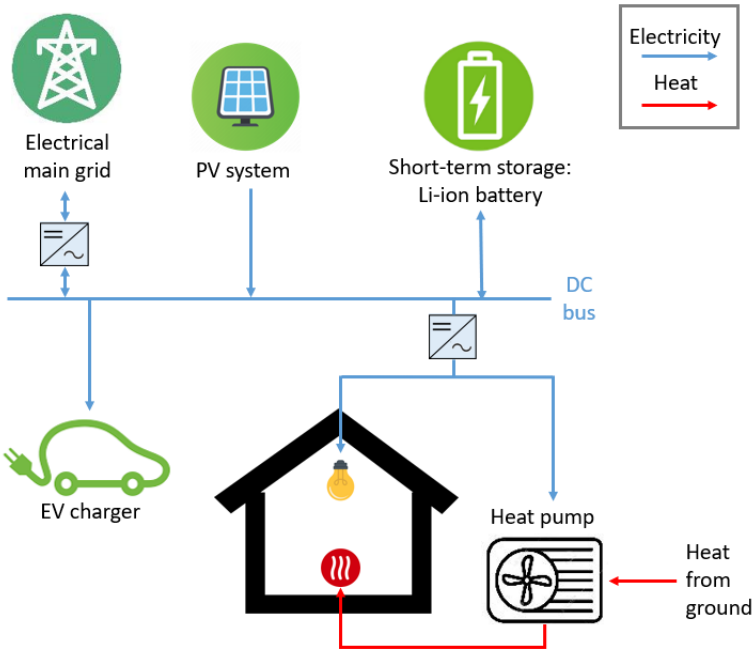

Figure 15. The first energy system configuration

Both space heating and DHW are provided by a centralized GSHP, shown in Figure 16. The electricity to operate heat pump is provided by the installed PV. This means that heat provision very much relies on electricity availability. If electricity is unavailable, then heat is unavailable as well. Nevertheless, commercial heat pump systems are usually equipped with a

backup, such as gas-fired boiler [42]. In this study, however, the heat pump will be sized appropriately, according to the houses' heat demand, so the backup system does not need to operate throughout the year, and the houses will be 100% powered by renewable energy.

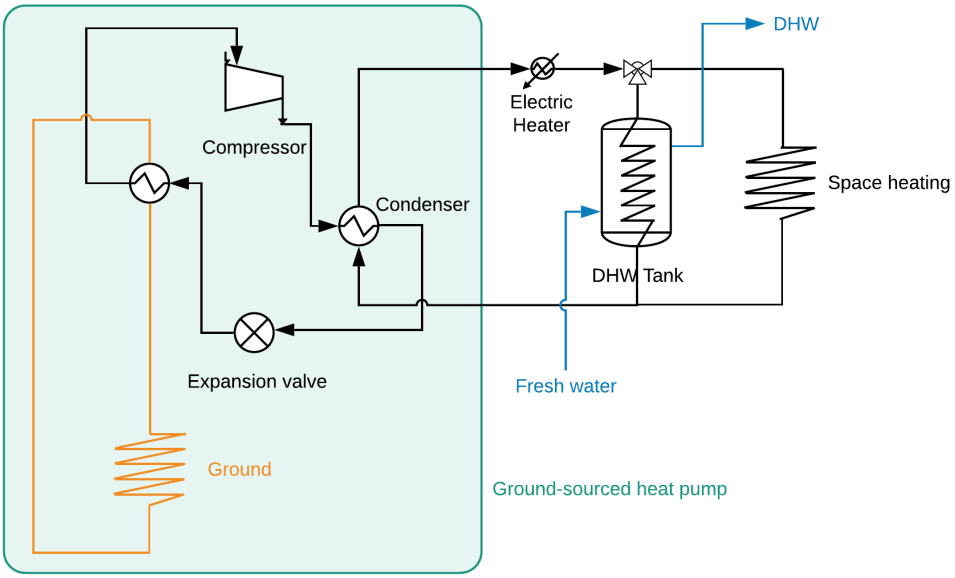

Figure 16. Layout of heating system in the first and third energy system configuration

3.1.2 Configuration 2: PV/T - Li-ion – LHS

The second concept consists of a PV/T system equipped with Li-ion battery as well; however, the heating system is different. Instead of using a heat pump, a PV/T is installed, equipped with an LHS. As explained in section 2.2.4, the PCM used is SAT, so it is possible to use it either as daily storage or seasonal storage. Figure 17 shows the second energy system configuration layout.

The electricity output of PV/T provides energy for base demand (lighting, appliances, cooking), EV demand, and space cooling or air conditioner (AC) demand. Like the first configuration, the Li-ion battery shall provide electricity during the night or in days with a lot of overcasts. In this configuration, however, the heat pump is replaced by the thermal output of PV/T coupled with an LHS. This indicates that, unlike the first configuration, heat provision does not rely on electricity. By evaluating the first and second concept, one could determine how a heat-based and electric-based heating system would differ in performance, efficiency, and cost of the overall energy system in a group of tiny houses.

The layout of the heating system is shown in Figure 18. The thermal output of PV/T provides both DHW and space heating. When there is enough solar irradiance and there is a heat demand, the PV/T will provide heat through a heat exchanger that connects solar thermal collector loop with the demand loop. From there, the heat could be used for both space heating and DHW tank. DHW tanks are present in this configuration because direct discharge of LHS might not be able to fulfil the power demand for DHW draw off [55]. When the heat produced from PV/T is higher than the demand at a certain moment, the system would first prioritize heating up DHW tank until its maximum temperature (70°C), and then followed by heating up (charging) the LHS. When there is a space heating demand, the system will prioritize discharging heat from the DHW tank, but only limited until tank temperature goes down to

55°C. Once the DHW tank reaches that temperature, the system would then discharge energy from the LHS. When there is a DHW demand, but the tank is below its minimum temperature (50°C), the system would also discharge the LHS.

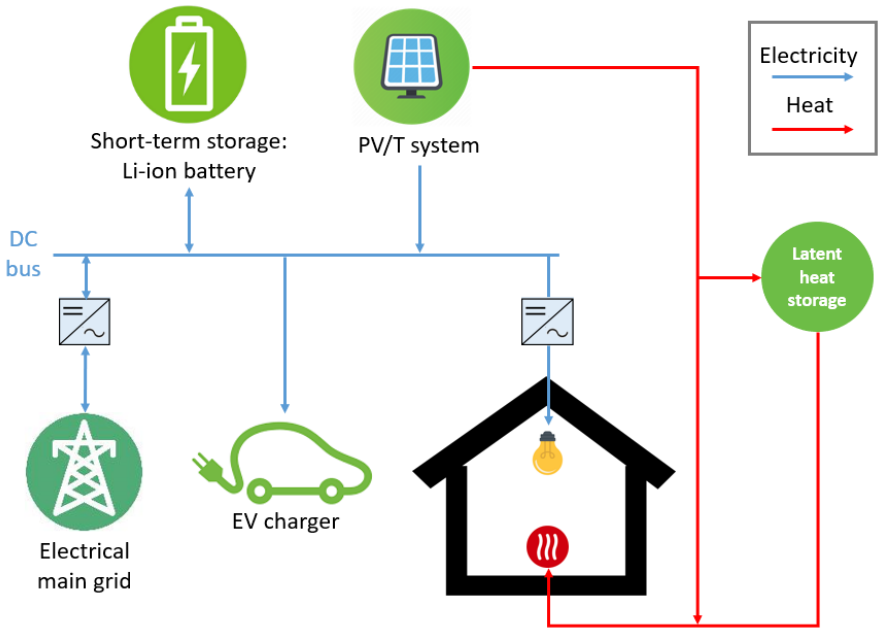

Figure 17. The second energy system configuration

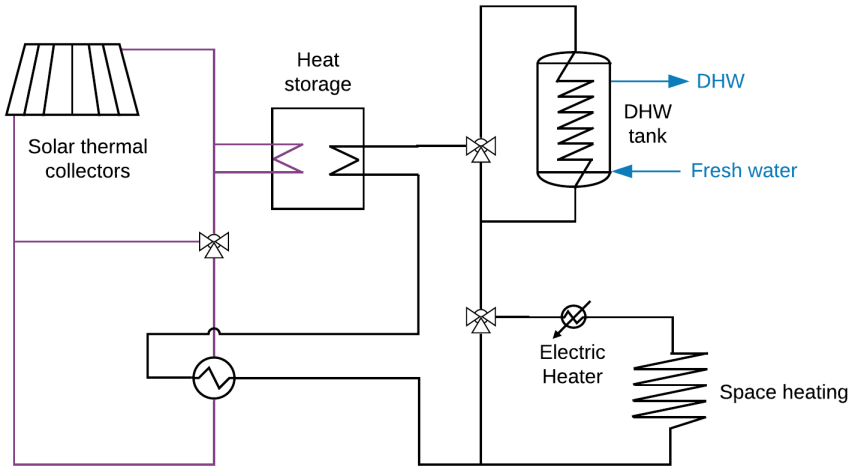

Figure 18. Layout of heating system in the second energy system configuration

3.1.3 Configuration 3: PV – Li-ion – Hydrogen - GSHP

The third concept has the most component and is the most complex, as it introduces hydrogen storage technology, depicted in Figure 19. The heating system layout is the same as that of the first concept, shown in Figure 16. Electricity is provided by PV as well, but the energy storage consists of seasonal energy storage in the form of hydrogen storage and daily energy storage in the form of Li-ion battery. In hydrogen storage, whenever there is a surplus of electricity, it is used to convert water into hydrogen and oxygen using an electrolyzer. The hydrogen is then compressed and stored inside a hydrogen tank. When electricity demand exceeds the supply, the hydrogen is discharged through a PEM fuel cell and converted back into electricity. Due to the presence of hydrogen storage, the total electricity demand not only

consists of base demand, EV demand, and heat pump demand, but also the hydrogen compressor.

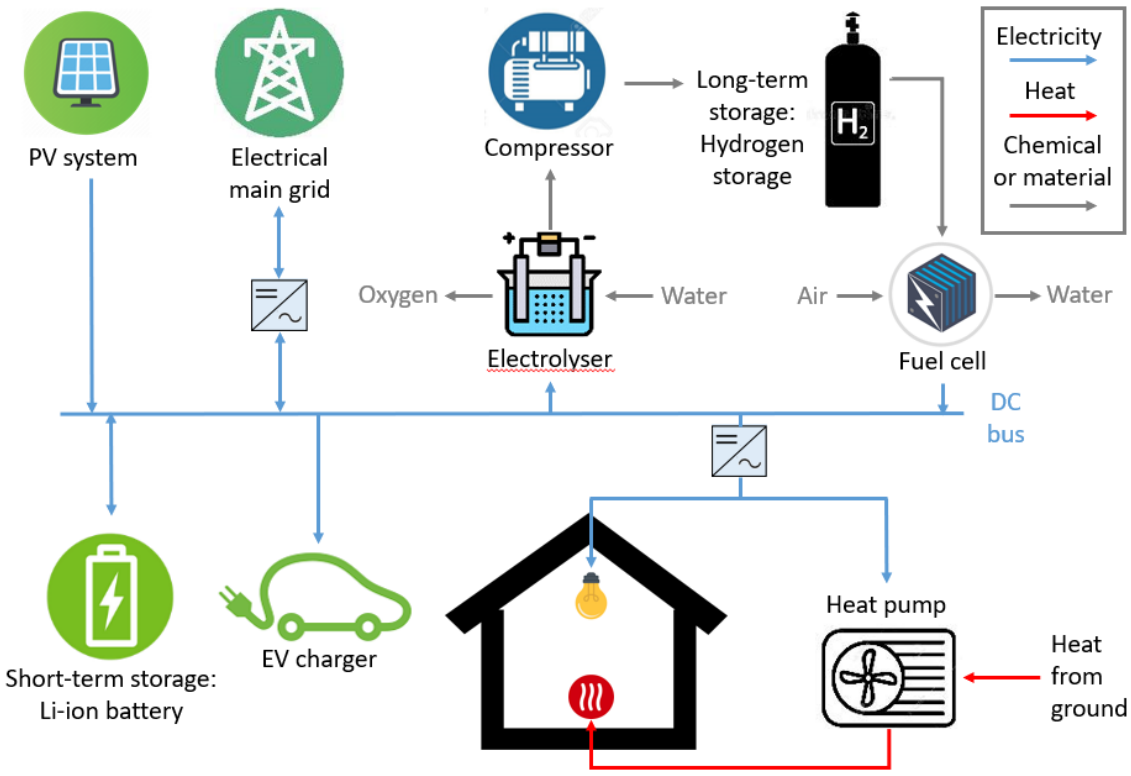

Figure 19. The third energy system configuration

When the PEM fuel cell operates, a certain amount of heat is generated, which could be utilized for space heating and DHW supply. This means that the fuel cell acts as a combined heat and power (CHP) unit. In such systems, the heat is a byproduct, meaning that a fuel cell is designed for electric energy supply rather than thermal [2].

When fuel cell does not operate, heat is provided by a heat pump. Besides its high efficiency, the reason of choosing heat pump is because the electricity system in the third configuration utilizes high-technology devices which ensures a more secure electricity availability, so the heating system should be electric-based and it should take advantage of this sophisticated technology. By evaluating the first and third concept, one could determine to what extent does hydrogen storage technology improve the energy system of tiny houses, and how it affects the cost. These are important questions because hydrogen storage with low-temperature fuel cell/electrolyzer technology has a low roundtrip efficiency, is not widely commercialized yet for households, and consists of expensive components. On the other hand, it can store energy for a longer period with smaller loss compared to Li-ion battery, assuming there is no leak on the hydrogen system.

3.2 Tiny House Design

There are six tiny houses with a total of eight occupants evaluated in this study. The house units are prefabricated by a company called EcoCabins, with general information presented in Table 7. There are three house types with different size and layout (e.g. window and door position), which affects the calculation of heat gain and heat loss on the next chapter. The house is well-insulated, as all surfaces (wall, roof, floor) has insulation layers and the windows

are triple-glazed. More detailed layers and dimensions of the house can be seen in Appendix A.2 and A.3.

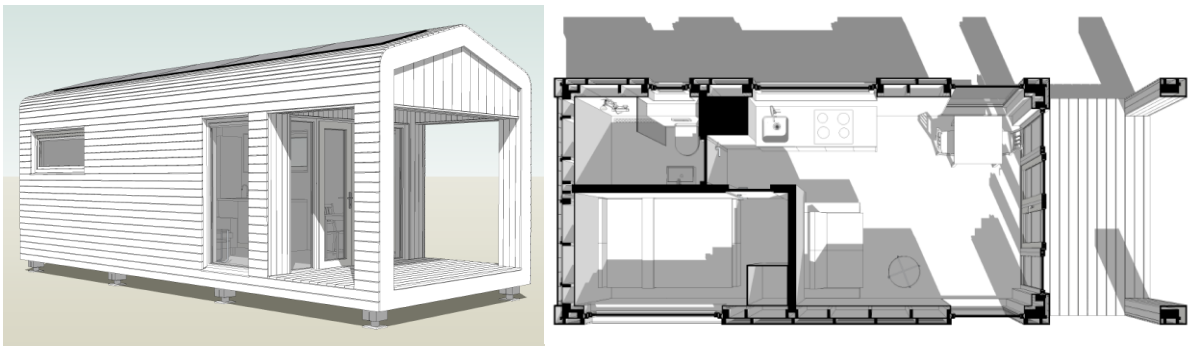

Figure 20. Illustration of exterior and interior the tiny house (EcoCabin TH25)

Table 7. Specifications of the tiny houses

House type	Number of units	Indoor area [m²]	Occupants
TH-25	2	25	1
TH-32	2	32	1
TH-40	2	40	2

3.3 Modelling of Components

To have a clear overview of the calculations done in this study, the energy system components will be explained separately in the next subsections. The components include solar energy generators (PV, PV/T, STC), li-ion battery, heat pump, latent heat storage, and hydrogen storage system (electrolyzer, compressor, hydrogen tank, and fuel cell).

3.3.1 PV, PV/T, STC

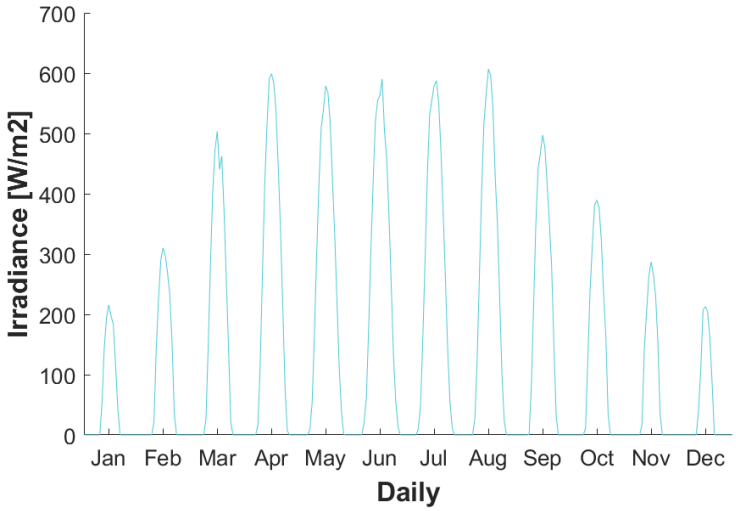

Figure 21. Average irradiance in Enschede, taken from PVGIS 2010-2016 data [6]

Irradiance data is taken from the European Commission's Photovoltaic geographical information system (PVGIS) [59]. The optimum tilt angle in Enschede is 38°, with an azimuth angle of 178°, which is almost completely facing the South. Referring to the mentioned assumptions, the irradiance profile is presented in Figure 21. As expected, the solar irradiance

is high in the middle of the year (summer) and low at the end and beginning of the year (winter). The annual sun irradiation is 1,216.8 kWh/m^2.yr or equal to an average of 3.3 kWh/m^2.day.

In this study, the rated capacity of one PV panel is 360 Wp, with an area of 2 m^2 [60]. The performance of PV systems depends on various factors, both internally and externally, which must be considered when determining the amount of electricity produced. PV performance is usually indicated by a parameter called the performance ratio (PR). It considers the losses that occur due to temperature, soiling, module mismatch, electrical losses, and other losses [61]. These losses are translated into efficiency and are used to determine the electricity produced by PV modules, according to equation (17)-(19) in Appendix A.4 [62]. It was found that PR is 88.25%, while the PV efficiency varies around 20% throughout the year.

Theoretically, the electrical efficiency of PV/T should be higher than that of PV because heat is extracted by the heat transfer fluid below it, which would lower the PV module temperature. However, it is not always the case in actual application, especially if the PV has a glass cover, a low emissivity coating, or anti-reflective coating [46]. Therefore, in this study, the electrical efficiency of PV/T is assumed to be the same as that of PV. On the other hand, the thermal efficiency is lower compared to regular solar thermal collectors. This is because there is a higher emissivity from PV laminate and a lower absorption factor due to the withdrawal of electrical energy in PV/T [46]. Essentially, the advantage of using PV/T is the reduced area that it requires to produce both heat and electricity. It is assumed that the thermal efficiency of PV/T ($\eta_{\text{th,PVT}}$) is 31.81% [63], while STC ($\eta_{\text{th,STC}}$) is 50%.

PV/T and STC are only specific to the second energy system configuration. When the required PV/T area for electricity output exceeds the required heat collecting area, then separate PV modules would be added on top of the PV/T panels. Conversely, when the required heat collecting area exceeds the required PV area for electricity, then separate solar thermal collectors (STC) would be added. Because STC thermal efficiency is higher than that of PV/T, the area required for STC would follow proportionally. This condition of synchronizing between PV/T and STC area is summarized in Appendix A.4.

3.1.1 Lithium-ion battery

Li-ion battery is present in all configurations. In this study, Li-ion battery is viewed from a macro perspective, by evaluating the energy that charges into and discharges from the battery. In all configurations, it is assumed that Li-ion battery has a 93% charge-discharge efficiency (η_{bat}) and operates with 80% depth of discharge (DoD). The self-discharge is only a few percent per month [64]; hence, it is neglected in this study.

The energy stored inside the battery is evaluated on an hourly basis. During charging mode, the energy stored inside the battery is expressed as follow:

$$E_{bat}^{i+1} = E_{bat}^{i} + (P_{prod}^{i} - P_{cons}^{i}) \quad (2)$$

Where E_{bat}^{i} and E_{bat}^{i+1} are the energy stored at hour-i and i+1 respectively, P_{prod}^{i} is the generated power and P_{cons}^{i} is the electricity demand at the corresponding hour. During discharging mode, the formula is the same, but (P_{prod}^{i} - P_{cons}^{i}) are divided by the battery efficiency (η_{bat}), which represents the whole charging and discharging loss. The complete charging and discharging logic of Li-ion battery will be explained later in section 3.4 about the optimization of energy component size because it is related to the whole system.

3.3.2 Heat pump

A heat pump is present in the first and third configuration. It requires work input for its compressor, in the form of electricity. The amount of this electricity demand depends on the heat output (or heat input for cooling mode) and the COP of the heat pump from Table 23 (Appendix A.4). The COP cooling is assumed to be equal to COP heating subtracted by one. The heat output is a combination of space heating (or cooling) and DHW, and is calculated using a series of heat balance equations, according to a temperature control system. The heat balance and control system will be explained in section 3.4.2 and 3.6.

The heat source of heat pump in this study is the ground/soil. Soil temperature's fluctuation is less extreme compared to ambient air. In the winter, the soil temperature is warmer than that of air, while in the summer, it is the opposite, as depicted in Figure 22. That is why the soil is a better heat source than air.

In heating mode, ground acts as the source, while water inside the heater acts as the sink. Conversely, in cooling mode, the ground is the sink, while water inside the cooler is the source. Both ground temperature and water in heater temperature vary every hour; thus, COP also changes accordingly. Equation (20) in Appendix A.4 shows how the heat pump's electricity demand is calculated.

Air conditioner (AC) is basically ASHP that is unable to operate reversibly, so it only acts as a room cooler. Due to this specification, the cost of AC is assumed to be cheaper. The presence of AC is only specific for the second energy system configuration because this configuration does not have any GSHP. They are installed individually in each house. The COP of AC is assumed to be fixed at 2.93.

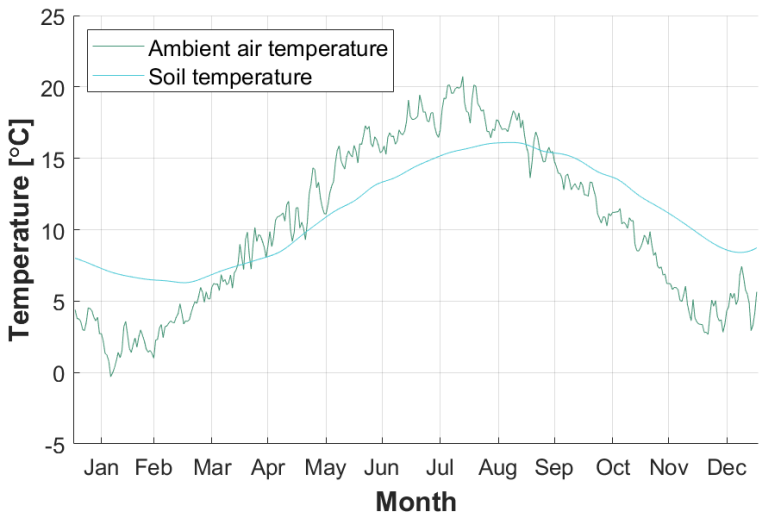

Figure 22. The temperature of ambient air and soil under grass at 1m-depth [31] [119]

3.3.3 Latent heat storage

Latent heat storage is only present in the second configuration. The thermal output of PV/T or STC charges the heat storage, making the temperature increase. The opposite happens when heat is discharged. It is assumed that the working temperature of heat storage is between 40°C to 80°C, which means that below 40°C, the storage is not capable of fulfiling heat demand. In this case, immersion (electric) heater will step in. However, the second configuration's goal is

to not rely on electricity for heat provision; therefore, the fraction of immersion heater use throughout the year is limited up to 1%. The sizing of PVT or STC capacity and latent heat storage must, therefore, comply with this condition. The complete charging and discharging logic of latent heat storage will be explained later in section 3.4.2 about the optimization of energy component size because it is related to the whole system.

The storage capacity of 1 unit of heat storage (Q_{unit}) device is 34.26 kWh, which is estimated using equation (21)-(23) in Appendix A.4. Throughout the storage period, there are some heat losses to the environment that is calculated hourly using equation (24) in Appendix A.4. Finally, the energy stored inside the LHS is evaluated on an hourly basis. During charging and discharging mode, the energy stored inside LHS is expressed as follow:

$$h_{LHS}^{i+1} = h_{LHS}^{i} + (Q_{prod}^{i} - Q_{cons}^{i}) - Q_{loss}^{i} \quad (3)$$

where h_{LHS}^{i} and h_{LHS}^{i+1} are the heat stored at hour-i and i+1 respectively, Q_{prod}^{i} is the generated heat and Q_{cons}^{i} is the heat demand at the corresponding hour. The complete charging and discharging logic of latent heat storage will be explained later in section 3.4.2 about the optimization of energy component size because it is related to the whole system.

3.3.4 Hydrogen storage: electrolyzer, compressor, hydrogen tank, fuel cell

Hydrogen storage is only present in the third configuration. The system is evaluated according to:

- The amount of electricity consumed by electrolyzer to convert water into hydrogen, which is assumed to be fixed at 54.3 kWh/kg H_2 produced [65]. This happens when energy is being charged into the hydrogen storage.
- The amount of electricity consumed by hydrogen compressor to transfer hydrogen from electrolyzer into hydrogen tank. This translates into additional electricity demand that must be provided by PV.
- The amount of electricity produced by the fuel cell to convert hydrogen into water, which is assumed to be 20 kWh/kg H_2 consumed [66]. This happens when energy is being discharged from the hydrogen storage.
- The amount of waste heat produced by fuel cell that could support heat provision for the houses; hence, reducing the burden of heat pump.

It is assumed that the outlet pressure of compressor (P_2) is 200 bar [67], while the inlet is 1 bar. The hydrogen temperature at compressor's inlet (T) is assumed to be 80°C, referring to PEM electrolyzer's operating temperature, 50-80°C [65]. Compressor's overall efficiency (η_{comp}) is assumed to be 85%. The required compression work is calculated using equation (33) in Appendix A.4.

The heat from fuel cell is calculated according to the amount of hydrogen that enters the fuel cell. In a stoichiometric reaction, the number of moles of hydrogen is equal to the number of moles of water produced. But in fuel cell reaction, there is usually remaining 15% of unreacted hydrogen, so the formula to calculate water mass at the end of the reaction is shown by equation (4). Fuel cell's operating temperature is around 80°C, so it is assumed that the water also exits at this temperature. The heat from fuel cell is obtained from equation (5).

$$m_{H2O} = n_{H2O}\, Mr_{H2O} = n_{H2}(1 - 0.15)\, Mr_{H2O} = \frac{m_{H2}}{Mr_{H2}}(1 - 0.15) Mr_{H2O} \quad (4)$$

$$Q_{FC} = m_{H2O}\, Cp_{H2O}\, (80°C - T_{ref}) \quad (5)$$

The hydrogen storage is evaluated in terms of the mass of hydrogen at a given hour (m^i_{H2}). The electrolyzer efficiency (η_e) represents a conversion factor from electricity into hydrogen mass (54.3 kWh/kg), while fuel cell efficiency (η_{fc}) represents a conversion factor from hydrogen mass into electricity (20 kWh/kg). During charging and discharging mode, the amount of hydrogen stored inside the tank is expressed as follows, respectively:

$$m^{i+1}_{H2} = m^i_{H2} + \frac{P^i_{prod} - P^i_{cons} - \left(E^{max}_{bat} - E^i_{bat}\right)}{\eta_e} \tag{6}$$

$$m^{i+1}_{H2} = m^i_{H2} - \frac{P^i_{cons} - P^i_{prod} - \left(E^i_{bat} - E^{min}_{bat}\right)}{\eta_{fc}} \tag{7}$$

where m^i_{H2} and m^{i+1}_{H2} are the amount of hydrogen stored at hour-i and i+1 respectively, P^i_{prod} is the generated power and P^i_{cons} is the electricity demand at the corresponding hour, E^i_{bat} is the energy stored in Li-ion battery at the corresponding hour, E^{min}_{bat} and E^{max}_{bat} are the minimum and maximum energy stored in Li-ion battery. The complete charging and discharging logic of hydrogen storage will be explained later in section 3.4.3 about the optimization of energy component size because it is related to the whole system.

3.4 Optimization of Energy Component Size

The simulation and optimization of energy systems are achieved by building calculation algorithms in MATLAB. In all energy system configurations, it is desired to get the most optimum size of each energy components, to prevent excessive unused energy, efficiency losses, and high cost. To achieve this, firstly, the energy system components are considered as variables, which are divided into independent and dependent variables (see Table 8). Independent variables are set to be varied, and their values affect the dependent variables. For instance, in the first configuration, the Li-ion size is viewed as an independent variable, and is varied from 100 kWh to 10,000 kWh with an interval of 100 kWh. Using iterations, the minimum PV capacity to achieve 100% self-sufficiency can be determined. Therefore, in this case, PV capacity is seen as a dependent variable. Essentially, for any size of storage systems, the energy generator's capacity is increased until the system is fully able to fulfil its own demand without the help of the main grid. This algorithm will be further explained in subsection 3.4.1 to 3.4.2.

Next, finishing the iterations would lead to different sizes of system components, which means that there would be hundreds of configurations. Therefore, the most optimum component size is achieved by minimizing the capital cost. Capital cost is chosen as the parameter because capital costs are usually the highest cost in energy systems. Once this is done, the optimum component size for each energy system configurations are obtained, and they can be compared with each other for further analysis.

Table 8. Variables in each energy system configuration

Parameter	**1st configuration**	**2nd configuration**	**3rd configuration**
Variables	• PV capacity • Li-ion size	• PV, PV/T, STC capacity • Li-ion size • LHS size	• PV capacity • Li-ion size • H_2 storage
Control variable	Self-sufficiency: 100%	Self-sufficiency: 100%	Self-sufficiency: 100%
Independent variable	Li-ion size: 100 – 10,000 kWh	LHS: • Seasonal	Li-ion size: 15 - 105 kWh PV size: 36 - 54 kW

		• Daily: 50 – 300 kWh Li-ion size: 100 – 10,000 kWh	
Dependent variable	PV capacity	PV, PV/T, STC capacity	Size of H_2 tank. Rated capacity of: • Electrolyzer • Compressor • Fuel cell

3.4.1 Sizing of PV and Li-ion

If Li-ion battery is present in a configuration without the presence of hydrogen storage, the algorithm on Figure 54 (Appendix A.5) takes place. This algorithm is adapted from a previous study by Ghussain et al. [62]. When electricity produced (P_{prod}) by PV is greater than the demand (P_{cons}), the system will charge the battery if there is still remaining space left ($E_{bat}^{i} < E_{bat}^{max}$). Otherwise, the energy excess (electricity) would be sent to the main grid (D_{excess}). Conversely, when P_{prod} is less than P_{cons}, the system would discharge the battery if there is still energy contained in it. When energy inside the battery at a given hour (E_{bat}^{i}) is insufficient to provide for the demand, the system would then draw electricity from the grid (D_{grid}). However, in this study, the goal is to not draw any electricity from the main grid; thus, the energy components must be sized accordingly.

The minimum capacity (E_{bat}^{min}) of the battery is assumed to be (1-DoD)× E_{bat}^{max}, while the charging and discharging efficiency are combined into one variable, η_{bat}. D_{RES} represents the electricity demand that is met using the energy system. After simulating for a whole year, the fraction of demand that is fulfiled by the energy system (F_{RES}) is calculated using the following equation.

$$F_{RES} = \frac{D_{RES}}{P_{cons}} \tag{8}$$

To achieve 100% self-sufficiency, the value of F_{RES} must be 1. If the F_{RES} is less than 1, then the number of PV panels (represented by their area, A) shall be added until the power supply is enough, and the algorithm reaches F_{RES} 1. The PV area when F_{RES} reaches one is then used to calculate the PV capacity (PV_{cap}). This PV capacity will be considered as the most optimum for the given battery size. These steps are done for various sizes of battery, in order to find the combination with the least capital cost.

3.4.2 Sizing of PV/T and latent heat storage

If latent heat storage (LHS) is present in a configuration, two approaches are considered in varying the PV/T and heat storage size combinations; the first one has the goal of minimizing PV/T panels because the available area is limited, while the second one has the goal of minimizing heat storage size because commercial latent heat storage is quite expensive. The minimum heat storage size is taken from the day with the longest night and the highest heat demand, which was found to be 110 kWh. The minimum PV/T area required can be estimated according to the yearly heat demand and sun irradiation, using the following equation. The minimum PV/T area found was 74 m^2.

$$\text{A PVT } [m^2] = \frac{\text{Heat demand per year [Wh/yr]}}{\text{Irradiation [Wh/m}^2\text{]} \times \eta_{th}} \tag{9}$$

In both approaches, the algorithm on Figure 55 (Appendix A.5) takes place. When heat produced (Q_{prod}) is greater than the demand (Q_{cons}), the heat output from PV/T or solar thermal collectors (STC) would be transferred into the LHS until it reaches its maximum temperature (T_{max}). Otherwise, the excess heat would be wasted (D_{waste}). Conversely, when Q_{prod} is less than Q_{cons}, the system would first check if the storage temperature at hour-i (T^i) is above its minimum working temperature (T_{min}). If it is, then heat would be discharged from the storage; otherwise, the electric immersion heater would step in. However, as mentioned in section 3.3.3, However, in a configuration with LHS, the goal is to not rely on electricity for heat provision. Therefore, the fraction of immersion heater use throughout the year is limited up to 1%.

The heat storage is evaluated in terms of the energy contained, using the enthalpy value at a given hour (h^i_{LHS}). Because temperature affects the charging and discharging mode of heat storage, one needs to estimate the storage temperature. This can be done by a calculation based on the storage enthalpy and the heat capacity ($C_{p,s}$ and $C_{p,l}$). There are three possibilities of PCM phase, which are completely solid ($h^i_{LHS}<h_s$), a mix of solid and liquid ($h_s<h^i_{LHS}<h_i$), and completely liquid ($h^i_{LHS}>h_i$), as depicted in Figure 53 (Appendix A.4). Each phase requires a different formula to calculate its temperature, as follows:

$$T = \begin{cases} \dfrac{h_{LHS}}{C_{p,s} m_{PCM}}, \text{if } h^i_{LHS} < h_s \\ T_{melt}, \text{if } h_s < h^i_{LHS} < h_l \\ \dfrac{h_{LHS} - h_l}{C_{p,l} m_{PCM}}, \text{if } h^i_{LHS} > h_l \end{cases}$$

3.4.3 Sizing of PV, Li-ion, and hydrogen storage

If Li-ion battery and hydrogen storage are both present, there are three variables: PV capacity, battery size, and hydrogen storage size. The Li-ion battery size is varied from 15 kWh to 105 kWh with an interval of 15 kWh. For each battery size, the PV capacity is varied from 100 panels (36 kWp) to 150 panels (54 kWp). Finally, the minimum hydrogen storage tank size to achieve 100% self-sufficiency is calculated. The sizing algorithm is shown in Figure 56 (Appendix A.5). In the case of both charging and discharging energy, the system prioritizes the short-term storage first, followed by the long-term storage. For example, when electricity produced (P_{prod}) by PV is greater than the demand (P_{cons}), the system would charge the Li-ion battery until it reaches its maximum capacity (E^{max}_{bat}). Otherwise, the system would charge the hydrogen storage. If the hydrogen storage is also full (m^{max}_{H2}), the excess electricity would finally be sent to the main grid (D_{excess}). Conversely, when P_{prod} is less than P_{cons}, the system would discharge the Li-ion battery first until it reaches the minimum capacity (E^{min}_{bat}), followed by the hydrogen storage.

The goal here is also to achieve an F_{RES} of 1 by adding the number of PV panels. At the end of the algorithm loop, one can determine the PV capacity based on the area, as well as the electrolyzer, compressor, and fuel cell capacity based on the maximum hydrogen rate that passes through each device.

Once the explained algorithm is finished, one can find out the additional electricity demand to operate the compressor, so the P_{cons} is recalculated, and the whole algorithm loop takes place again. Furthermore, as mentioned in section 3.3.4, one needs to take into account the heat released by fuel cell as a byproduct. This heat will be used to support the heat pump in providing heat for the house. The amount of heat will then be subtracted from the heat pump

output, and the electricity input into the heat pump will be reduced. Once again, this means that the total electricity demand needs to be recalculated, and the algorithm loop is conducted again. This iteration loop is presented in Figure 57 (Appendix A.5).

3.5 Energy Demand

Generating energy demand profile is an important step in this study because it is the base of all component sizing calculations. Energy demand is unique for every system, depending on its location, climate, and even economic condition. For instance, in developing countries, the use of dishwater is uncommon, so electricity demand is lower than in developed countries. To understand the system clearly, energy demand in this study is divided into two types, which are heat and electricity. Both types of demand will be detailly explained in the next subsections. In all the three energy system configurations, we start with determining the heat demand first, followed then by the electricity demand. This is because the heat (and cooling) demand affects the electricity demand of heat pump (in the first and third configuration) and air conditioner (in the second configuration).

3.5.1 Heat Demand

In this subsection, both heating demand for room and DHW, as well as cooling demand for the room, will be discussed. Space heating and cooling demand are based on heat balance, affected by various parameters such as ambient temperature and building material. The DHW demand is obtained from available data, but a heat balance is still required to determine the DHW heat profile throughout the year. Each of these demands will be explained in the next subsections. The overall heating and cooling demand in this study are depicted in Figure 23. The annual heat demand for DHW and space heating of six tiny houses are 9,907 kWh and 19,076 kWh. The annual cooling demand for space is 5,634 kWh (extracted heat).

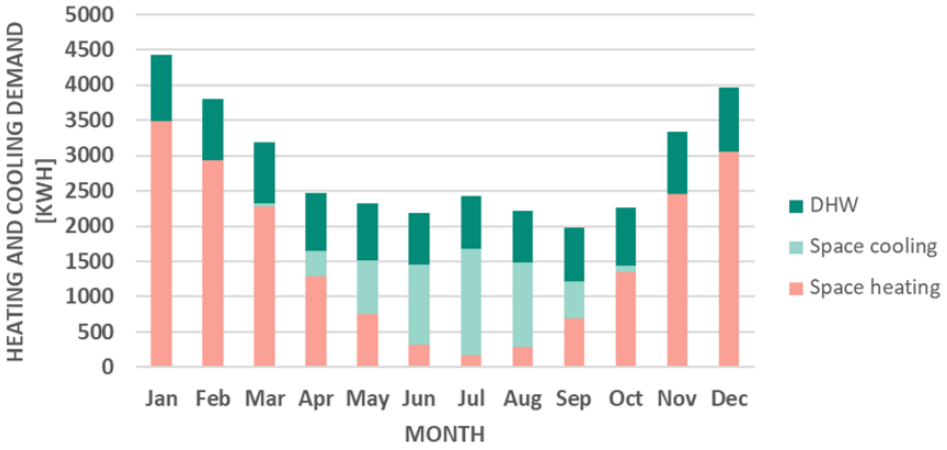

Figure 23. Overall heating and cooling demand for six tiny houses

3.5.1.1 Heat Balance of Room

The heat balance of rooms is calculated using the following equation. The derivation of this equation is explained in Appendix A.6.

$$\frac{dT_{in}}{dt} = \frac{1}{V_{room}\,\rho_{air}\,Cp_{air}}\left[\left((UA)_{rad}(T_h - T_{in}) + \frac{dQ_{rad}}{dt} + \frac{dQ_{pla}}{dt}\right) - ((UA)_{floor} + (UA)_{window} + (UA)_{wall} + (UA)_{roof} + 1.2\ ACH\ V_{room})(T_{in} - T_{out})\right] \quad (10)$$

Equation (10) shows that heater temperature and outdoor ambient temperature are variables that affect the indoor temperature. The parameters that affect the indoor temperature are the size of the room (V_{room}) and the air mass inside it, the thermal properties of house's material, the surface area of the house, and the thermal properties of radiators. The outdoor temperature varies every hour throughout the whole year and is depicted in Figure 24.

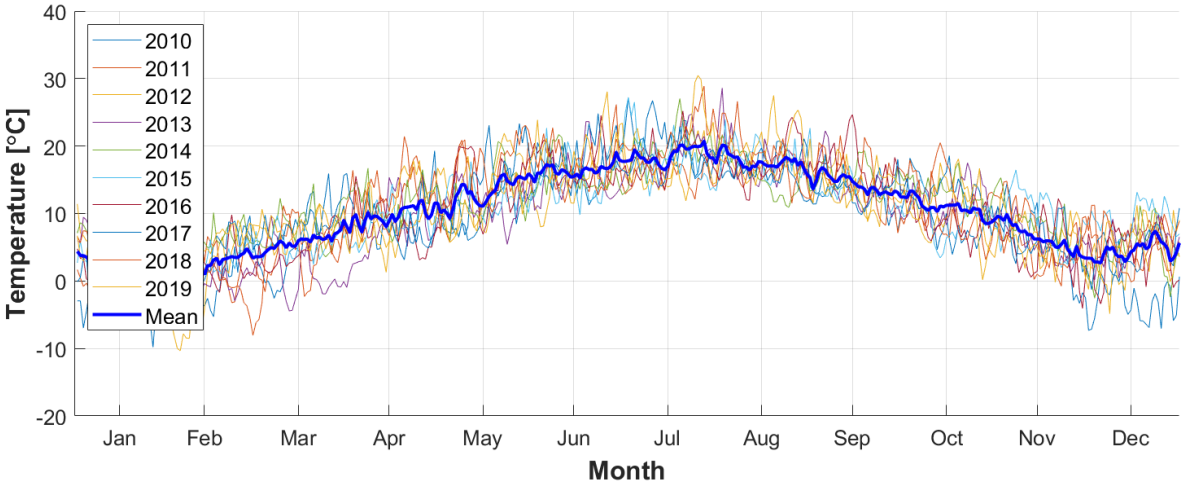

Figure 24. Daily average temperature of Twenthe region [31]

3.5.1.2 Heat Balance of DHW Tank

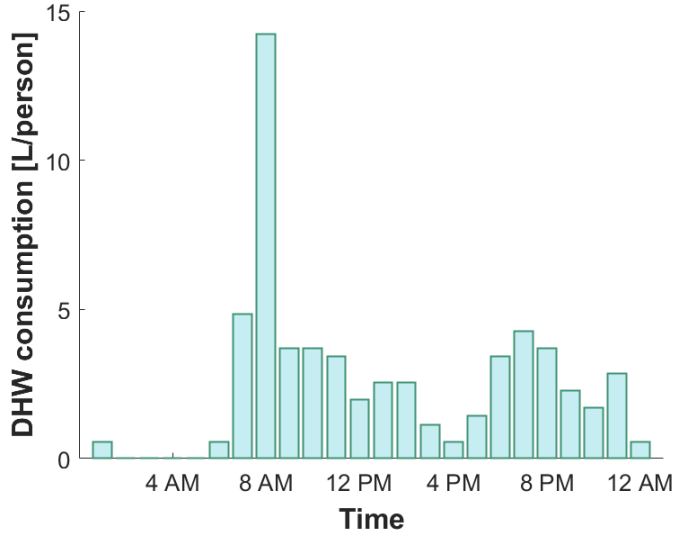

Figure 25. Hourly DHW consumption in a day

According to Edwards et al. [68], there are four DHW consumption patterns in households, namely predominantly morning, predominantly evening, predominantly late night, and dispersed throughout the day. In this study, the predominantly morning pattern is chosen because the houses are located on the campus, so it is assumed that the occupants have to start their daily activity in the morning. The typical DHW temperature is between 50°C to 60°C.

As mentioned in section 3.1.1, DHW tanks are present to ensure continuous availability. Generally, one person would require 50L of DHW tank [69]. Based on this reference, houses with eight occupants would need a 400L-tank. In this study, two 200L DHW tanks are in place. The heating medium is also water, and it runs through the heating coil, as depicted in Figure 26. The water inside the coil comes from the system's heater, such as a heat pump.

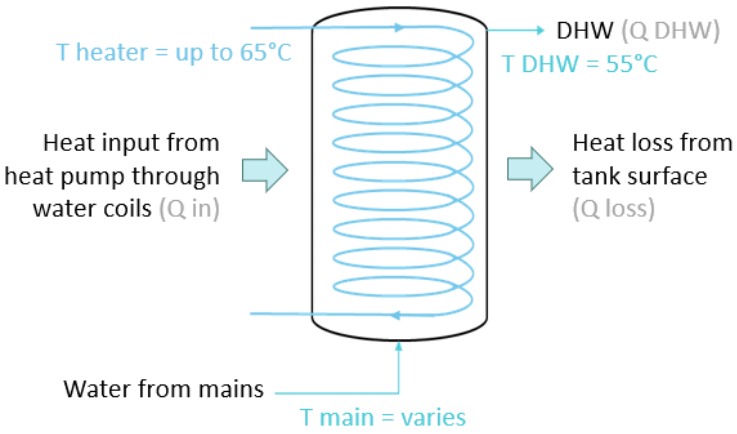

Figure 26. DHW tank

The heat balance of DHW tanks is calculated using the following equation. The derivation of this equation is explained in Appendix A.6.

$$\frac{dT_{water}}{dt} = \frac{1}{V_{tank}\,\rho_{water}\,Cp_{water}}[Q_{in} - \dot{m}_{DHW}\,Cp_{water}\,(T_{DHW} - T_{mains}) - (UA)_{tank}\,(T_{DHW} - T_{out})] \quad (11)$$

3.5.2 Electricity Demand

The base electricity demand is for the purposes of lighting, cooking, and appliances (not including heater and air conditioner). In addition, there is a demand for charging one electric vehicle (EV) is also considered. According to Bloomberg New Energy Finance (BMEF), EV will make 10% of global passenger vehicle sales in 2025, with that number rising to 28% in 2030 and 58% in 2040 [70]. Therefore, at least one EV is considered in this study as a load. However, EV is not considered as additional energy storage in this study. The demand for DHW and space heating's circulation pump, as well as for PV/T circulating pump, are neglected.

The base demand profile is obtained from NEDU in collaboration with other parties, namely Energie Data Services Nederland (EDSN), Essent/RWE, Nuon/Vattenfall, and Eneco [71]. Tiny houses in this study are occupied by one or two people. The average base demand per year for a one-person and two-person households are 1,825 kWh and 2,860 kWh, respectively [72]. Therefore, the annual base electricity demand for six tiny houses with eight inhabitants is 13,020 kWh, topped by 1 EV demand of 4,051.5 kWh.

It is assumed that the campus EV is used to travel around the University of Twente (UT) campus daily. One round of trip at the campus is about 7.3km, and the car travels six round trip every day, so the total distance is about 44km. It is claimed that the Renault Zoe EV has the ability to travel about 300km using a 52-kWh battery [73]. Referring to this data, a 44km trip would require 7.4 kWh of energy. With a 3.7-kW charger, the EV would need to be charged for 2 hours per day. It is assumed that the EV is scheduled to be charged at 02:00 a.m. every day, when the base demand is at its lowest. Figure 27 shows the average daily base and EV demand profile with the explained assumptions. The peak is 3.7 kW, which happens when EV is charged.

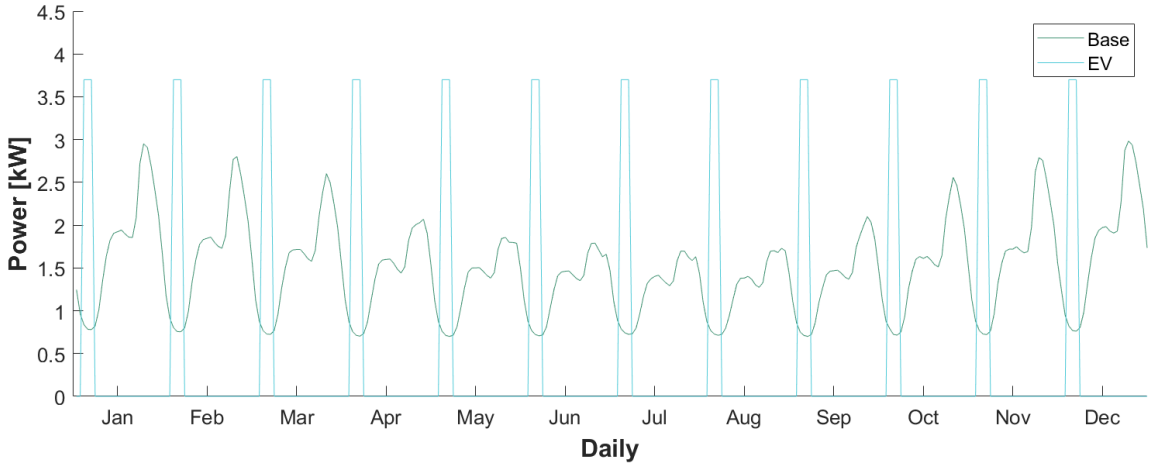

Figure 27. Base and EV electricity diurnal demand profile of six tiny houses in the Netherlands

In the first and third energy system configurations, the heating system uses GSHP; thus, it needs work input in the form of electricity. This means that there is an additional electricity demand for heat pump, on top of the base and EV demand, as depicted in Figure 28. The annual electricity demand for the heat pump that covers six houses heat demand is 8,205 kWh.

In the second energy system configuration, the heat pump is absent because heating demand is provided by PV/T and heat storage. However, cooling demand is fulfiled by an air conditioner (AC), so there will be additional electricity demand for this unit. The annual electricity demand for air conditioner of six tiny houses is 1,915.2 kWh. The electricity components for each configuration is summarized in Table 9.

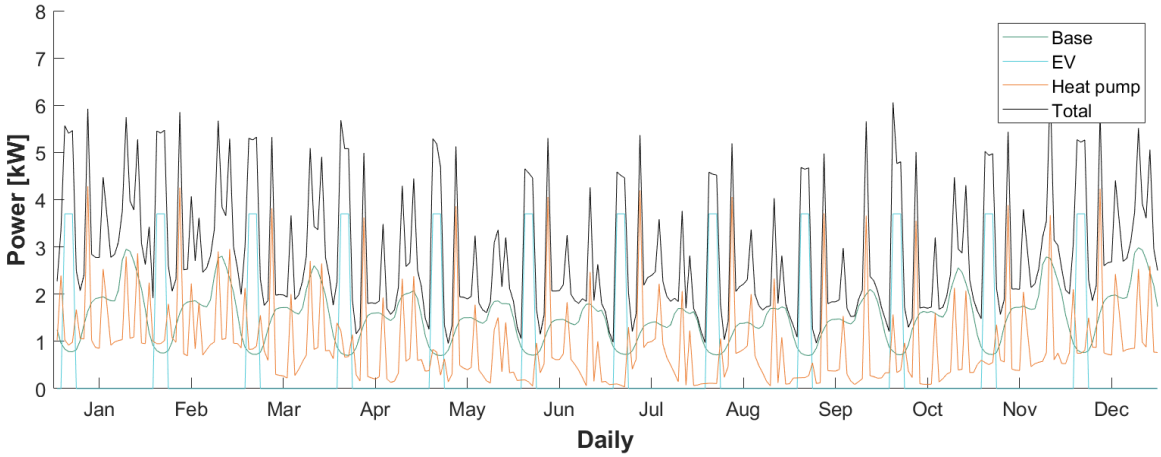

Figure 28. Base, EV, and heat pump demand profile of six tiny houses in the Netherlands

Table 9. Components that consume electricity in each energy system configurations

Component	**1st configuration**	**2nd configuration**	**3rd configuration**
Base (cooking, lighting, appliances)	Yes	Yes	Yes
EV	Yes	Yes	Yes
Heat pump	Yes	No	Yes
Air conditioner (AC)	No	Yes	No
Hydrogen compressor	No	No	Yes

3.6 DHW and Room Temperature Control Strategies

3.6.1 Room temperature control

There are two indoor temperature control strategies considered in this study, which are the on-off control that supplies heat intermittently, and the proportional–integral–derivative (PID) control that supplies heat continuously. According to Saleh & Mosa [74], a PID control strategy results in less indoor temperature fluctuation compared to the on-off strategy, as depicted in Figure 29. According to Oughton & Hodkinso [75], the human body is sensitive to temperature variations of more than 5% in short periods, which means that the on-off control would not give the desired level of comfort. If the temperature fluctuation limit of on-off control is reduced, it would increase the frequency of heater's on-off mode, and thus reduce its reliability. The PID control is, therefore, chosen for this study. However, it is worth to mention that the cumulative energy consumption of the two control strategies is actually similar [74].

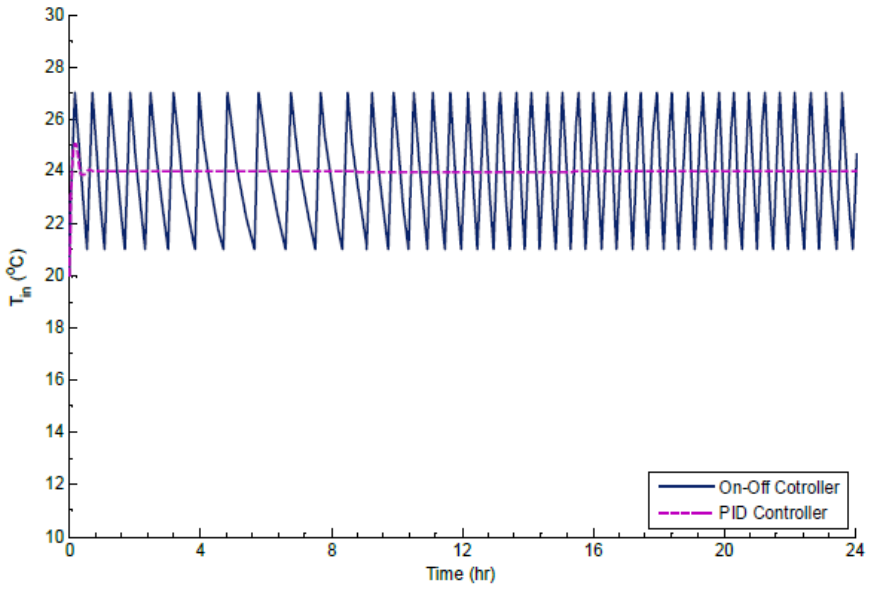

Figure 29. Effects of on-off and PID control strategies on indoor temperature [12]

The PID control loop is presented in Figure 30. Simulink is used to model the room temperature according to equation (10), with a set point indoor temperature of 21°C at 05:00 – 23:00 and 18°C at 23:00 – 05:00. The setpoint is lower during the night to save some energy, which is a common recommendation. Assuming that the occupants are sleeping in blankets during the night, this strategy would not disturb their level of comfort. Figure 31 shows a 2-day sample of room temperature profile during the winter. The end result of this model is the amount of heat that needs to be supplied by the heater throughout the year.

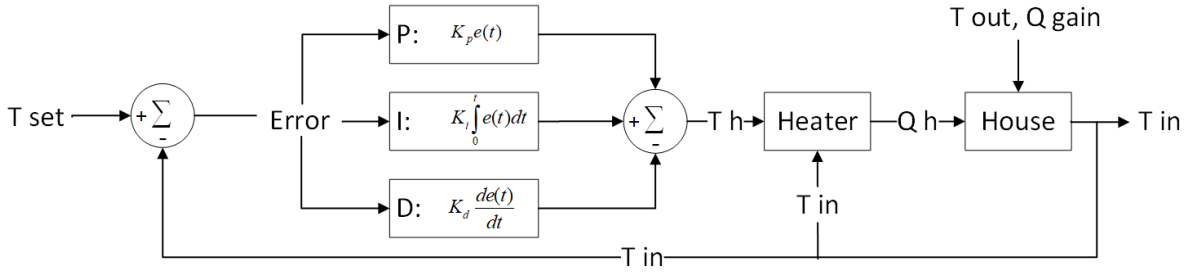

Figure 30. Closed-loop PID control system for room temperature

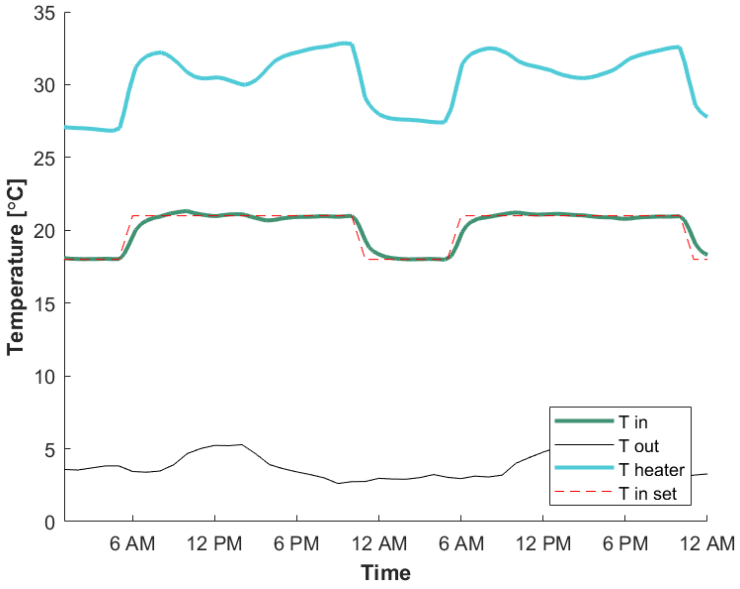

Figure 31. A data sample of room temperature profile of EcoCabin TH25 based on controlled heating in the winter

3.6.2 DHW temperature control

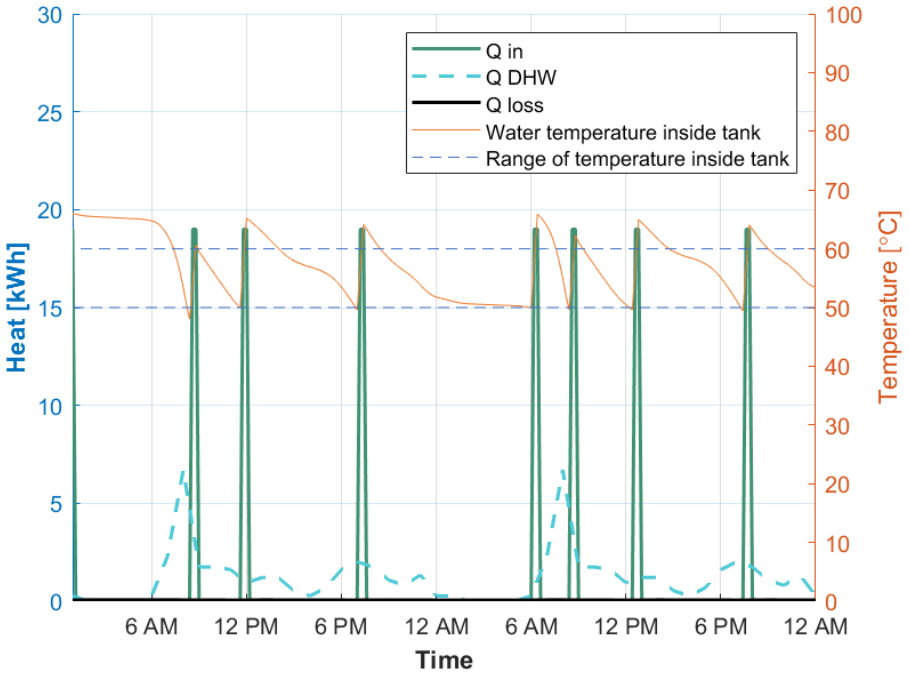

Figure 32. A data sample of DHW load and water temperature inside tank for six tiny houses

Unlike the space heating system, the DHW system uses on-off control because we would not want the DHW heater to operate continuously, as the heat pump also needs to provide heating and cooling for room. This is possible because DHW tanks are present, which means that the heat is kept inside the tanks. When water temperature inside the tank reaches below 50°C, the tank will be heated up until the temperature reaches 60°C. Above that, the heater will turn off. The same cycle takes place once the temperature reaches below 50°C again. Figure 32 shows the DHW load profile based on equation (11) and the explained control strategy. Q in is the heat entering the DHW tank, Q DHW is the heat required to increase the temperature of water from mains to the target DHW temperature, Q loss is the heat loss from DHW tank to the environment. The end result

of this control simulation is the amount of heat that needs to be supplied for DHW throughout the year.

3.7 Cost Model

The costs of systems are evaluated based on their present value, using a parameter called net present cost (NPC). NPC represents all the costs incurred over a system's lifetime, subtracted by its revenue. The cost in this study includes capital cost (CC), replacement cost, operation & maintenance (O&M) cost, while the revenue includes salvage value (SV) at the end of the period (year-n) and the feed-in tariff [76]. The CC, replacement cost, and O&M cost used in this study are shown in Table 28 (Appendix A.9). In this study, the period considered is 20 years, and the annual interest rate (r) is 8% [11]. Formula (15) shows how NPC is calculated.

$$\mathrm{NPC} = \mathrm{CC} + \left(\sum_{t=1}^{n} \frac{\mathrm{ACost}}{(1+\mathrm{r})^{t}}\right) - \frac{\mathrm{SV}}{(1+\mathrm{r})^{n}} \tag{12}$$

Where n is the evaluated period expressed in a number of years and ACost is the annual cost minus annual revenue.

The feed-in tariff refers to the Dutch SDE+ scheme, so the value received is a function of various parameters, such as PV rated capacity, the phase of SDE+ application, and the maximum load hours per annum [77]. Referring to this guide, it is estimated that the feed-in tariff for a PV system is 0.074 €/kWh.

The salvage value of a component at the end of its lifetime is assumed as zero, so the value of them in the middle of its lifetime follows proportionally. For instance, if the capital cost of a 1-kW PV system with a 25-year lifetime is €890, then its salvage value after ten years of operation is (25-10)/25*890, or equal to €534.

Most of the capital costs are simply obtained according to the price per kW or per kg in literature, except for compressor. The capital cost (CC) of a compression system includes the compressor itself and auxiliary components such as cooling and control system. It is estimated according to a reference hydrogen compression system with a capacity (Q_{ref}) of 50 kg/h, pressure ratio (r_{ref}) of 30, and outlet pressure (P_{2ref}) of 200 bar. The formula is as follows [78].

$$\mathrm{CC\ compressor} = A\left(\frac{Q}{Q_{ref}}\right)^{a} + B\left(\frac{Q}{Q_{ref}}\right)^{b}\left(\frac{P_2/P_1}{r_{ref}}\right)^{c}\left(\frac{P_2}{P_{2ref}}\right)^{d} \tag{13}$$

The first term refers to the site cost, which is neglected in this study. The second term refers to the compression system cost, which will be used to estimate the compressor capital cost in this study. Q is the compressor's capacity in kg/h, P_1 and P_2 are compressor's inlet and outlet pressure respectively. The rest coefficients are presented in Appendix A.9.

The economic feasibility is evaluated using a term called levelized cost of energy (LCOE), which represents the cost of energy production by dividing NPC with the energy produced throughout the energy system's lifetime. The amount of energy produced is either self-consumed (D_{RES}), sent to the grid (D_{excess}), or wasted (D_{waste}). This study focuses on the amount of energy produced that is self-consumed, so instead of dividing the NPC with the total energy production, we divide NPC by D_{RES}. The equation to calculate LCOE is shown below.

$$\mathrm{LCOE} = \frac{\mathrm{NPC}}{\sum_{t=1}^{n} \frac{D_{RES}}{(1+r)^t}} \tag{14}$$

LCOE will be divided into the cost of heat and the cost of electricity because, in the residential utilities, they have different costs. To divide between these two, the energy components shall be categorized into heat and electricity, so the costs are distributed accordingly. Table 29 in Appendix A.9 shows the categorization between the two.

Chapter 4

Results and Discussions

In this chapter, section 4.1 explains about the optimum component size and the comparison between each configuration. All component sizes are for a total of six houses. Next, the energy flow and operations are discussed in section 4.2, in order to understand the energy losses, energy excess, how the energy demand is fulfiled, and how the storage capacity utilization is. The economic analysis, covering NPC and LCOE, is then discussed in section 4.3. Lastly, section 4.4 gives an overview of the whole performance of the energy system, so a conclusion can be made.

4.1 Optimum Component Size

In the first energy system configuration, different combinations of PV capacity and Li-ion battery size can be installed to reach the goal of 100% self-sufficiency. Smaller Li-ion battery size means that it acts as a daily or short-term storage, while larger size means it acts as long-term storage. The capital cost was calculated for these different combinations.

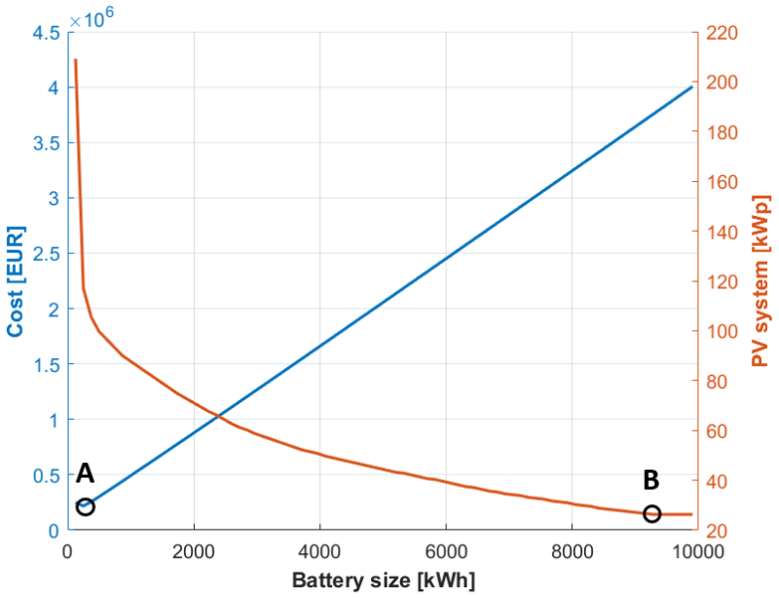

Figure 33. Configuration 1: Relation between Li-ion battery size and PV system (100% self-sufficiency), along with the total capital costs

In Figure 33, the orange line shows that the amount of PV reduces exponentially with increasing battery size. This trend is similar to the result of Weniger's et al. [79] research, shown on Figure 34 (a); however, this graph only shows the trend for 10% to 80% self-sufficiency instead of 100% self-sufficiency. To get a better comparison, a graph for these self-sufficiencies was created, shown in Figure 34 (b). It can be observed that both graphs have the same tendency; the degree of self-sufficiency saturates with a larger PV system size. This is because there is more excess energy or PV surplus that is not consumed by the system. The same tendency of saturation is also observed with larger battery size because the large-sized battery is only partially discharged during the night; hence, there is still remaining energy in the next day [79]. These tendencies also apply to 100% self-sufficient system, as depicted in Figure 33.

In Figure 33, the blue line shows that there is a slight decrease of capital cost from a battery size of 124 kWh to 248 kWh. This is because the PV capacity required for a 124-kWh battery is significantly higher than that of 248 kWh (209 kWp versus 117 kWp). After this minimum point (point A), the capital cost goes up linearly. This shows that above 248 kWh battery, the PV capacity reduction is not very significant, so the battery price will be the primary parameter that drives the cost.

(a)

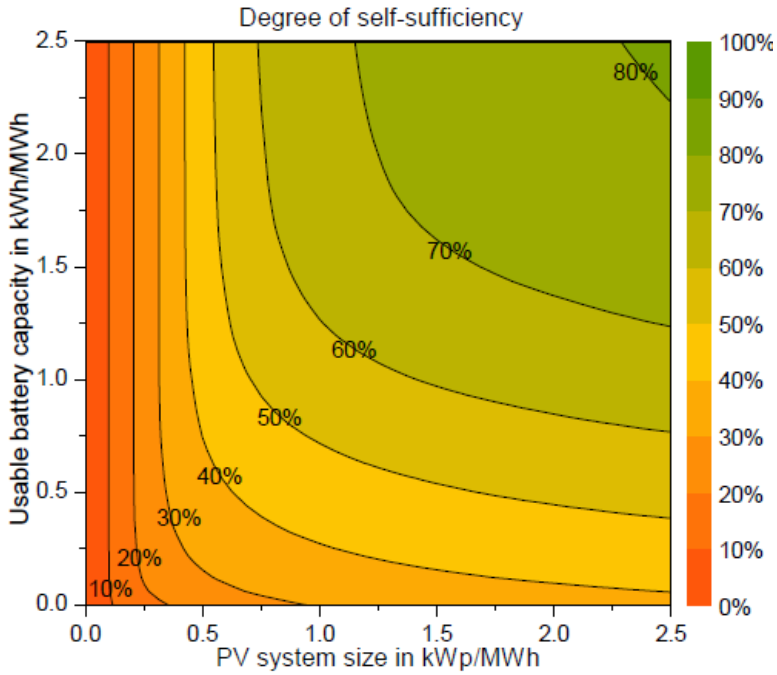

(b)

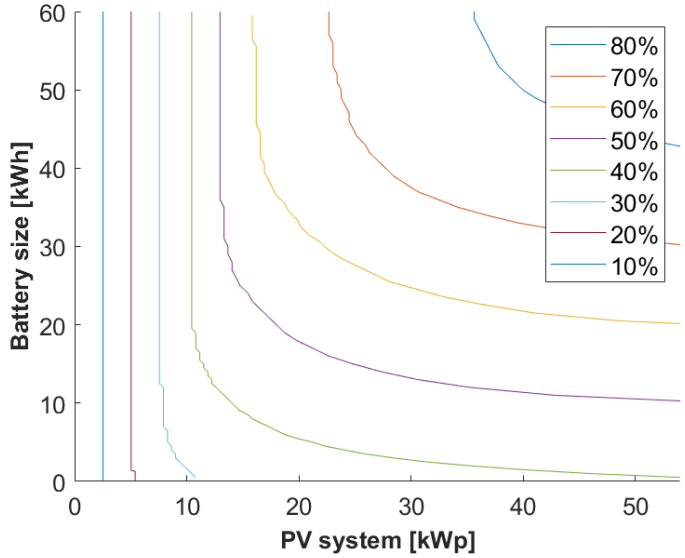

Figure 34. Annual degree of self-sufficiency for various PV system and battery size by (a) Weniger et al. [10] and (b) in this study

It needs to be highlighted that 117 kWp of PV system for six houses is quite large, requiring an area of 650 m^2. In this study, however, the land acquisition cost is not considered because the tiny houses evaluated are assumed to be located inside the University of Twente campus.

It is possible to reduce the PV capacity down to 26.3 kWp (point B in Figure 33); however, the compromise is a very large Li-ion battery size, around 9,000 kWh. This results in a very expensive capital cost (€3.76 million). With very large Li-ion battery size, we would also need a more sophisticated cooling system, which would increase the cost even more. Therefore, the chosen combination of the first energy system configuration is the one that shows minimum capital cost (€217,117), with 248 kWh Li-ion battery and 117 kWp PV system. This configuration will be used for further analysis of energy flow and economic feasibility.

Table 10 shows the comparison between configuration 1 with another study that is similar, consisting of PV and battery to power several houses in a Malaysian village. However, the battery type used in the Malaysia case is Lead-acid instead of Li-ion. The electricity demand for the reference is about twice as much as this study, but it requires smaller PV and battery size. As a result, the excess electricity of the reference study is lower, 37.5% from the produced electricity. There are two main reasons for this, which are the location and the degree of self-sufficiency. Malaysia is located around the equatorial area; thus, the sun intensity throughout the year is relatively stable. The lowest average monthly solar irradiation in Kuala Lumpur, Malaysia is 136 kWh/m^2, while in Enschede, it is 18 kWh/m^2 [59]. This significant difference allows Malaysia's case to have smaller PV and battery sizes. In addition, as displayed in Table 10, the average daily irradiation in Kuala Lumpur is also 1.5 times higher than the Netherlands. Due to these facts, the Malaysia case does not require large PV and battery sizes to fulfil the demand. Secondly, the self-sufficiency in the reference study is less than 100%. As explained in the previous paragraph, the degree of self-sufficiency saturates with a larger PV system size. Therefore, increasing the degree of self-sufficiency from 97.9% to 100% would require a large addition of PV size.

Table 10. Comparison of configuration 1 with another study

Parameter	**This study, Netherlands case – conf.1**	**Malaysia case** [6]
PV [kW]	117	62
Battery size [kWh]	248	72
Electricity production [kWh]	123,764	102,605
Electricity loss [kWh]	2,446 (2.0%)	14,985 (14.6%)
Electricity demand [kWh]	25,621 (20.7%)	49,125 (47.9%)
Self-sufficiency	100%	97.9%
Excess electricity [kWh]	95,697 (77.3%)	38,495 (37.5%)
Average daily irradiation [kWh/m^2.day]	3.3	4.8

As explained in section 3.4.2, there are two approaches in designing the heating system for the second energy system configuration, which are (1) to use PCM as short-term (daily) heat storage system with a consequence that the PV/T area will be large, and (2) to use PCM as long-term (seasonal) heat storage. For the daily heat storage system, the storage size is varied from 50 to 300 kWh to see how much PV/T area is required to achieve at least 99% of heat provided without immersion heater (F_{TH}). Figure 35 shows that the required PV/T area to achieve the same F_{TH} increases for a smaller size of heat storage. We can even observe that a heat storage size of 50 kWh and 100 kWh are not capable of achieving the targeted F_{TH}. Therefore, this leaves us with a choice of 150-300 kWh heat storage size. At 99% F_{TH}, the PV/T area for 150 kWh, 200 kWh, 250 kWh, and 300 kWh battery are 520 m^2, 500 m^2, 480 m^2, and 480 m^2 respectively. The capital cost of LHS and PV/T for these four options were calculated and presented in Figure 36. The positive slope shows that the increased size of LHS

more dominantly affects the cost compared to PV/T. The lowest cost is shown by a combination of 150 kWh LHS and 520 m^2 PV/T; therefore, this is chosen to be compared with the second approach of using LHS as seasonal storage. The size comparison is shown in Table 11.

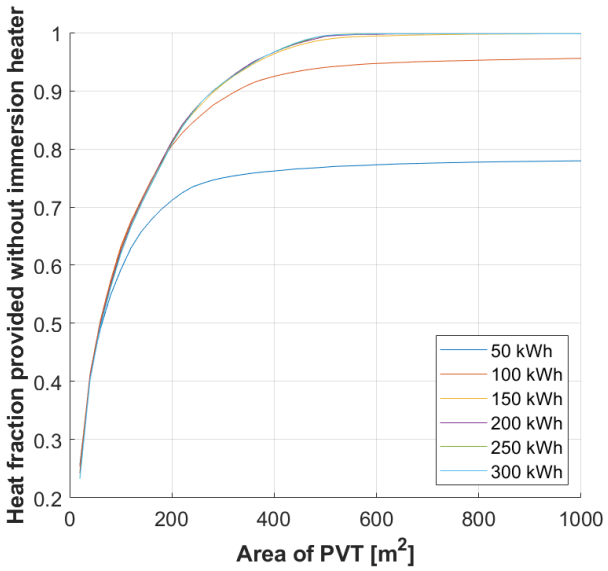

Figure 35. Configuration 2: The effect of different heat storage and PV/T sizes towards the heat fraction provided without immersion heater

After obtaining the data in Table 11, the total capital cost of the system is then evaluated, including the electrical components (li-ion battery) and other components (DHW tank, air conditioner). As explained in section 3.3.1, when the required PV area required for electricity exceeds the required heat collecting area, then separate PV modules would be added on top of the PV/T panels. Conversely, when the required heat collecting area exceeds the required PV area for electricity, then separate solar thermal collectors (STC) would be added. It needs to be noted that STC thermal efficiency is higher than that of PV/T, so the area required would follow proportionally. The result is presented in Figure 37.

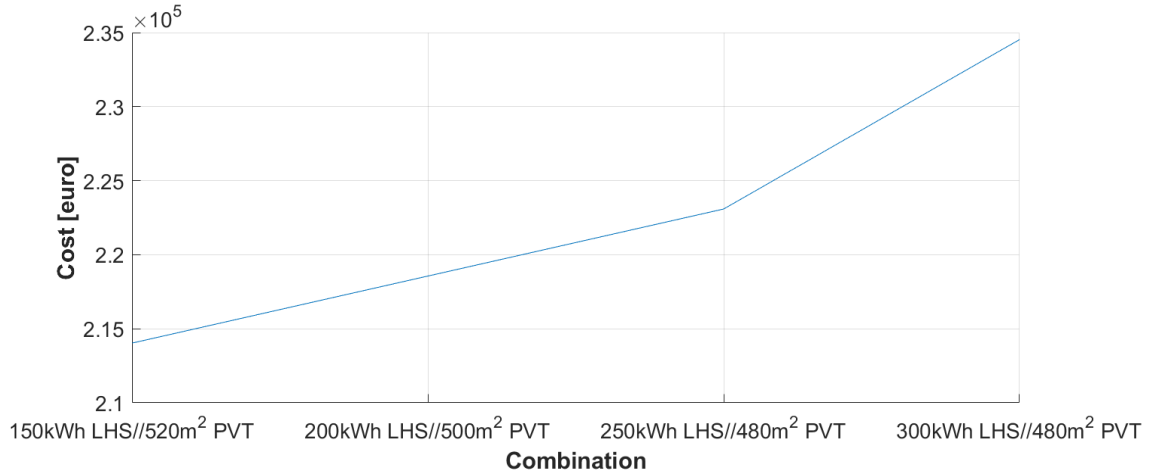

Figure 36. Configuration 2: The capital cost of different PV/T and daily LHS combinations

Table 11. Comparison of two approaches in heating system component combination in the second energy system configuration

Parameter	**1st approach: PCM as daily heat storage**	**2nd approach: PCM as seasonal heat storage**
Amount of PCM [ton]	1.2 (150 kWh)	201 (12616 kWh)
PV/T heat collecting area [m^2]	520	74.7

One can observe Figure 37 and see that the minimum capital cost is significantly higher for the second approach (€3 million), which uses PCM as seasonal heat storage. Although the

area of PV/T and STC required for the first approach is notably higher than the second approach, the overall cost is still cheaper. This is because the cost of PCM heat storage is still very expensive. Although the cost of SAT material itself is not high (up to €11.84/kWh [80]), the cost of the actual unit of heat storage is high due to the sophisticated control system. As explained in section 2.2.4, the supercooling nature of SAT needs to be well-controlled. In addition, a large aspect of the technology is still under development and not widely commercialized yet, so it might need a few years for learning curve and economy of scale to achieve a lower price. In conclusion, the first approach of using PCM as daily heat storage is chosen for further analysis of energy flow and economic feasibility. The minimum capital cost for this approach is €263,910 (point C); that is when the battery size is 163 kWh, PV/T area is 440 m^2, and STC area is 51 m^2.

(a)

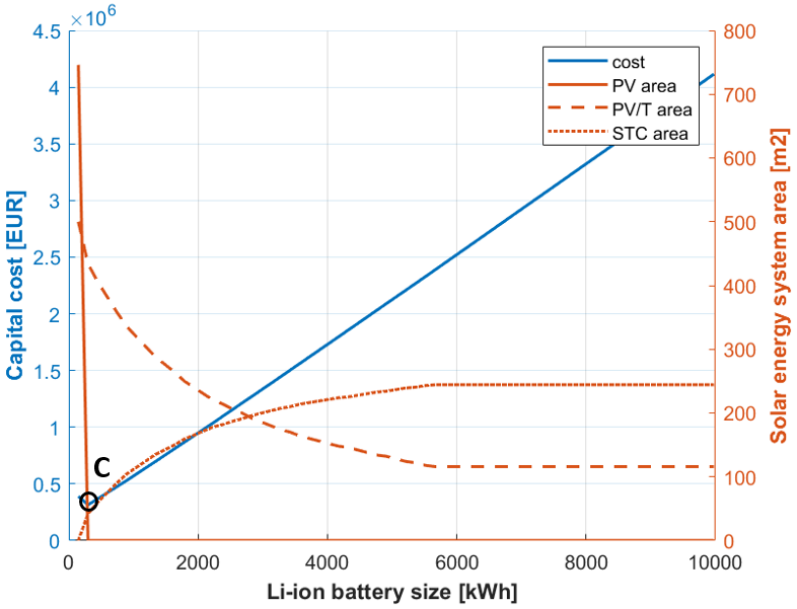

(b)

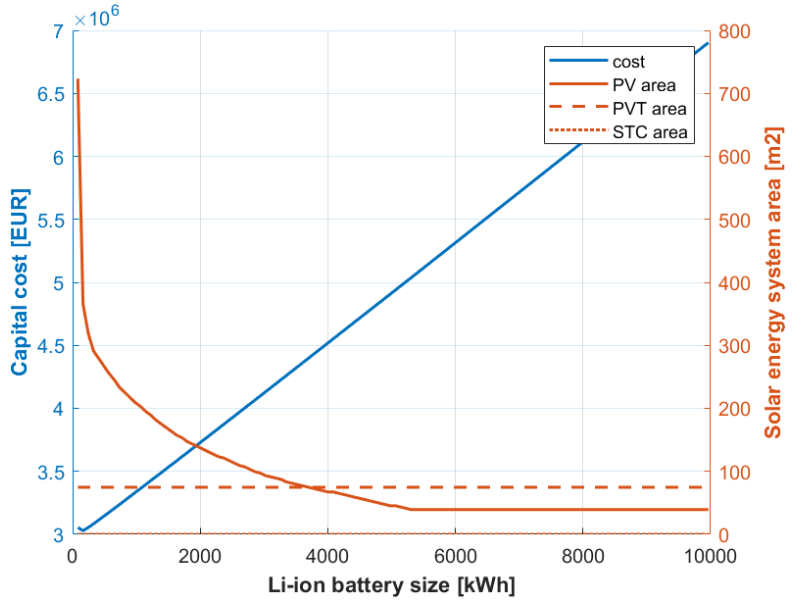

Figure 37. Configuration 2: Relation between Li-ion battery size and PV/T system, along with the total capital costs, using (a) daily heat storage and (b) seasonal heat storage

In Yumrutaş and Ünsal's study [81], it was shown that a system in Gazientep, Turkey with 12,222 kWh/year heat demand requires 20 m^2 of STC and 300 m^3 of underground hot water tank storage (HWTS) with a heat pump to be 83% self-sufficient [14]. In this study, the heat demand is 28,983 kWh, which is about twice as high as the Turkey case. However, the heat storage size in this study is significantly smaller (1.2 m^3) because this study uses latent heat technology, while the Turkey case uses sensible heat technology. The STC area in the Turkey case is significantly smaller than this study because the HWTS only acts as a heat source for the heat pump to improve the COP. The study did not mention the requirement of PV size to operate the heat pump itself. In addition, the Turkey case can only fulfil 83% of the demand, while this study fulfils 100% of the demand.

In the third energy system configuration, the size of Li-ion battery and PV are varied to obtain the required hydrogen tank capacity that fulfils 100% energy self-sufficiency. Figure 38 (a) shows that the required hydrogen tank capacity gets larger with smaller PV capacity because the system can store more amount of energy in the summer and discharge it in the winter. If the hydrogen tank size is smaller, then the system requires more PV panels to store energy into Li-ion battery during days with low solar irradiation. The figure also shows that at the same PV capacity, a larger size of Li-ion battery results in a smaller hydrogen tank size requirement because they complement with each other. However, above 75 kWh, it is apparent that the reduction in hydrogen tank capacity is insignificant.

After obtaining the variation of these components' sizes, the capital cost of Li-ion battery, PV, and hydrogen tank can be calculated to determine which combination is the least expensive. Figure 38 (b) shows that the cost consistently increases with larger hydrogen tank, even though the PV capacity reduces. This means that the increase of hydrogen tank size is more dominant than the reduction of PV capacity. We can continue to increase the PV capacity to achieve lower cost, but the area required would be too large. Therefore, a limit was set for the third configuration; it is assumed that each house can only have a maximum PV capacity of 54kW (150 panels). It is understood that the first and second configuration has larger PV or PV/T capacity, but in the third configuration, we need to take into account the space required for the hydrogen tanks. At this PV size, the lowest cost is shown by a 75kWh Li-ion battery size, as depicted on point D (€205,233) in Figure 38 (b). Therefore, the chosen third configuration component size is 54 kW PV, 75 kWh Li-ion battery, and 142.8 kg hydrogen tank.

Table 12 shows the comparison between configuration 3 with other similar studies. The hydrogen tank size is much larger in this study, compared to the East Malaysian case, because Malaysia's sun intensity is relatively stable throughout the year, hence, seasonal storage is not essential for this system. The battery size between the two are similar, but the PV size of the East Malaysian study is larger simply because the electricity demand is also higher.

The amount of produced electricity in the Saudi Arabia case is about one-third of this study, but the PV size is nine times smaller, and the hydrogen tank size is significantly smaller. There are two possible reasons for this, which are location and electricity demand profile. As displayed in Table 12, Saudi Arabia has the highest average daily irradiation compared to the other two cases. Like in the Netherlands, solar irradiation is highest in the middle of the year and lowest in the beginning and at the end of the year. However, the lowest average monthly solar irradiation in Riyadh, Saudi Arabia is 134 kWh/m^2, while in Enschede, it is 18 kWh/m^2 [59]. This significant difference allows Saudi Arabia's case to have smaller PV and battery sizes. Secondly, the electricity demand profile in the Saudi Arabia case is not explained, so it is possible that the electricity load is dominant during the day. If the load is kept low during the night, then the system does not need large sizes of PV and hydrogen tank. In the case of Saudi

Arabia, there are no batteries present; thus, the demand during the night is always fulfiled by hydrogen storage through a fuel cell. This is possible to do; however, fuel cell's lifetime depends on its operating hours. Therefore, the fuel cell in the Saudi Arabia case might need to be replaced more frequently compared to this study.

(a)

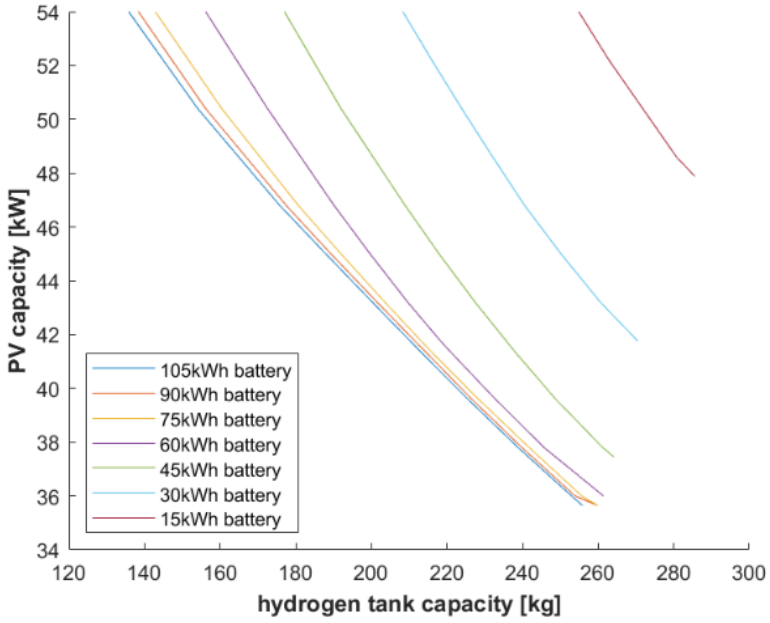

(b)

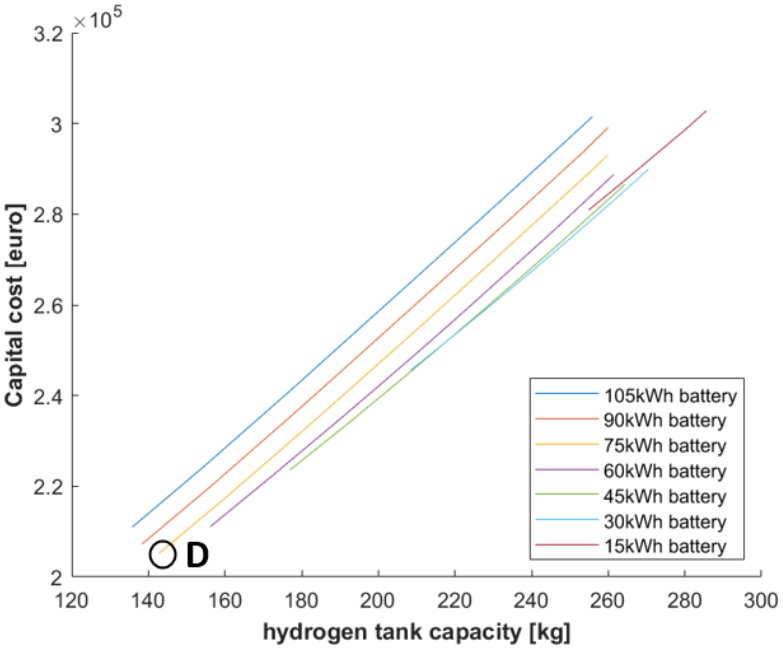

Figure 38. (a) Relation between hydrogen tank capacity with PV capacity for different battery size and (b) the capital cost of PV, battery, hydrogen tank

Table 12. Comparison of configuration 3 with other studies

Parameter	**This study, Netherlands case – conf.3**	**East Malaysia case** [6]	**Saudi Arabia case** [82]
PV [kW]	54	71	6
Battery size [kWh]	75	72	0

Hydrogen tank size [kg]	143	2	7
Electricity production [kWh]	44,174	102,755	14,629
Electricity demand [kWh]	39,661	56,734	14,629
	8.7 kW peak	20.85 kW peak	
Self-sufficiency	100%	98.2%	100%
Average daily irradiation [kWh/m².day]	3.3	4.8	5.6

The summary of size and capital cost of all configurations is presented in Table 13. One can compare seasonal electricity storage using hydrogen (configuration 3) with seasonal heat storage using PCM (configuration 2). It was explained that seasonal heat storage using PCM would result in a capital cost starting around €3 million, while hydrogen storage starts around €200,000. In fact, the hydrogen storage covers both heat and electricity demand (through a heat pump), while PCM storage only covers the heat demand. The cost difference is due to the large amount of PCM required for seasonal storage, and commercial LHS technology is still quite expensive. Table 28 shows that the capital cost of LHS is 229 €/kWh, while hydrogen tank is 890 €/kg. Assuming that hydrogen lower heating value (LHV) is 33.3 kWh/kg and hydrogen storage round-trip efficiency is 36.8%, the cost of hydrogen tank is 73 €/kWh; thus, it's about three times cheaper. Therefore, it is more preferred to opt with hydrogen for seasonal energy storage, instead of LHS. If the seasonal heat storage uses sensible heat technology (e.g. BTES, ATES, etc.) and the energy system scale is larger, then there is a chance that this solution is more cost-competitive, because this type of setup has been installed in several neighbourhoods [14].

Table 13. Summary of component size and capital cost of all energy system configuration*

Component	**Unit of size**	**1st configuration: PV – Li-ion - GSHP**		**2nd configuration: PV/T – Li-ion - LHS**		**3rd configuration: PV - Li-ion - H_2 storage - GSHP**	
		Size	**Capital cost [€]**	**Size**	**Capital cost [€]**	**Size**	**Capital cost [€]**
PV	kW	117 (650 m²)	104,130			54 (300 m²)	48,060
PV/T	m²			440	152,064		
STC	m²			51	8,601		
Li-ion	kWh	248	99,185	163	65,425	75	30,038
Electrolyzer	kW					34	33,701
Compressor	kg/h					1	36,457
Hydrogen tank	kg					143	127,135
Fuel cell	kW					9	30,901
Heat pump	kW	24	9,887			17	5,476
Air conditioner	unit			6	2,334		
Ground coils	unit	1	2,750			1	2750
DHW tank	L	2x200	1,165	2x200	1,165	2x200	1,165
LHS	kWh			150	34,320		
Total	**€**		**217,117**		**263,910**		**315,682**

**Capital cost already considers subtraction from government subsidy*

After the size of all components are selected, one can evaluate the area required for solar energy system, as well as the volume required for other energy components. The power density and energy density for these components are shown in Appendix A.7.

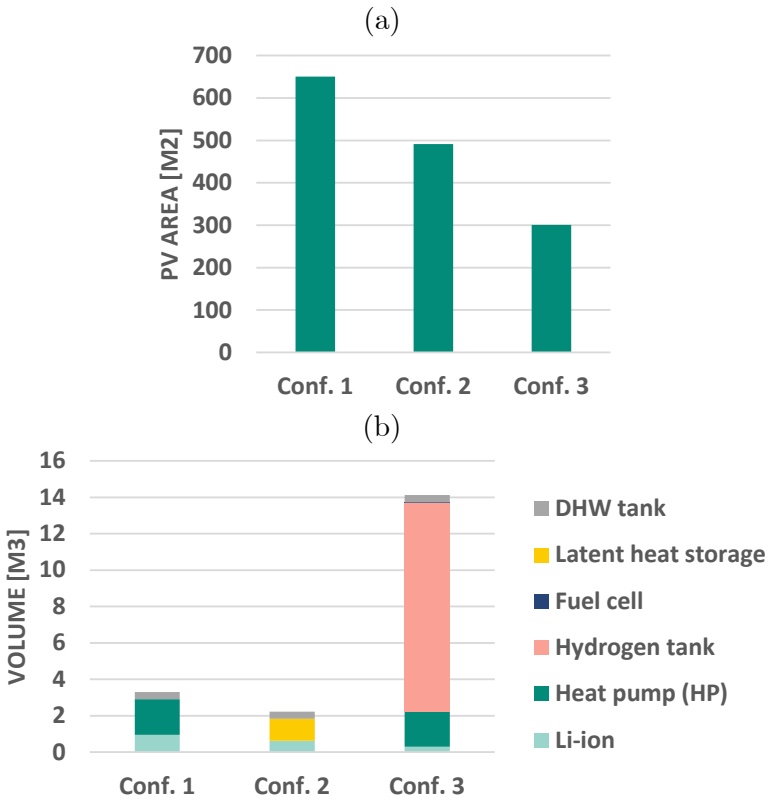

Figure 40. The required PV or PV/T (a) area and the (b) volume of energy components of all energy system configurations

Figure 40 shows that the PV area reduces from configuration 1 to 3. The third configuration requires the least amount of PV due to the presence of hydrogen storage that acts as seasonal storage. It is capable of storing excess electricity produced during the summer and discharge it during the winter; thus, the PV capacity is not excessive. In the case of daily electricity storage such as the first and second configuration, the system requires a large amount of PV during days with low solar irradiation, to ensure that there is enough electricity for the house during the night. Therefore, relying on daily-sized batteries for 100% self-sufficiency would result in a large PV capacity requirement. Lastly, PV/T technology allows the second configuration to have a smaller solar energy generation area compared to the first configuration.

In all configurations, it is estimated that the houses' roofs are not wide enough to accommodate the PV area, because the floor area of all houses is 194 m^2. This means that PV panels have to be installed on the ground or other areas besides the houses' roofs. Looking at the area around the planned location, it is possible to place the PV at the car parking area (Figure 39), even for the first configuration that requires an area of 650 m^2. It needs to be noted that the actual area during installation would be larger than 650 m^2, but there is still some remaining area left around the car parking area.

Figure 39. Possible area for PV installation

In terms of component volume, the largest is shown by the third configuration because of the hydrogen storage system, especially the hydrogen tank (11 m^3). It is possible to reduce the tank's

volume if the storage pressure is higher. However, this study already assumes a pressure of 200 bar, which is typically used for hydrogen tank.

In the first configuration, the component volumes comprise of Li-ion battery (1 m^3), heat pump (2 m^3), and DHW tanks (0.4 m^3). In the second configuration, the component volumes comprise of Li-ion battery (0.6 m^3), LHS (1.2 m^3), and DHW tanks (0.4 m^3). It is still possible to distribute some components inside each house, but it is recommended to install a small building unit for these utilities. In the third configuration, however, it is clear that the components must be placed in a designated space, such as a 20ft (6.1 m) container. The area and volume of components will be considered in the final selection of energy system configuration on section 4.4.

4.2 Energy Flow and System Operation

The optimum sizes of each configurations' components have now been determined. Simulations using MATLAB were carried out, and the overall energy flow is analyzed. Figure 41 shows the comparison of energy production and consumption in all configurations.

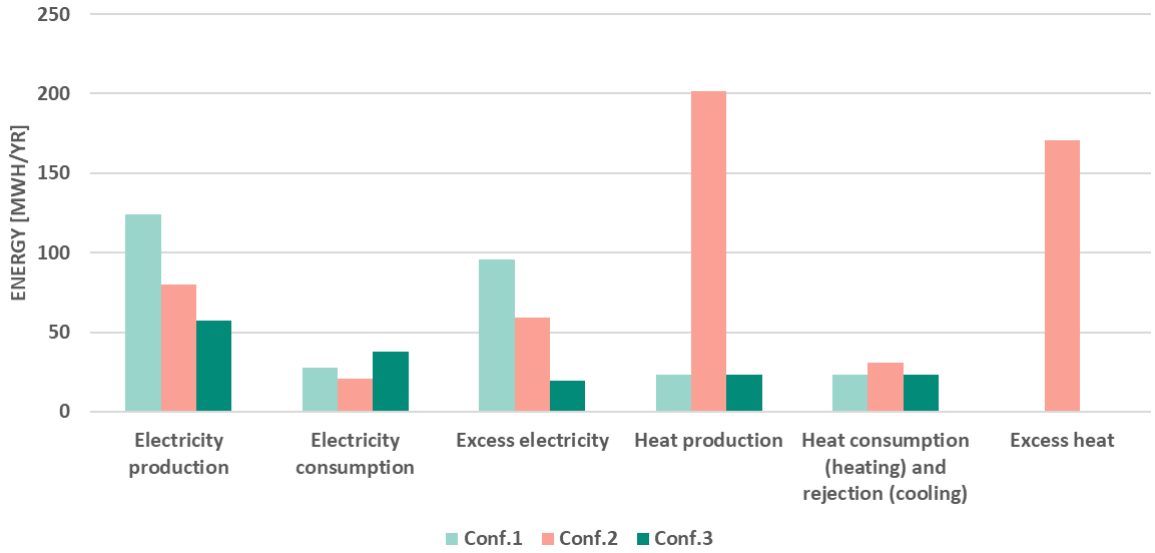

Figure 41. Comparison of energy production and consumption in all configurations

One can observe that in all cases, electricity production is always higher than the actual consumption, which results in excess electricity. In the case of grid-connected houses, this is still tolerable because the excess can be injected into the grid and homeowners receive certain revenue. However, in stand-alone houses, the excess electricity will just go to waste. This excess in production is the result of using the intermittent solar energy to provide 100% of the energy demand. The sizing of these systems is in such a way that the system can still fulfil the demand even on the darkest day.

There are some variations in electricity consumption because there are different electrical components in each configuration. The second configuration has the lowest electricity consumption because it does not use an electric-based heater for the houses, as opposed to the first and third configuration. The first configuration shows 33% higher electricity consumption compared to the second configuration due to the use of a heat pump. Meanwhile, the third configuration has a higher electricity consumption compared to the first configuration because the hydrogen storage system requires additional electricity input for the compressor and to compensate for the roundtrip losses of hydrogen storage.

In the case of electricity, the first configuration shows the highest production excess, mainly due to the fact that it uses a daily-sized Li-ion battery. In days with low sun irradiation, the houses require a lot of PV panels to catch the amount of energy used during the night. However, this size of PV panels would produce excess electricity in days with high solar irradiation, such as summer. This occurrence is best explained in Figure 42.

Figure 42 (a) shows the SoC of battery, electricity production and consumption in the winter (20^{th} – 26^{th} of December). The sun irradiation in day 1 is very low that electricity production is also low. During this day, the battery cannot be charged as much as other days, so the SoC is further reduced during the night and the next day. If the size of PV is reduced, then the battery would be charged even less, and it would not be able to fulfil the demand during the night or the next day.

On the other hand, with this size of PV, there is a high excess of electricity produced during the summer (1^{st} – 7^{th} of August). Figure 42 (b) shows that electricity production is significantly higher than the demand, and the battery is charged up to its maximum capacity every day. Although the second configuration also uses daily-sized Li-ion battery, the electricity consumption is lower, resulting in smaller PV capacity and lower production excess.

The third configuration shows the lowest electricity excess due to the presence of hydrogen storage that acts as seasonal storage. It is capable of storing excess electricity production during the summer and discharging it during the winter. In conclusion, relying on daily-sized batteries for 100% self-sufficiency would result in a large PV capacity requirement, resulting in excessive production at certain times.

Figure 43 (a) shows that the Li-ion battery is only charged with a small amount of energy because the sun irradiation is very low. However, it is not an issue because, during those days, hydrogen storage is being discharged to fulfil the electricity demand. In Figure 43 (b), one can observe that there is less excess electricity compared to the first configuration because it is being charged into the hydrogen storage.

In the case of heat, the consumption of the second configuration is observed to be more than the first and third. This is due to the presence of LHS. Although insulated, LHS would still have a small amount of heat losses to the environment, especially if the LHS size is large.

Furthermore, excess heat production is only observed in the second configuration. This is because the first and third configurations use a heat pump, which is essentially an electric-based heater. The heat pump only operates when there is a heat demand; hence, the production is equal to the consumption. The second configuration uses the thermal output of PV/T and STC, equipped with LHS, to provide heat. Therefore, the excess in heat production is also due to the use of the intermittent solar energy.

The reason behind high excess heat production is the same as in the case of electricity, which was explained in previous paragraphs. Figure 44 (a) was made according to winter days. It shows that the heat production on day 1 is low that the heat storage goes down to the minimum useful temperature (40°C), so the immersion heater is turned on briefly in day 2. The heat production is also low on day two that immersion heater is turned on again. This only happens during the day with the lowest irradiation, and the fraction of immersion heater supply is only less than 1% throughout the year. After day 2, however, the heat production is sufficient, and all demand is fulfiled by either the PV/T or the LHS. This shows that the PV/T has been sized appropriately to fulfil at least 99% of the heat demand. If PV/T size is reduced, then the frequency of immersion heater operation would be even more. On the other hand, Figure 44

(b) shows that the heat production is much more than the demand in the summer, which is why there is a lot of excess heat.

(a)

(b)

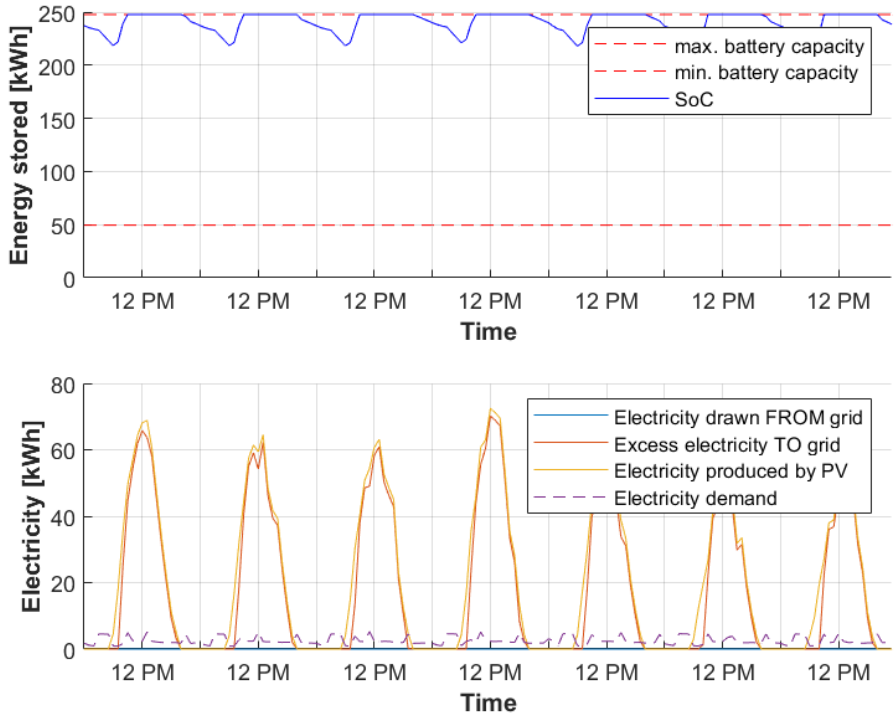

Figure 42. Configuration 1: Interaction of electricity supply and demand, along with Li-ion battery SoC during the winter (a) and the summer (b) for seven days

(a)

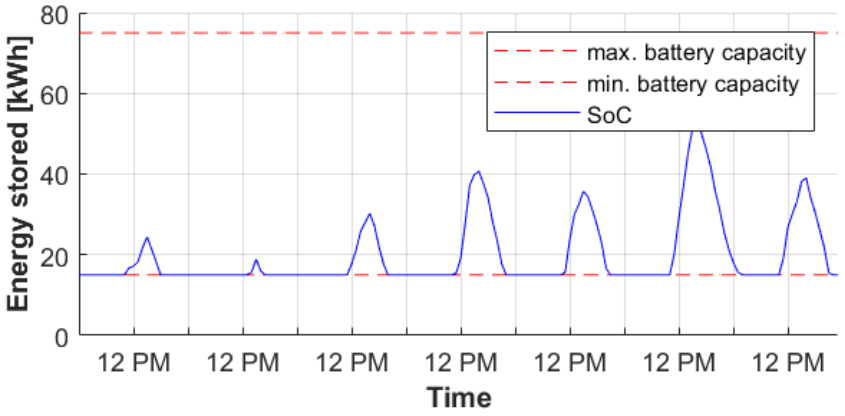

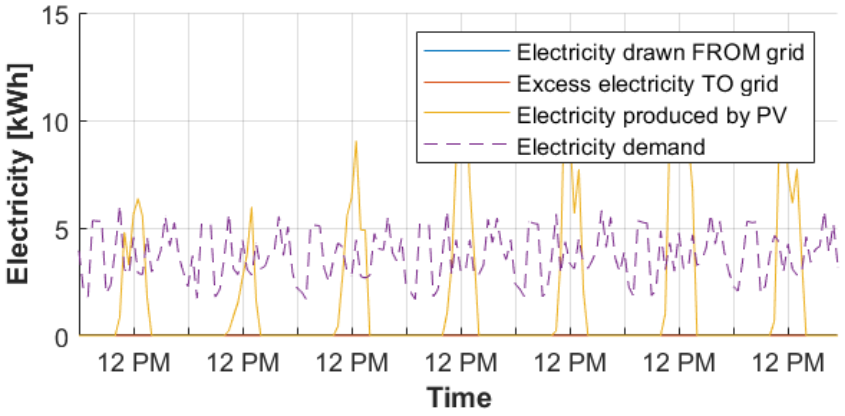

(b)

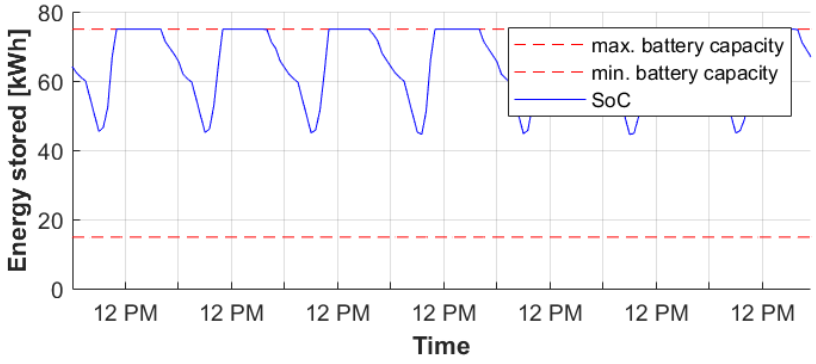

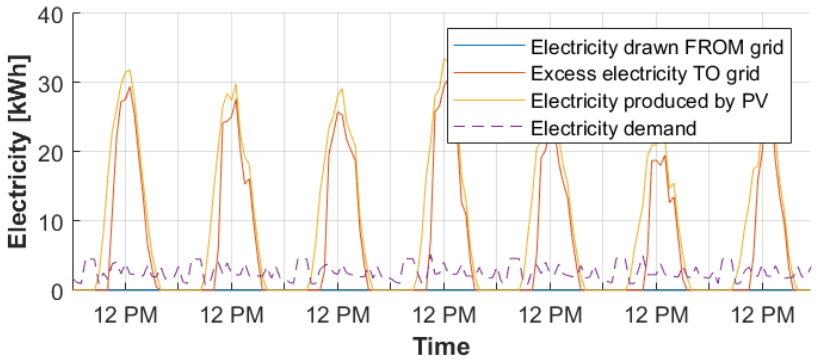

Figure 43. Configuration 3: Interaction of electricity supply and demand, along with Li-ion battery SoC during the winter (a) and the summer (b) for seven days

(a)

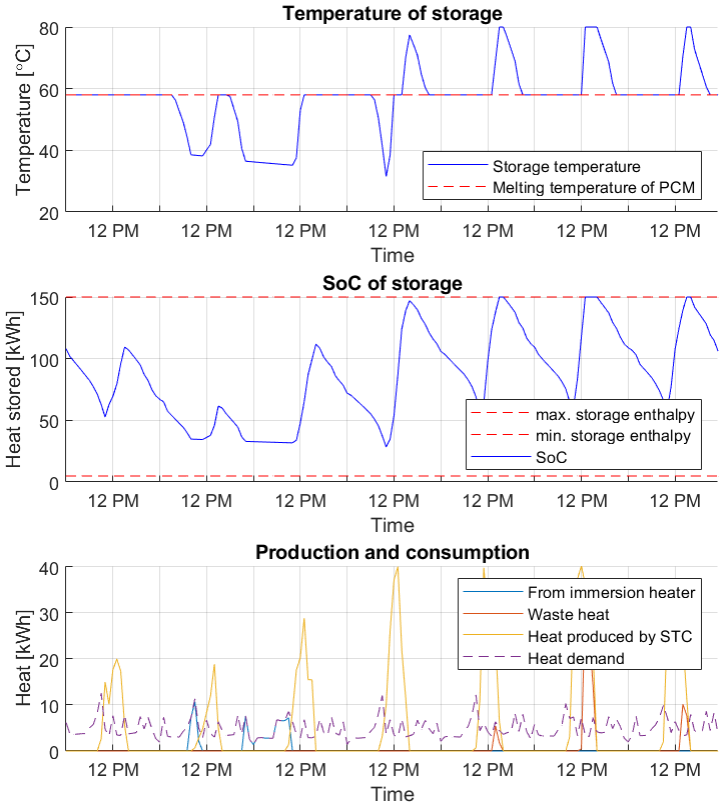

(b)

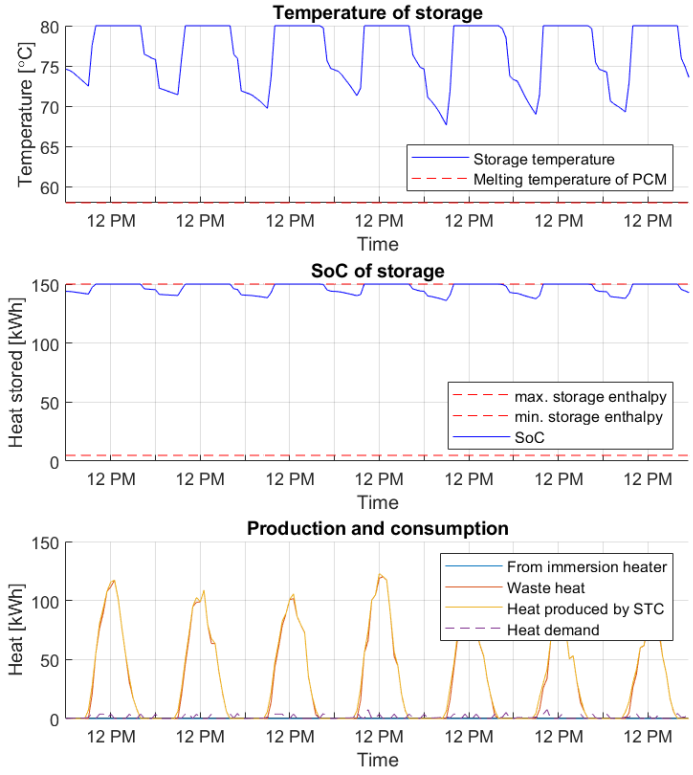

Figure 44. Configuration 2: Interaction of heat supply and demand, along with storage temperature during the winter (a) and the summer (b) for seven days

4.2.1 Energy Losses and Energy Excess

The detailed energy flow and losses that occur in each energy systems are analyzed using Sankey diagrams, presented in Appendix A.8. Energy loss is defined as losses due to a device's efficiency (e.g. inverter, electrolyzer, fuel cell) or due to temperature differences (e.g., DHW tank and LHS). Unused energy or energy excess is defined as the amount of energy that is produced or could be produced by PV PV/T, and STC, but not consumed by the houses due to the absence of demand or because the energy storage has been fully charged. Excess electricity can be sold to the main grid if the houses are grid-connected, but excess heat is just wasted.

In the first configuration (Figure 58, Appendix A.8), the losses come from inverter's efficiency, Li-ion battery charging-discharging efficiency, and DHW tank loss to the environment. The losses account for 6.7% of the total energy input, which comes from PV and ground (heat pump). The Sankey diagram also visualizes how big the energy excess is, which is 3.4 times more than the PV energy being consumed by the house.

In the second configuration (Figure 59, Appendix A.8), the losses come from not only the inverter, battery, and DHW tank, but also LHS. The LHS loss is about 10% of the heat supplied by LHS, while the overall loss is 7.5% from the PV/T energy that goes to the house. The loss is higher compared to the first configuration due to the presence of LHS. The second configuration has 2.9 times excess electricity, and 5.6 times excess heat, making the overall energy excess 4.5 times than the required amount. Therefore, the overall energy excess in the second configuration is even more than the first configuration.

The energy loss in the third configuration (Figure 60, Appendix A.8) is the highest one compared to the other two configurations. This is because the hydrogen storage has a roundtrip efficiency of 36.8%, in which the losses comes from electrolyzer and fuel cell. The overall energy loss of the third configuration is 23.7%; however, the energy excess is less than the other two configurations. Here, the energy excess is 0.5 times from the PV energy being consumed by the house.

In section 4.1, we considered various size combinations of the third energy system configuration, and we chose the cheaper option that minimizes the hydrogen storage size. However, it needs to be highlighted that if we choose other option that minimizes PV capacity, the energy excess will be zero, as shown by Figure 61 (Appendix A.8). If energy excess is considered as loss, then the losses are 80%, 83%, 56%, 30% for the first, second, third (hydrogen storage minimized), and third (PV capacity minimized) configuration.

4.2.2 Energy Storage Capacity Utilization

Figure 45 shows the SoC of Li-ion battery for the first and third configuration. The graph for the second configuration is very similar to the first configuration because they both use daily Li-ion battery for electrical energy storage. The battery sizes are different for each configuration, with the first configuration being the largest and the third configuration being the smallest. One can observe that the battery capacity is not utilized most of the time in the first configuration, as indicated by the white area inside the battery capacity limit. They are only discharged until its maximum DoD at the end of the year. This is seen as a waste of energy storage capacity. On the positive side, the cycle life of batteries could be longer if it is not frequently discharged until its maximum DoD. On the other hand, the battery capacity utilization in the third configuration is more effective, as indicated by the smaller white area inside the battery capacity limit.

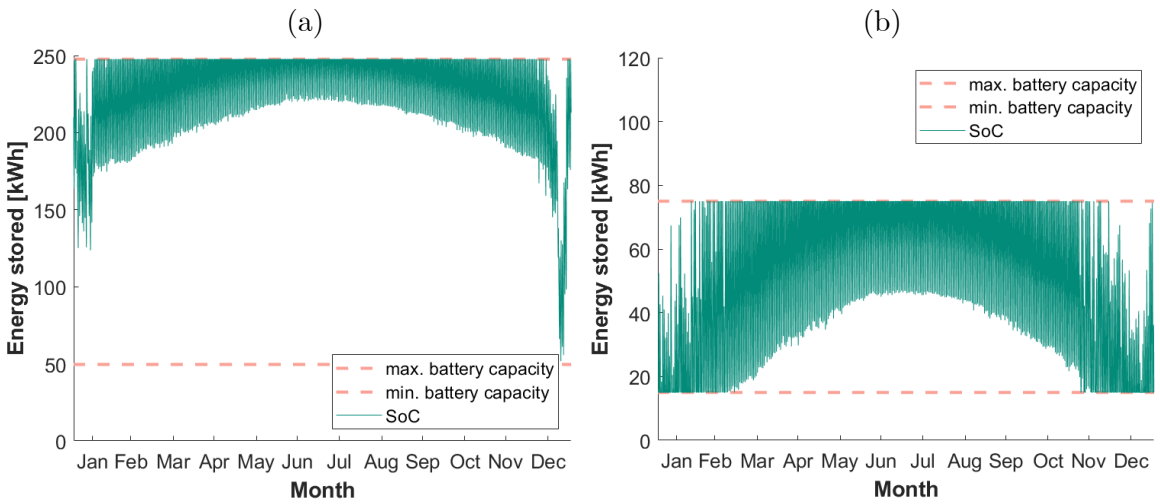

Figure 45. SoC of Li-ion battery in configuration 1 (a) and 3 (b)

4.2.3 Energy Demand Fulfilment

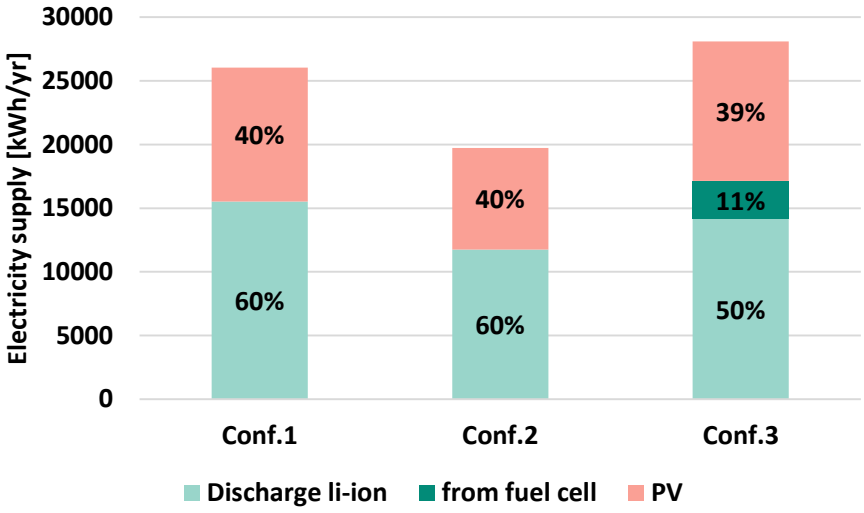

Figure 46. Overall electricity demand fulfilment for all configurations

Figure 46 shows how electricity demand is fulfiled in all configurations. In the first and second configuration, the demand is either supplied directly from the PV or by the Li-ion battery. In the third configuration, a hydrogen storage system is present; hence, the demand is fulfiled by a fuel cell in addition to PV and Li-ion battery. The hydrogen storage is charged from March to October to fulfil the demand in November to February, as shown in Figure 47. 11% of the annual electricity demand is supplied by a fuel cell. Although it seems like a small percentage, it holds an important role in the energy system because it supplies the largest portion of electricity in December and January, where solar irradiation is the lowest. Seasonal storage allows an energy system to be 100% self-sufficient without the need of installing a massive amount of PV system.

Figure 48 shows how heat demand is fulfiled. In the first configuration, heat is fully supplied by a heat pump. In the second configuration, heat can be supplied by the thermal output of PVT/STC, LHS, and immersion heater. In the third configuration, heat can either be supplied by a heat pump or fuel cell (heat as a byproduct).

About 60% of heat fulfilment in the second configuration is done by LHS, so it holds an important role. Immersion heater only steps in when there is not enough heat from PV/T, STC, and LHS, which happens in December and January (see Figure 49 (a)). In the third configuration, almost 100% of heat is supplied by a heat pump. As explained in previous

paragraphs, fuel cell only operates from November until February. With fuel cell's operation to supply electricity, the amount of high-temperature water produced by the fuel cell is only 1,343 kg/year, and unreacted hydrogen is 26 kg/year, which takes place in November until February (see Figure 49 (b)). Assuming a working temperature of 40°C to 80°C in the heat exchanger, it is only equivalent to 66 kWh/year, which is significantly less than the annual heat demand of around 29,000 kWh/year.

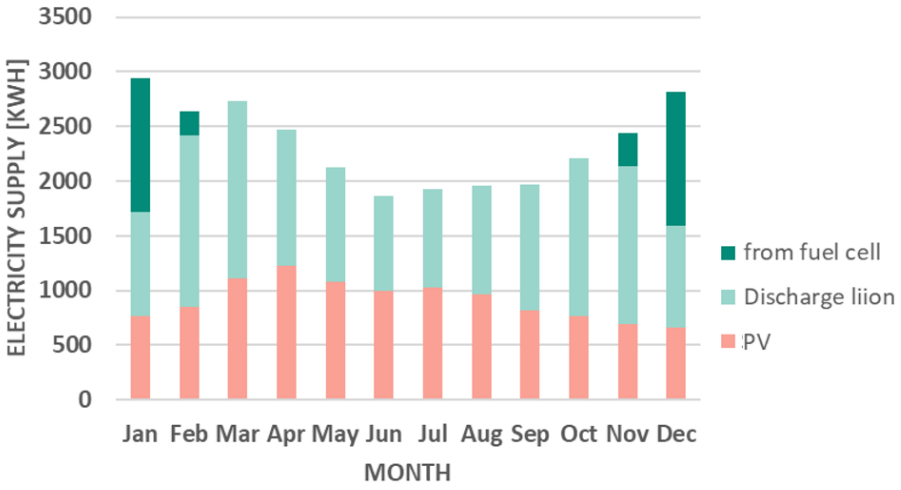

Figure 47. Electricity demand fulfilment every month in configuration 3

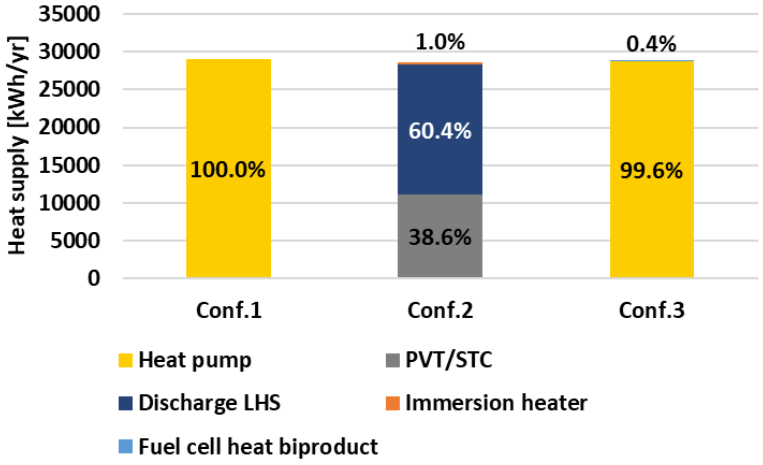

Figure 48. Overall heat demand fulfilment for all configurations

(a)

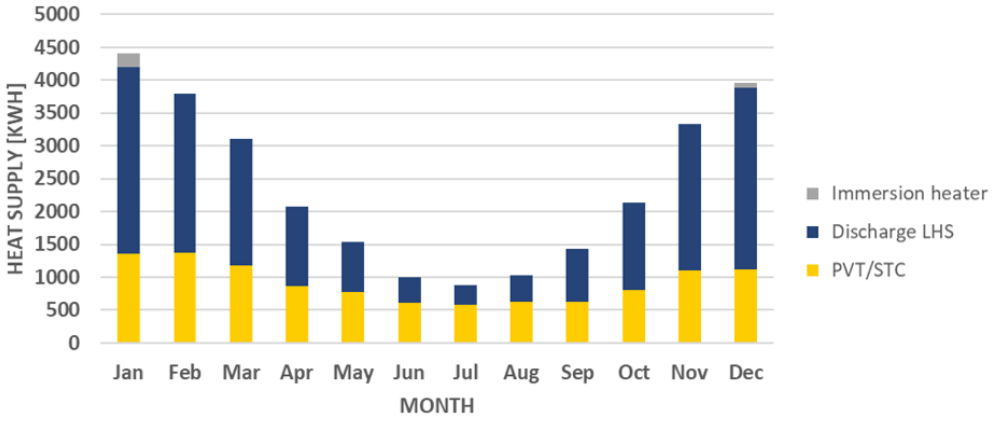

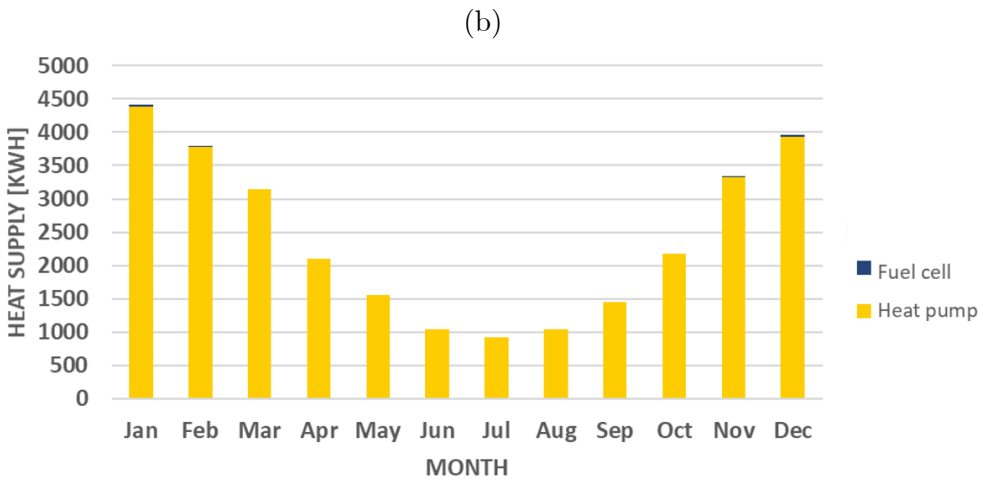

Figure 49. Heat demand fulfilment in configuration 2 (a) and 3 (b)

4.3 Economic Analysis

In this section, a cash flow for each configuration was made, and is shown in Appendix A.9. The net present cost (NPC) of each energy components is depicted in Figure 50. The NPC increases from the first to the third configuration. It is apparent that the third configuration shows the highest NPC because of the hydrogen storage system. Although the Li-ion and PV cost of the third configurations are significantly lower than the first and second configuration, the hydrogen system is still the main driver of the overall NPC.

In the second configuration, PV/T and STC are the components with the highest NPC, and it highly affects the overall NPC. As explained in section 4.2, a large size of PV/T is required to fulfil all energy demand. Although the PV/T and STC area in the second configuration is smaller than the first configuration, the overall PV/T cost is still higher because the cost of PV/T per Watt and per unit area is still higher than PV. This is aligned with Mellor et al.'s study [83] that states the technology and market readiness level of PV/T is much lower than that of PV and STC. Advancement of PV/T is the key to allow it to become financially competitive with separate PV and STC. A promising solution is to use an Argon-filed cavity and low-e coating, which could improve PV/T's thermal efficiency by 70% and improve its financial payback by 20% [83]. Lastly, the feed-in tariff income of the second configuration is less than the first configuration; thus, the overall NPC is higher than the first configuration.

In the first configuration, the NPC of Li-ion batteries is the highest among all three configurations because it is the one and only energy storage in the first configuration. The second configuration has Li-ion batteries and LHS, while the third configuration has Li-ion battery and hydrogen storage. The NPC of PV is about the same as the Li-ion battery. The feed-in tariff is the highest compared to the other two configurations because it produces the highest excess electricity. This indicates that if excess electricity cannot be injected to the main grid, the NPC would be higher.

When feed-in tariff is not considered as an income, the NPC of first, second, and third configuration increase by €70,000, €42,000, and €17,000. Although the first configuration's NPC is increased more than the second configuration, the Figure 50 (b) shows that the overall NPC of the second configuration is still higher than the first one, with a difference of €28,000.

Figure 51 shows the present value of cost components. In all configurations, the capital cost is the highest cost component. The capital cost increases from the first to the third configuration,

respectively, and so does the NPC. This is due to the high-cost sophisticated technology that the hydrogen storage system uses. Among the hydrogen storage components, hydrogen tank system gives the highest cost because the required capacity is 142.8 kg, and the cost per kg is 890 €/kg. The highest replacement and O&M costs are also shown by the third configuration; however, the differences are not as significant as the capital cost.

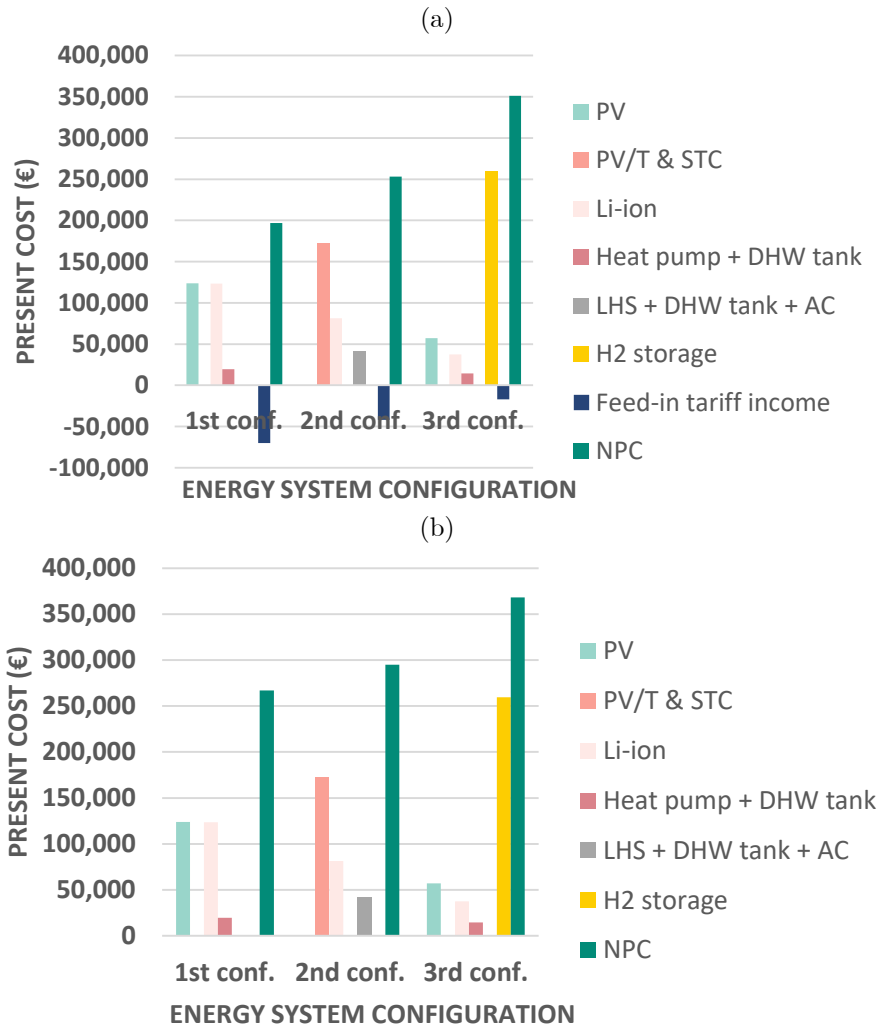

Figure 50. Net present cost (NPC) per energy component (a) with feed-in tariff and (b) without feed-in tariff

After obtaining the NPC of each configuration, we can now determine the LCOE. The LCOE of all configurations with and without feed-in tariff is shown in Figure 52. One can compare the system's LCOE with PV LCOE in Germany (300 kWh/m^2.year of global horizontal irradiation), ranging from €0.0495/kWh to €0.0843/kWh [84]. However, they are not well-comparable because those values are specific for a PV system, while in this study, the components are much more than just a PV system.

Therefore, as a reference, one can compare the system's LCOE with the current cost of buying energy from utility companies, because homeowners normally buy energy from them. The cost of buying electricity from the main grid is €0.2169/kWh [85], while gas is €0.74132/m^3 [85] (equivalent to €0.073/kWh [86]). From the graph, it is observed that for both cases where feed-in tariff is considered and not considered, the LCOE of all configurations are higher than the reference.

In both cases of feed-in tariff, the cost of electricity is highest for the third configuration, mainly due to the hydrogen storage components. The second configuration has a lower cost of electricity compared to the first one because it does not use an electric-based heating system. On the contrary, the cost of heat for the second configuration is the highest compared to the other two. The overall LCOE increases from the first to the third configuration, respectively, according to their NPC, which was explained in the previous paragraph.

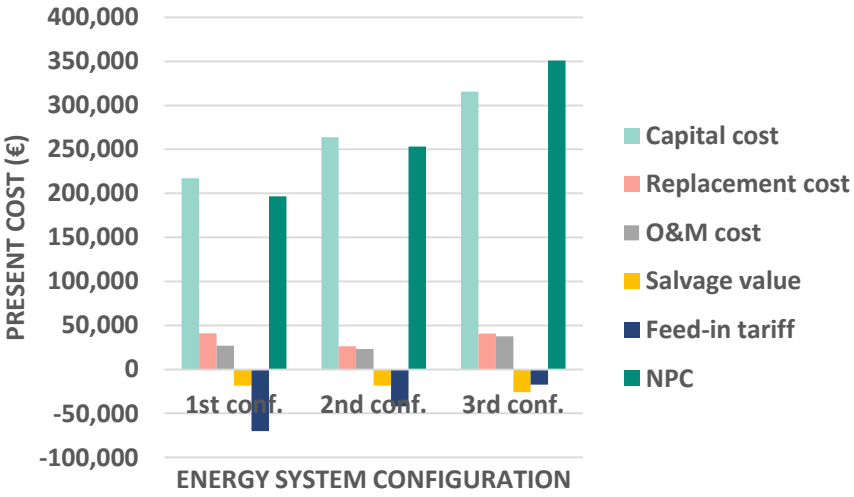

Figure 51. Present value of cost components

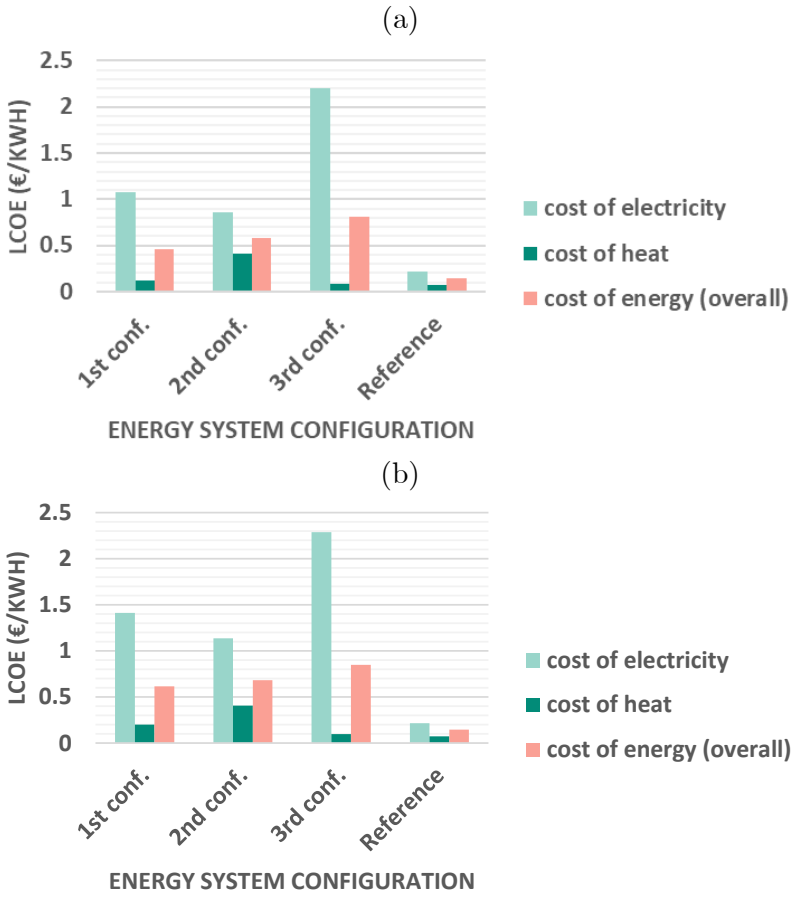

Figure 52. LCOE of all energy system configurations (a) with feed-in tariff and (b) without feed-in tariff

4.4 Recommendation of Energy System Configuration

A matrix was created to have an overview of the advantages and disadvantages of each configuration. Six parameters that have been discussed in this chapter were considered. In the final matrix (Table 18), a high score represents a positive outcome, while a low score represents a negative outcome. The explanation of each parameters' scores are listed below:

- **Area and volume**: high score = less area and volume, low score = more area and volume
- **Reliability**: high score = more reliable, low score = less reliable
- **Energy loss**: high score = less loss, low score = more loss
- **Energy excess**: high score = less excess, low score = more excess
- **Li-ion battery capacity utilization**: high score = higher utilization, low score = lower utilization
- **Technology complexity**: high score = less complex, low score = more complex
- Cost: high score = lower cost, low score = higher cost

The most important parameters are area & volume, reliability, as well as cost, with weight factors of 5. This is because the study considers tiny houses; thus, the space is limited. In addition, the system would need other building's roofs or additional land area to install the PV system, which could increase the cost even further. Reliability is important because power outage highly affects the home occupants, and this needs to be prevented. Cost is also considered as the most important parameter because homeowners' budget is limited, and it is a major consideration in an investment or a project.

Energy loss due to efficiency and energy excess are the second most important aspects, with weight factors of 4, because they are seen losses for the homeowners, and they consistently happen throughout the operations. Lastly, storage capacity utilization and technology complexity are given weight factors of 3 because they do not affect the homeowners directly in terms of their gain or loss. For instance, the impact of complex technology is mostly during its installation stage and annual maintenance, which are usually not handled by homeowners. In the next paragraphs, each factor's scoring will be explained.

The required area and volume for all configurations were shown in Figure 40. To make area and volume comparable, it is assumed that all components with calculated volume have a height of 0.5 m. Therefore, the area is equal to volume divided by height, as shown in Table 14. Using this method, the total required area can be calculated. The largest area is assigned a score of 1, while the smallest area has a score of 10. The area in between is calculated proportionally by interpolation.

Table 14. Defining score for area and volume

Parameter	1st configuration	2nd configuration	3rd configuration
PV, PV/T, STC area [m^2]	650.3	491.2	300.3
Volume of all components [m^3]	3.3	2.2	14.1
Area of components with calculated volume [m^2]	3.3/0.5=6.6	2.2/0.5=4.5	14.1/0.5=28.2
Total required area [m^2]	656.9	495.7	328.6
Score	1	5	10

In the case of energy excess and energy loss, the scores are determined based on the amount of energy, in which the highest excess or loss is assigned a score of 1, while a score of 10 means that the energy excess is zero. The loss and excess in between are calculated proportionally by interpolation.

Table 15. Defining score for energy excess and energy loss

Parameter	**1st configuration**	**2nd configuration**	**3rd configuration**
Energy excess [kWh/year]	95,697	229,773	19,486
Score for energy excess	6	1	9
Energy loss [kWh/year]	2,915	3,948	12,369
Score for energy loss	10	9	1

In the case of cost, a score of 10 is assigned to the reference cost (the price of buying energy from utility companies), and a score of 1 is assigned to the most expensive combined heat and electricity LCOE. The cost in between is calculated proportionally by interpolation. The LCOE used to define these scores are the ones that do not consider feed-in tariff, because it can be applied for both grid-connected and stand-alone system. If the LCOE with feed-in tariff is used, then it is only applicable for grid-connected cases.

Table 16. Defining score for cost

Parameter	**1st configuration**	**2nd configuration**	**3rd configuration**	**Reference**
LCOE (heat and electricity) [€/kWh]	0.62	0.68	0.85	0.14
Score	4	3	1	10

In the case of Li-ion battery capacity utilization, the fraction of unused capacity throughout the year was calculated. A score of ten is assigned for the lowest unused fraction, and a score of 1 is assigned for the highest unused fraction. The capacity utilization in between is calculated proportionally by interpolation.

Table 17. Defining score for battery capacity utilization

Parameter	**1st configuration**	**2nd configuration**	**3rd configuration**
Fraction of unused battery capacity	74%	76%	25%
Score	1	5	10

Reliability score of the third configuration is higher than the first and second because it has seasonal energy storage. In terms of technology complexity, the first configuration has the highest score because the components used have high technology readiness level (TRL), as opposed to the second and third configuration that have LHS and hydrogen storage. The second configuration is assigned the same score as the third because LHS control still needs to be further improved, and the third configuration requires various high-technology components.

Finally, according to the matrix of choice (Table 18), the highest score is shown by the third configuration, which means that it is more preferred than the other two. However, it needs to be highlighted that the LCOE is 7.4 times higher than the typical energy bill, but it might be considered as the "price" for going more sustainable. If economic feasibility is the primary selection factor, then the first configuration is the best choice.

The first main obstacle of the implementation of configuration 3 is the high cost of hydrogen storage. A possible solution is to implement hydrogen storage for a larger scale energy system, because according to Saba et al. [87], the capital cost per kW of electrolyzer reduces exponentially with larger capacity. Their study showed that the cost is significantly higher when the capacity is below 2 MW. The same reducing exponential trend was observed by Greener et al. [88] for PEM fuel cell, in which the cost is much higher when the capacity is below 50 kW. Furthermore, NREL's data [65] shows that the capital cost per kW of rectifier, electrolyzer, and compressor could potentially reduce by 54%, while the capital cost per kW of inverter and fuel cell could reduce by 48% in the future. The capital cost of storage tank per kWh has a potential of reducing by 49%. Therefore, hydrogen storage technology has great potential for future self-sufficient houses.

Another option to reduce the cost of hydrogen storage is by using geologic storage, such as salt cavern [65]. However, this solution is limited because not all places have salt caverns. The capital cost of storage per kWh using salt caverns is 438 times lower than using tanks. In addition, unlike tank storage, the LCOE of fuel cell and geologic storage actually reduces with longer storage duration.

The second obstacle of the implementation of configuration 3 is the high energy loss due to the low roundtrip efficiency of hydrogen storage. The efficiency of hydrogen storage has the potential to be improved through technological advancement of electrolyzer and fuel cell.

Table 18. Matrix of choice for the final energy system configuration

Parameter	**Weight factor (1-5)**	**Score**		
		1st configuration	**2nd configuration**	**3rd configuration**
Area and volume	5	1	5	10
Reliability	5	5	5	8
Energy loss	4	10	9	1
Energy excess	4	7	1	9
Battery capacity utilization	3	3	2	8
Technology complexity	3	8	3	3
Cost	5	4	3	1
Total = weight factor × score		151	120	171

There is an opportunity to improve the first and second configuration by combining both concepts partially. When comparing the first and second configuration, all parameters of the first configuration has higher score, except for the area and volume. Since the weakness of the first configuration is its large area, then the combined concept shall use PV/T to minimize the area. Consequently, the cost would be higher, but the difference of cost score between the two configurations are not significant. Therefore, it can be compromised. In this combined concept, heat demand during the day is fulfilled directly by the thermal output of PV/T, so ideally, the heat pump does not need to operate. If the heat pump does not operate during the day, then a larger portion of the produced electricity can be allocated to charge Li-ion battery. During the night, heat demand will be fulfilled by the heat pump that draws electricity from the Li-ion battery.

Chapter 5

Conclusions and Recommendations

In this study, three energy system configurations for six tiny houses with eight inhabitants were evaluated. The configurations are listed as follows:

- **Configuration 1**: PV, Li-ion battery, GSHP
- **Configuration 2**: PV/T, STC, Li-ion battery, LHS
- **Configuration 3**: PV, Li-ion battery, GSHP, hydrogen storage (electrolyzer, compressor, hydrogen tank, fuel cell)

The energy demand was modelled by dividing them into heat and electricity. The heat demand profile is built according to the houses' heat balance, based on the Netherland's climate. Heat demand of the second configuration is 31.5% higher than the others because there are some heat losses from LHS, while other configurations use a heat pump that operates according to demand. In the first and third configuration, the heat demand increases electricity demand by 33% because an electric-based heater (heat pump) is used. Hydrogen storage increases electricity demand by 37% due to the roundtrip loss and additional electricity demand for the hydrogen compressor.

In configurations with daily-sized energy storage, a large size of solar energy generator is required to ensure the batteries are charged enough to make energy available during the night and during days with low solar irradiation. This applies to both heat (PV/T and STC) and electricity (PV and PV/T). That is why the required area for the first and second configuration are 1.5 and 2 times larger than the third configuration, respectively.

Integrating heat and electricity as one whole system creates the opportunity to improve efficiency in two ways. Firstly, utilizing fuel cell's heat byproduct to fulfil the heating demand partially. However, the study shows that the amount of heat produced by the fuel cell is insignificant, reducing only 0.4% of the heat pump's load. Secondly, reducing the area of energy generation using PV/T. There is a reduction of 24% area when using PV/T and STC (configuration 2), as compared to just PV (configuration 1), to fulfil the same heat and electricity demand. However, this area reduction results in a higher cost because; (1) the thermal efficiency of PV/T is lower than STC and (2) the cost per Watt and per unit area of PV/T is still higher than separate PV and STC. Currently, the TRL of PV/T is much lower than that of PV and STC; therefore, the cost of PV/T could be more competitive in the future.

Moreover, it was found that the energy loss of the second configuration is higher compared to the first and third configuration, due to the heat loss from LHS. In addition, the yearly unused heat excess is also higher. Therefore, it is more beneficial to use a high-efficiency electric-based heater such as a heat pump (configuration 1), compared to a thermal-based heater (configuration 2).

As a result of the large PV or PV/T size, there is a high amount of unused energy during days with high solar irradiation, which mostly happens during the summer. The electricity excess

of the first and second configuration (daily Li-ion battery without seasonal hydrogen storage) are 3.5 and 2.9 times higher than the actual consumption, respectively. This excess is 3-5 times higher than the third configuration because they do not have seasonal hydrogen storage. Electricity excess is not seen as a loss if it can be sent to the main grid, but it is also not profitable to sell electricity back to the grid as the price per kWh is lower than the normal electricity tariff. There is no heat excess for the first and third configuration due to the use of an electric-based heater, but the heat excess of the second configuration (daily LHS) is 5.6 times the actual consumption throughout the year. Overall, the second configuration with a thermal-sourced heating system has the highest excess of energy compared to other configurations. Although the third configuration shows the least energy excess, its overall energy loss is 3-4 times larger than other configurations due to the low roundtrip efficiency of hydrogen storage.

Essentially, the main advantage of having seasonal energy storage is its less energy excess, higher reliability, and more effective battery capacity utilization, but it comes with more complex technology and a higher cost. The LCOE of the third configuration (seasonal hydrogen storage) is 1.4 to 1.8 times higher than the configurations with no seasonal energy storage when feed-in tariff is considered. Even if the electricity excess is considered as loss, or in other words, there is no feed-in tariff, the LCOE of the third configuration is still 1.2 to 1.4 times higher than the first and second configurations, respectively.

In all configurations, the cost of electricity is significantly higher than the price to buy electricity from utility companies, ranging from 4-10 times more if feed-in tariff is considered, and 5-11 times more if feed-in tariff is not considered. The cost of heat, on the other hand, is a bit better, ranging from 1-6 times more expensive. When heat and electricity costs are combined, configuration 1 shows the lowest LCOE, indicating that new technologies like LHS and hydrogen storage need improvement to be able to compete. Possible solutions include making the system scale larger to achieve the economy of scale, technology advancement that could drive the cost down and improve the roundtrip efficiency, or increasing the price of fossil fuel so that clean technologies become competitive.

Finally, if the parameter of choice is only economic feasibility, then the first configuration is recommended because it shows the lowest LCOE amongst all configurations, although it is still higher than the reference cost. This higher cost might be considered as the cost to be sustainable. For a better system, the PV in the first configuration can be replaced by PV/T to reduce the area required. However, if we consider all factors besides cost such as area, reliability, energy excess, then the third configuration with seasonal hydrogen storage would be the best recommendation.

For future work, it is recommended that the cost components are more detailed, for instance, by considering labour, construction, tax, overhead, and other components. The costs should also be varied through a sensitivity analysis. Moreover, in this study, most of the components are evaluated on a macro scale, based on the energy flow. The energy components could be modelled more accurately by considering the voltage and current of electricity. For instance, the amount of hydrogen produced by electrolyzer and consumed by fuel cell could be calculated based on the electricity current received/produced. Lastly, a sensitivity analysis based on the scale of the energy system is a good subject to discuss because the result can be applied more generally for other sizes of buildings.

Bibliography

[1] European Commission, "2050 long-term strategy," [Online]. Available: https://ec.europa.eu/clima/policies/strategies/2050_en.

[2] Global Alliance for Buildings and Construction; International Energy Agency (IEA); United Nations (UN) Environment Programme, "2019 Global Status Report for Buildings and Construction: Towards a Zero-Emission, Efficient and Resilient Buildings and Construction Sector," 2019.

[3] European Commission,, "Energy statistics - an overview," [Online]. Available: https://ec.europa.eu/eurostat/statistics-explained/index.php?title=Energy_statistics_-_an_overview#Final_energy_consumption.

[4] O. S. Burheim, Engineering Energy Storage, Academic Press, 2017.

[5] LIFE, "Living Project for Future Innovative Environments (LIFE) - Project Plan," Enschede, 2020.

[6] H. S. Das, C. W. Tan, A. Yatim and K. Y. Lau, "Feasibility analysis of hybrid photovoltaic/battery/fuel cell energy system for an indigenous residence in East Malaysia," *Renewable and Sustainable Energy Reviews,* vol. 76, pp. 1332-1347, 2017.

[7] D. Nelson, M. Nehrir and C. Wang, "Unit sizing and cost analysis of stand-alone hybrid wind/PV/fuel cell power generation systems," *Renewable Energy,* vol. 31, pp. 1641-1656, 2006.

[8] D. Bezmalinović, F. Barbir and I. Tolj, "Techno-economic analysis of PEM fuel cells role in photovoltaic-based systems for the remote base stations," *Int. J. of Hydrogen Energy,* vol. 38, pp. 417-425, 2013.

[9] S. Kharel and B. Shabani, "Hydrogen as a Long-Term Large-Scale Energy Storage Solution to Support Renewables," *energies,* vol. 11, 2018.

[10] O. H. Mohammed, Y. Amirat, M. Benbouzid and A. Elbast, "Optimal Design of a PV/Fuel Cell Hybrid Power System for the City of Brest in France," *IEEE ICGE,* pp. 119-123, 2014.

[11] D. N. Luta and A. K. Raji, "Decision-making between a grid extension and a rural renewable off-grid system with hydrogen generation," *Int. J. of Hydrogen Energy,* vol. 43, pp. 9535-9548, 2018.

[12] V. Mudgal, K. S. Reddy and T. K. Mallick, "Techno-Economic Analysis of Standalone Solar Photovoltaic-Wind-Biogas Hybrid Renewable Energy System for Community Energy Requirement," *Future Cities and Environment,* vol. 5, no. 1, 2019.

[13] A. Ramos, M. A. Chatzopoulou, I. Guarracino, J. Freeman and C. N. Markides, "Hybrid photovoltaic-thermal solar systems for combined heating, cooling and power provision in the urban environment," *Energy Conversion and Management,* vol. 150, pp. 838-850, 2017.

[14] A. Hesaraki, S. Holmberg and F. Haghighat, "Seasonal thermal energy storage with heat pumps and low temperatures in building projects — A comparative review," *Renewable and Sustainable Energy Reviews,* vol. 43, pp. 1199-1213, 2015.

[15] EC - Intelligent Energy Europe, "Solar Combi systems promotion and standardisation," [Online]. Available: https://ec.europa.eu/energy/intelligent/projects/en/projects/combisol.

[16] C. Leonhardt and D. Muller, "Latent Heat Storage Devices for Heat Pump and Solar Heating Systems," E.ON Energy Research Center, 2011.

[17] J. Zhao, Y. Ji, Y. Yuan, Z. Zhang and a. J. Lu, "Energy-Saving Analysis of Solar Heating System with PCM Storage Tank," *energies,* vol. 11, no. 237, 2018.

[18] W. Lin, Z. Ma, H. Ren, J. Liu and K. Li, "Solar Thermal Energy Storage Using Paraffins as Phase Change Materials for Air Conditioning in the Built Environment," Intechopen, 2019.

[19] IPS; CRES; TEISTE; UOI; GEOTEAM; SGGW; RUB; PCM PRODUCTS; ECOSERVEIS Z&X, "TESSE2B - Thermal Energy Storage Systems for energy efficient building an integrated solution for residential building energy storage by solar and geothermal resources D8.5 Training Material," TESSE2B Project, 2018.

[20] M. S. Buker and S. B. Riffat, "Solar assisted heat pump systems for low temperature water heating," *Renewable and Sustainable Energy Reviews,* vol. 55, pp. 399-413, 2016.

[21] A. Heinz and H. Schranzhofer, "Thermal Energy Storage with Phase Change Materials – A Promising Solution ?," 2010.

[22] R. Heimrath and M. Haller, "The Reference Heating System, the Template Solar System of Task 32. A Report of IEA Solar Heating and Cooling programme - Task 32. “Advanced storage concepts for solar and low energy buildings”," IEA, Austria, 2007.

[23] International Energy Agency (IEA), "World Energy Model - Sustainable Development Scenario," IEA, 11 2019. [Online]. Available: https://www.iea.org/reports/world-energy-model/sustainable-development-scenario. [Accessed 17 6 2020].

[24] Affairs, Ministry of Economic, "Energy Report: Transition to sustainable energy," Ministry of Economic Affairs, Den Haag, 2016.

[25] S. A. Kalogirou, Solar Energy Engineering: Processes and Systems, vol. 2, Academic Press, 2014.

[26] S. O. Amrouche, D. Rekioua, T. Rekioua and S. Bacha, "Overview of energy storage in renewable energy systems," *Int. J. of Hydrogen Energy,* vol. 41, pp. 20914-20927, 2016.

[27] P. Komarnicki, P. Lombardi and Z. Styczynski, Electric Energy Storage System: FLexibility Options for Smart Grids, Berlin: Springer, 2017.

[28] PACE, "Fuel Cell micro-Cogeneration," PACE, [Online]. Available: http://www.pace-energy.eu/micro-cogeneration/.

[29] J. Töpler and J. Lehmann, Hydrogen and Fuel Cell: Technologies and Market Perspectives, Berlin: Springer, 2016.

[30] Home Power Solutions, "HPS System – Picea," [Online]. Available: https://www.homepowersolutions.de/en/product. [Accessed 17 6 2020].

[31] KNMI, "Climatology - Hourly weather data for the Netherlands," [Online]. Available: http://projects.knmi.nl/klimatologie/uurgegevens/selectie.cgi.

[32] H. Burroughs and S. J. Hansen, Managing Indoor Air Quality, vol. 5, The Fairmont Press, Inc. & CRC Press, 2011.

[33] Fraunhofer-ISI; Fraunhofer-ISE; IREES; Observ'ER; TU Wien-EEG; TEP, "Mapping and analyses of the current and future (2020 - 2030) heating/cooling fuel deployment (fossil/renewables)," European Commission, 2016.

[34] Y. A. Cengel and M. A. Boles, Thermodynamics: An Engineering Approach, 8th ed., McGraw Hill Education, 2015.

[35] I. Sarbu and C. Sebarchievici, Ground-Source Heat Pumps: Fundamentals, Experiments and Applications, Academic Press, 2016.

[36] International Energy Agency (IEA), "Tracking Building - Heating," IEA, 6 2020. [Online]. Available: https://www.iea.org/reports/tracking-buildings-2020/heating#abstract. [Accessed 17 6 2020].

[37] International Renewable Energy Agency (IRENA), "Renewable Energy Prospects for the European Union," European Commission, 2018.

[38] R. Niessink and H. Rosler, "Developments of Heat Distribution Networks in the Netherlands," ECN, Utrecht, 2015.

[39] International Energy Agency (IEA), "Renewables 2019: Market Analysis and Forecast from 2019 to 2024," IEA, October 2019. [Online]. Available: https://www.iea.org/reports/renewables-2019/heat.

[40] (CBS), Centraal Bureau voor de Statistiek, "Use of air-source heat pumps has increased," 8 10 2018. [Online]. Available: https://www.cbs.nl/en-gb/news/2018/40/use-of-air-source-heat-pumps-has-increased#:~:text=At%20the%20end%20of%202017,systems%20(air%20conditioning%20units)..

[41] D. Thorpe, Sustainable Home Refurbishment: The Earthscan Expert Guide to Retrofitting Homes for Efficiency, Earthscan, 2010.

[42] N. P. Garcia, K. Vatopoulos, A. K. Riekkola, A. P. Lopez and L. Olsen, "JRC Scientific and Policy Reports: Best available technologies for the heat and cooling market in the European Union," European Commission, Luxembourg, 2012.

[43] I. Sarbu and C. Sebarchievici, "A Comprehensive Review of Thermal Energy Storage," *Sustainability,* vol. 10, 2018.

[44] A. Huang, "Comparison Sheet Evacuated Heat Pipe Collectors versus Flat-Plate Solar Panels," [Online]. Available: http://mcensustainableenergy.pbworks.com/f/FlatvsEvac2.pdf.

[45] M. Nájera-Trejoa, I. R. Martin-Domíngueza and J. A. Escobedo-Bretadoa, "Economic feasibility of flat plate vs evacuated tube solar collectors in a combisystem," *Energy Procedia,* vol. 91, pp. 477-485, 2016.

[46] R. Santbergen, C. Rindt, H. Zondag and R. v. Zolingen, "Detailed analysis of the energy yield of systems with covered sheet-and-tube PVT collectors," *Solar Energy,* vol. 84, pp. 867-878, 2010.

[47] Sunamp, "Sunamp Residential," Sunamp, [Online]. Available: https://www.sunamp.com/residential/. [Accessed 17 6 2020].

[48] International Energy Agency - Energy Technology Systems Analysis Program (IEA-ETSAP); International Renewable Energy Agency (IRENA), "Thermal Energy Storage - Technology Brief," IEA-ETSAP and IRENA, 2013.

[49] A. H. Abedin and M. A. Rosen, "A Critical Review of Thermochemical Energy Storage Systems," *The Open Renewable Energy Journal,* vol. 4, pp. 42-46, 2011.

[50] T.-T. Nguyen, V. Martin, A. Malmquist and C. A. Silva, "A review on technology maturity of small scale energy storage technologies," *Renew. Energy Environ. Sustain.,* vol. 2, no. 36, 2017.

[51] M. Shahi, *Energy Storage - Thermal energy storage systems - Lecture 2019,* Enschede, 2019.

[52] J. B. Johansen, G. Englmair, M. Dannemand, W. Kong, J. Fan, J. Dragsted, B. Perers and S. Furbo, "Laboratory Testing of Solar Combi System with Compact Long Term PCM Heat Storage," *Energy Procedia,* vol. 91, pp. 330-337, 2016.

[53] T. M. Letcher, Storing Energy: with Special Reference to Renewable Energy Sources, Durban: Elsevier, 2015.

[54] L. F. Cabeza, Advances in thermal energy storage systems - methods and applications, Woodhead Publishing, 2015.

[55] M. Dannemand, J. M. Schultz, J. B. Johansen and S. Furbo, "Long term thermal energy storage with stable supercooled sodium acetate trihydrate," *Applied Thermal Engineering,* vol. 91, pp. 670-678, 2015.

[56] Daikin, "Daikin Altherma HPC," Daikin, [Online]. Available: https://www.daikin.eu/en_us/product-group/daikin-altherma-hpc.html.

[57] Viessmann, "How does a hot water tank work?," Viessmann, [Online]. Available: https://www.viessmann.co.uk/heating-advice/how-does-a-hot-water-tank-work.

[58] PVPMC Sandia, "CEC Inverter Test Protocol," PVPMC Sandia, [Online]. Available: https://pvpmc.sandia.gov/modeling-steps/dc-to-ac-conversion/cec-inverter-test-protocol/#:~:text=Inverter%20efficiency%20is%20the%20ratio,voltage%2C%20and%20sometimes%20inverter%20temperature..

[59] E. Commission, "Photovoltaic Geographical Information System," European Commission, [Online]. Available: https://re.jrc.ec.europa.eu/pvg_tools/en/tools.html#PVP.

[60] LIFE, "Technical Specifications of LIFE Project," Enschede, 2020.

[61] A. Reinders, P. Verlinden, W. v. Sark and A. Freundlich, Photovoltaic Solar Energy: From Fundamentals to Applications, John Wiley & Song, Ltd, 2017.

[62] L. Al-Ghussain, O. Taylan and D. K. Baker, "An Investigation of Optimum PV and Wind Energy System Capacities for Alternate Short and Long-term Energy Storage Sizing Methodologies," *International Journal of Energy Research,* vol. 43, pp. 204-218, 2018.

[63] J. H. Lee, S. G. Hwang and G. H. Lee, "Efficiency Improvement of a Photovoltaic Thermal (PVT) System Using Nanofluids," *energies,* vol. 12, 2019.

[64] y. C. N. Truong, M. Naumann, R. C. Karl, M. Müller, A. Jossen and H. C. Hesse, "Economics of Residential Photovoltaic Battery Systems in Germany: The Case of Tesla's Powerwall," *Batteries,* vol. 2, no. 2, 2016.

[65] M. Penev, N. Rustagi, C. Hunter and J. Eichman, *Energy Storage: Days of Service Sensitivity Analysis,* National Renewable Energy Laboratory (NREL), 2019.

[66] D. Thomas, "“RENEWABLE HYDROGEN: THE MISSING LINK BETWEEN THE POWER, GAS, INDUSTRY AND TRANSPORT SECTORS”," Hydrogenics Europe N.V., June 2018. [Online]. Available: https://hydrogeneurope.eu/sites/default/files/2018-06/2018-06_Hydrogenics_Company%20presentation.compressed.pdf.

[67] M. Trifkovic, M. Sheikhzadehl, K. Nigim and P. Daoutidis, "Modeling and Control of a Renewable Hybrid Energy System With Hydrogen Storage," *IEEE TRANSACTIONS ON CONTROL SYSTEMS TECHNOLOGY,* vol. 22, no. 1, pp. 169-179, 2014.

[68] S. Edwards, I. Beausoleil-Morrison and A. Laperriere, "Representative hot water draw profiles at high temporal resolution for simulating the performance of solar thermal systems," *Solar Energy,* vol. 111, pp. 43-52, 2015.

[69] John, "Direct hot water cylinder buying guide," ManoMano, [Online]. Available: https://advice.manomano.co.uk/direct-hot-water-cylinder-buying-guide-n2969.

[70] T. Sylvia, "The future of cars is electric – but how soon is this future?," PV Magazine, [Online]. Available: https://pv-magazine-usa.com/2020/05/19/the-future-of-cars-is-electric-but-how-soon-is-this-

future/#:~:text=In%20the%20report%2C%20BNEF%20outlines,3%25%20of%20global%20car%20sales..

[71] NEDU, "Consumption profiles," [Online]. Available: https://www.nedu.nl/documenten/verbruiksprofielen/.

[72] NIBUD, "Energy and water," [Online]. Available: https://www.nibud.nl/consumenten/energie-en-water/.

[73] Renault, "Driving range, battery & charging: New Renault Zoe," [Online]. Available: https://www.renault.co.uk/electric-vehicles/zoe/battery.html.

[74] A. Saleh and M. Mosa, "Analysis of Control Strategies and Simulation of Heating System using Simulink/Matlab Potential," *Thermal Engineering,* vol. 2, no. 5, pp. 921-927, 2016.

[75] D. Oughton and S. Hodkinso, Heating and Air Conditioning of Buildings, 9 ed., Oxford: Butterworth-Heinemann, 2002.

[76] HOMER , "Total Net Present Cost (NPC)," HOMER Energy, [Online]. Available: https://www.homerenergy.com/products/pro/docs/latest/total_net_present_cost.html.

[77] Rijksdienst voor Ondernemend Nederland (RVO), "SDE+ Spring 2018: Instructions on how to apply for a subsidy for the production of renewable energy," 2018. [Online]. Available: https://english.rvo.nl/sites/default/files/2018/02/Brochure-SDE-Spring-2018.pdf.

[78] Tractebel Engie; Hinicio, "Study on Early Business Cases for H2 in Energy Storage and More Broadly Power to H2 Applications," Fuel Cells and Hydrogen Joint Undertakin (FCH-JU), Brussels, 2017.

[79] J. Weniger, T. Tjaden and V. Quaschning, "Sizing of residential PV battery system," *Energy Procedia,* vol. 46, pp. 78-87, 2014.

[80] J. Hirschey, K. R. Gluesenkamp, A. Mallow and S. Graham, "Review of Inorganic Salt Hydrates with Phase Change Temperature in Range of 5°C to 60°C and Material Cost Comparison with Common Waxes," *2018 Purdue Conferences,* 2018.

[81] R. Yumrutaş and M. Ünsal, "Energy analysis and modeling of a solar assisted house heating system with a heat pump and an underground energy storage tank," *Solar Energy,* vol. 86, no. 3, pp. 983-993, 2012.

[82] A. Al-Sharafi, A. Sahin, T. Ayar and B. Yilbas, "Techno-economic analysis and optimization of solar and wind energy systems for power generation and hydrogen production in Saudi Arabia," *Renewable and Sustainable Energy Reviews,* vol. 69, pp. 33-49, 2017.

[83] A. Mellor, D. A. Alvarez, I. Guarracino, A. Ramos, A. R. Lacasta, L. F. Llin, A. Murrell, D. Paul, D. Chemisana, C. Markides and N. Ekins-Daukes, "Roadmap for the next-generation of hybrid photovoltaic-thermal solar energy collectors," *Solar Energy,* vol. 174, pp. 386-398, 2018.

[84] C. Kost, S. Shammugam, V. Julch, H.-T. Nguyen and T. Schlegl, "LEVELIZED COST OF ELECTRICITY RENEWABLE ENERGY TECHNOLOGIES," Fraunhofer-ISE, 2018.

[85] Engie, "Engie - Bereken uw maandbedrag," Engie, [Online]. Available: https://www.engie-energie.nl/.

[86] The Engineering Toolbox, "Fuels - Higher and Lower Calorific Values," [Online]. Available: https://www.engineeringtoolbox.com/fuels-higher-calorific-values-d_169.html.

[87] S. M. Saba, M. Muller, M. Robinius and D. Stolten, "The investment costs of electrolysis - A comparison of cost studies from the past 30 years," *Int. J. of Hydrogen Energy,* vol. 43, pp. 1209-1223, 2018.

[88] D. L. Greene, K. Duleep and G. Upreti, "Status and Outlook for the U.S. Non-Automotive Fuel Cell Industry: Impacts of Government Policies and Assessment of Future Opportunities," Oak Ridge National Laboratory, Oak Ridge, Tennessee, 2011.

[89] ASHRAE, 2001 ASHRAE Handbook: Fundamentals - Chapter 28: Residential Cooling and Heating, Atlanta: ASHRAE, 2001.

[90] ASHRAE, 1997 ASHRAE Handbook: Fundamentals - Chapter 29: Fenestration, Atlanta: ASHRAE, 1997.

[91] A. TenWolde, J. D. McNatt and L. Krahn, Thermal Properties of Wood and Wood Panel Products for Use in Buildings, Oak Ridge National Laboratory, 1988.

[92] Forestia, "Declaration of Performance," [Online]. Available: https://www.retbouwproducten.nl/producten/downloads/dl/file/id/256/product/6680/dop_walls2paint.pdf. [Accessed 27 May 2020].

[93] Insulation, Knauf, "Glass Wool - Naturoll 032," [Online]. Available: https://www.knaufinsulation.nl/producten-van-knauf-insulation/naturoll-032. [Accessed 27 May 2020].

[94] N. P. Bansal and R. Doremus, Handbook of Glass Properties, Academic Press, Inc, 1986.

[95] NIBE, "Installer manual NIBE F1255 Ground source heat pump," [Online]. Available: https://www.nibe.eu/assets/documents/16708/231531-6.pdf.

[96] R. Waser, S. Maranda, A. Stamatiou, M. Zaglio and J. Worlitschek, "Modeling of solidification including supercooling effects in a fin-tube heat exchanger based latent heat storage," *Solar Energy,* vol. 200, pp. 10-21, 2020.

[97] Sunamp, "UNIQ HEAT BATTERIES REFERENCE MANUAL_V2.3 Version: 2018_07_19_v2.3," 2018. [Online]. Available: https://www.sunamp.com/wp-content/uploads/2019/01/UniQ-Heat-batteries-reference-manual-ver_20180719_v2.3.pdf.

[98] E. Blokker and E.j.Pieterse-Quirijns, "Modeling temperature in the drinking water distribution system," *American Water Works Association,* pp. E19-E28, 2013.

[99] Daikin, "Daikin Altherma 3 Product catalogue 2018," 2018. [Online]. Available: https://www.daikin.eu/content/dam/internet-denv/catalogues_brochures/residential/Daikin%20Altherma%203%20product%20catalogue%20ECPEN18-786.pdf.

[100] NIBE, "NIBE Prijscatalogus 2020," 2020. [Online]. Available: https://www.nibe.eu/download/18.1cc0394d170d53b08f050cd/1588745727886/Prijscatalogus%202020%20LR%20def.pdf.

[101] F. Ning, X. He, Y. Shen, H. Jin, Q. Li, D. Li, S. Li, Y. Zhan, Y. Du, J. Jiang, H. Yang and X. Zhou, "Flexible and Lightweight Fuel Cell with High Specific Power Density," *ACS NANO,* vol. 11, no. 6, 2017.

[102] C. Wang, "MODELING AND CONTROL OF HYBRID WIND/PHOTOVOLTAIC/FUEL CELL DISTRIBUTED GENERATION SYSTEMS," Montana State University, Bozeman, 2006.

[103] R. Fu, D. Feldman and R. Margolis, "U.S. Solar Photovoltaic System Cost Benchmark: Q1 2018," NREL, 2018.

[104] WePowr, "How much maintenance to solar hot water systems require?," WePowr, [Online]. Available: http://wepowr.com/technology/shw/maintenance.

[105] Energy Star, "Save Money and More with ENERGY STAR Qualified Solar Water Heaters," Energy Star, [Online]. Available: https://www.energystar.gov/products/water_heaters/water_heater_solar/benefits_savings.

[106] International Renewable Energy Agency (IRENA), "ELECTRICITY STORAGE AND RENEWABLES: COSTS AND MARKETS TO 2030," IRENA, 2017.

[107] W. Cole and A. W. Frazier, "Cost Projections for Utility-Scale Battery Storage," National Renewable Energy Laboratory, Golden, CO, 2019.

[108] Tesla, "Tesla Powerwall Limited Warranty (USA)," 2017. [Online]. Available: https://www.tesla.com/sites/default/files/pdfs/powerwall/Powerwall_2_AC_Warranty_USA_1-1.pdf.

[109] Atlas Copco, "Cost Saving Opportunities for Compressors: Maintenance," Atlas Copco, [Online]. Available: https://www.atlascopco.com/en-au/compressors/wiki/compressed-air-articles/compressor-maintenance#:~:text=The%20annual%20maintenance%20cost%20is,filters%2C%20control%20and%20regulation%20equipment).

[110] Arista - Michael Rosone, "Heat Pump Maintenance: FAQ and Checklist," 2018. [Online]. Available: https://aristair.com/blog/heat-pump-maintenance-faq-and-checklist/.

[111] Glasco, "HOW LONG SHOULD YOUR HEAT PUMP LAST?," [Online]. Available: https://glascohvac.com/heating/heat-pumps/long-heat-pump-last/#:~:text=The%20life%20expectancy%20of%20a,can%20last%20a%20bit%20longer..

[112] HomeAdvisor, "How Much Does It Cost To Service And Maintain An Ac?," HomeAdvisor, [Online]. Available: https://www.homeadvisor.com/cost/heating-and-cooling/service-maintain-ac-unit/#:~:text=AC%20Unit%20Service%20Costs,hour%20for%20an%20HVAC%20technician..

[113] urdesign, "AIR CONDITIONING LIFESPAN – HOW LONG SHOULD MY AIR CONDITIONER LAST," urdesign, 2019. [Online]. Available: https://www.urdesignmag.com/technology/2019/11/03/air-conditioning-lifespan-how-long-should-my-air-conditioner-last/.

[114] M. Bakker, H. Zondag, M. Elswijk, K. Strootman and M. Jong, "Performance and costs of a roof-sized PV/thermal array combined with a ground coupled heat pump," *Solar Energy,* vol. 78, pp. 331-339, 2005.

[115] Direct Heating Supplies, "Telford Tempest 200l Direct Unvented Stainless Steel Cylinder TSMD200," Direct Heating Supplies, 2020. [Online]. Available: https://www.directheatingsupplies.co.uk/telford-tempest-200-litre-direct-unvented-stainless-steel-cylinder.

[116] Gregory Heating and Plumbing Ltd, "VENTED AND UNVENTED SYSTEM MAINTENANCE," Gregory Heating and Plumbing Ltd, [Online]. Available: http://gregoryheatingltd.com/gregory-heating-and-plumbing-ltd/central-heating-maintenance/unvented-hot-water-cylinder.

[117] Smarter Homes, "Smart Guide: Hot Water Cylinder and Pipes," Smarter Homes, [Online]. Available: https://www.smarterhomes.org.nz/smart-guides/water-and-waste/hot-water-cylinders-and-pipes/#:~:text=How%20long%20do%20cylinders%20last,shorter%20at%2012%E2%80%9320%20years..

[118] Midsummer Wholesale, "Sunamp UniQ 12," Midsummer Wholesale, [Online]. Available: https://midsummerwholesale.co.uk/buy/sunamp-heat-batteries/sunamp-uniq-12.

[119] Sunamp, "Introducing the UniQTM Range," 2018. [Online]. Available: https://www.sunamp.com/wp-content/uploads/2018/06/Leaflet-3-Introduction-to-UniQ.pdf.

[120] Sunamp, "Sunamp," [Online]. Available: https://www.sunamp.com/.

[121] M. Carmo, D. L. Fritz, J. Mergel and D. Stolten, "A comprehensive review on PEM water electrolysis," *Int. J. of Hydrogen Energy,* vol. 38, pp. 4901-4934, 2013.

[122] International Renewable Energy Agency (IRENA), "HYDROGEN FROM RENEWABLE POWER: TECHNOLOGY OUTLOOK FOR THE ENERGY TRANSITION," IRENA, Abu Dhabi, 2018.

[123] A. F. Jacobs, B. G. Heusinkveld and A. A. Holtslag, "Long-term record and analysis of soil temperatures and soil heat fluxes in a grassland area, The Netherlands," *Agricultural and Forest Meteorology,* vol. 151, pp. 774-780, 2011.

Appendices

A.1 Heat from ventilation

Table 19. Air Exchange Rates (ACH) for Tight* Airtightness [89]

	Outdoor Design Temperature, °C								
	-12	-7	-1	4	10	29	32	35	38
ACH	0.49	0.47	0.45	0.43	0.41	0.33	0.34	0.35	0.36

**Tight: Good multifamily construction with close-fitting doors, windows, and framing is considered tight. New houses with full vapor retarder, no fireplace, well-fitted windows, weather-stripped doors, one story, and less than 140 m2 floor area fall into this category.*

$$Q_{vent} = 1.2\ ACH\ V_{room}\ {}^{1000}/_{3600}\ (T_{in} - T_{out}) \quad (15)$$

where ACH in 1/h, Vroom in m^3, Q_{vent} in W, T_{in} in °C.

A.2 Solar radiation heat gain [90]

$$Qrad = \frac{SHGF\ ref}{I\ ref} \text{ x I x SC x A} \quad (16)$$

Where SC is the shading coefficient for clear triple glazing (0.71), SHGF (W/m^2) is obtained from ASHRAE table [90], I is the irradiance in W/m^2, A is the glass window or door area in m^2. The surface area of house is shown on Table 20Error! Reference source not found..

Table 20. Surface Area of Houses

Façade	Part	House type		
		TH25	TH32	TH40
South	Wall	4.43	4.67	5.29
	Glass window & door	5.58	6.64	9.13
West	Wall	14.85	13.75	17.30
	Glass window	3.87	7.05	8.66
North	Wall	10.13	11.45	14.60
East	Wall	14.08	15.56	23.86
	Glass window	4.64	5.24	2.14
Top	Roof	21.34	26.72	38.11
Bottom	Floor	20.41	25.55	36.61

A.3 Transmission heat loss

Table 21. Heat Transfer Coefficient of House Surface

Part	**Layer**	**Thickness (d)** **mm**	**Thermal conductivity (λ)** **W/m°C**	**Convective heat transfer coefficient (h)** **W/m²°C**	**Thermal resistance (R)** **R=d/λ or R=1/h** **m²°C/W**	**Overall heat transfer coefficient (U)** **U=1/R** **W/m²°C**
Wall	Inside surface			8	0.125	
	Cladding spruce parts	21	0.12 [91]		0.175	
	Backwood firing preserved	70	0.12 [91]		0.583	
	Water-resistant, vapor-permeable & UV resistant film	0				
	Oriented Strand Board-3	12	0.13 [92]		0.092	
	Glass wool blanket insulation	120	0.032 [93]		3.750	
	Vapor barrier foil	0				
	Glass wool blanket insulation	45	0.032 [93]		1.406	
	Wall panels	13	0.13 [92]		0.100	
	Outside surface			23.63	0.042	
				TOTAL	6.274	0.159
Floor	Inside surface			8	0.125	
	Oriented Strand Board-3	22	0.13 [92]		0.169	
	Vapor barrier foil	0				
	Glass wool blanket insulation	220	0.032 [93]		6.875	
	Oriented Strand Board-3	8	0.13 [92]		0.062	
	Outside surface			23.63	0.042	
				TOTAL	7.273	0.138
Glass window or door	Inside & outside surface			12.80	0.078	
	3x glass	3 x 7	0.921 [94]		3 x 0.008	
	2x air	2 x 8	0.024 [34]		2 x 0.328	
				TOTAL	0.757	1.321

Roof	Inside surface			8	0.125	
	Cladding spruce parts	21	0.12 [91]		0.175	
	Backwood firing preserved	70	0.12 [91]		0.583	
	Water-resistant, vapor-permeable & UV resistant film	0				
	Oriented Strand Board-3	15	0.13 [92]		0.115	
	Glass wool blanket insulation	45	0.032 [93]		1.406	
	Glass wool blanket insulation	145	0.032 [93]		4.531	
	Vapor barrier foil	0				
	Glass wool blanket insulation	45	0.032 [93]		1.406	
	Wall panels	13	0.13 [92]		0.100	
	Cladding spruce parts	21	0.12 [91]		0.175	
	Backwood firing preserved	70	0.12 [91]		0.583	
	Outside surface			23.63	0.042	
				TOTAL	9.243	0.108

A.4 Technical specifications of energy components

PV

Table 22. Technical specifications of PV module

Parameter	Value
PV panel rated power (Wp)	360 [60]
A_{PV} (m^2)	2 [60]
$\eta_{PV,ref}$	(360 Wp/2 m^2)/(1000 W/m^2) = 18% [62]
β_{ref} (1/°C)	-0.0042 [62]
$T_{ref,STC}$ (°C)	25 [62]
T_{NOC} (°C)	45
$T_{ref,NOC}$ (°C)	20 [62]
I_{ref} (Wh/m^2)	800 [62]
η_{wire}	99% [61]
η_{inv}	95.25% [61]
η_{soil}	94.5% [61]
η_{mis}	97.25% [61]
$\eta_{charger}$	97% [61]

The definition of symbols in the following equations can be found on the nomenclature section, while the technical specifications are based on polycrystalline PV module (see Table 22).

$$E_{PV}^{i} = \eta_{PV}^{i} \, I_{T}^{i} \, A_{PV} \, N_{PV} \, PR \tag{17}$$

$$\eta_{PV}^{i} = \eta_{PV,ref}\left[1 - |\beta_{ref}|\left(T_{amb}^{i} + \left(T_{NOC} - T_{ref,NOCT}\right)\frac{I_{T}^{i}}{I_{ref}} - T_{ref,STC}\right)\right] \tag{18}$$

$$PR = \eta_{wire} \, \eta_{inv} \, \eta_{soil} \, \eta_{mis} \, \eta_{charger} \tag{19}$$

Condition of PV, PV/T, and STC area:

$$\text{PVT area} = \begin{cases} \text{PVT area, if PV area} > \text{PVT area} \\ \text{PV area, if PV area} < \text{PVT area} \\ \text{PVT area, if PV area} = \text{PVT area} \end{cases}$$

$$\text{PV area} = \begin{cases} \text{PV area} - \text{PVT area, if PV area} > \text{PVT area} \\ 0, \text{if PV area} < \text{PVT area} \\ 0, \text{if PV area} = \text{PVT area} \end{cases}$$

$$\text{STC area} = \begin{cases} 0, \text{if PV area} > \text{PVT area} \\ \eta_{th,PVT}/\eta_{th,STC}\,(\text{PVT area} - \text{PV area}), \text{if PV area} < \text{PVT area} \\ 0, \text{if PV area} = \text{PVT area} \end{cases}$$

Heat pump

Table 23. COP of heat pump at different source and sink temperatures*

T_{source} [°C]	T_{sink} [°C]	COP heating	COP cooling
$0 \leq T < 10$	$T \leq 35$	4.72 [95]	3.72
	$35 < T \leq 45$	3.61 [95]	2.61
	$45 < T \leq 55$	2.93	1.93
	$55 < T \leq 65$	2.5	1.5

T ≥ 10	T ≤ 35	6.49 [95]	5.49
	35 < T ≤ 45	4.79 [95]	3.79
	45 < T ≤ 55	3.79	2.79
	55 < T ≤ 65	3.17	2.17

**The COP values are based on Thorpe's* [41] *book, but adapted according to values from NIBE* [95]

Heat pump work input:

$$W_{in} = \frac{Q_{out,sink}}{COP\ heating};\ W_{in} = \frac{Q_{in,source}}{COP\ cooling} \quad (20)$$

Latent heat storage

Table 24. Matrix of choice for heat storage

Parameter	**Weight factor (1-5)**	**Score**		
		SHS (water)	**LHS**	**TCM**
Energy density (1=low, 5=high)	3	1	4	5
Power (1=low, 5=high)	3	4	1	1
Efficiency (1=low, 5=high)	3	3	4	4
Storage period (1=short, 5=long)	4	2	3	5
Cost (1=high, 5=low)	5	4	3	1
Technology readiness level (1=low, 5=high)	4	5	4	3
Heat loss (1=high, 5=low)	1	2	3	5
Total = weight factor × score		68	73	72

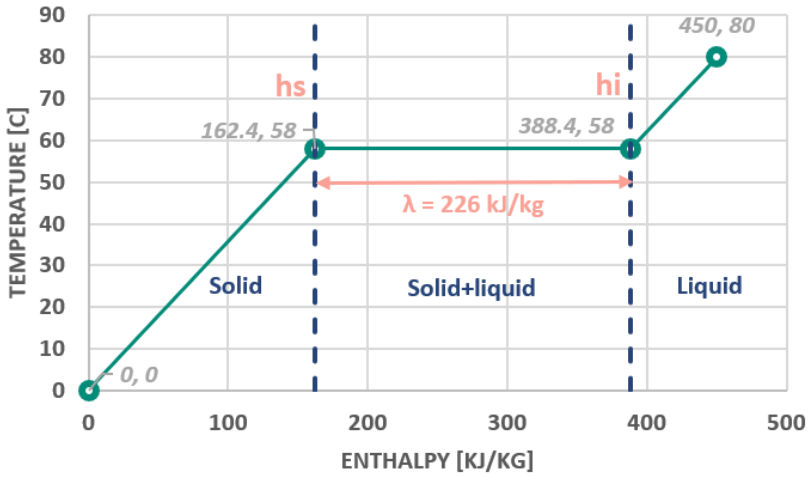

Figure 53. Temperature and enthalpy relation of sodium acetate trihydrate (without supercooling)

Table 25. Technical parameters of latent heat storage

Parameter	**Value**
Phase-changing material (PCM)	Sodium Acetate Trihydrate (SAT)
Melting temperature (T_{melt}) [°C]	58 [96]
Heat capacity (liquid) ($C_{p,l}$) [kJ/kg°C]	3.5 [96]
Heat capacity (solid) ($C_{p,s}$) [kJ/kg°C]	2.8 [96]
Latent heat capacity (λ) [kJ/kg]	226 [96]
Liquid density ($\rho_{SAT,l}$) [kg/m^3]	1180 [96]

Solid density ($\rho_{SAT,s}$) [kg/m^3]	1280 [96]
Minimum useful storage temperature (T_{min}) [°C]	40
Maximum storage temperature (T_{max}) [°C]	80
Dimension of 1 storage unit [cm]	36.5 x 57.5 x 107 [97]
Heat loss coefficient (U_{loss}) [W/m^2. °C]	0.28*

*estimated from Sunamp UniQ's [97] device that has 33.7W of heat loss for a surface area of 2.43 m^2. The temperature difference between PCM and ambient is assumed to be 50°C.

Heat storage capacity:

It is assumed that the device volume is the same as that of the PCM volume.

$$V_{unit} = l \times w \times h = 36.5cm \times 57.5cm \times 107cm = 0.2246\ m^3 \quad (21)$$

$$m_{SAT} = V_{unit}\ \rho_{SAT,l} = 264.99\ kg/unit \quad (22)$$

$$Q_{unit} = m_{SAT}\left[C_{p,s}(T_{melt} - T_{min}) + \lambda + C_{p,l}(T_{max} - T_{melt})\right] - 34.26\ kWh \quad (23)$$

Heat storage loss:

The heat loss area and coefficient refers to Sunamp UniQ size 12 [97], with details listed on Table 25. Symbol n in the equation refers to the number of storage unit required, assuming that 1 unit is 34.26 kWh. Since the storage temperature and ambient temperature vary according to time, then the Q_{loss} is also dependent on time. Moreover, the heat loss is a function of n (number of unit), hence, it changes according to the heat storage size.

$$Q^i_{loss} = n\ (UA)_{tank}\left(T^i_{LHS} - T^i_{out}\right) \quad (24)$$

Compressor work

$$P_{comp} = 2\dot{n}_{H2}\frac{\gamma RT}{\gamma - 1}\left[\left(\frac{P_2}{P_x}\right)^{\frac{\gamma-1}{\gamma}} - 1\right]\frac{1}{\eta_{comp}} \quad (25)$$

where γ is the polytropic exponent of hydrogen (γ=Cp/Cv=1.4 [34]), $\dot{n}_{H2}$ is the hydrogen molar flow rate in mol/s, R is the gas constant (8.248 J/mol.K [34]), P_x is the intermediate pressure ($\sqrt{P_1 P_2}$) in Pa, P_1 and P_2 are the inlet and outlet pressure of compressor in Pa.

A.5 Algorithm to find energy component sizes

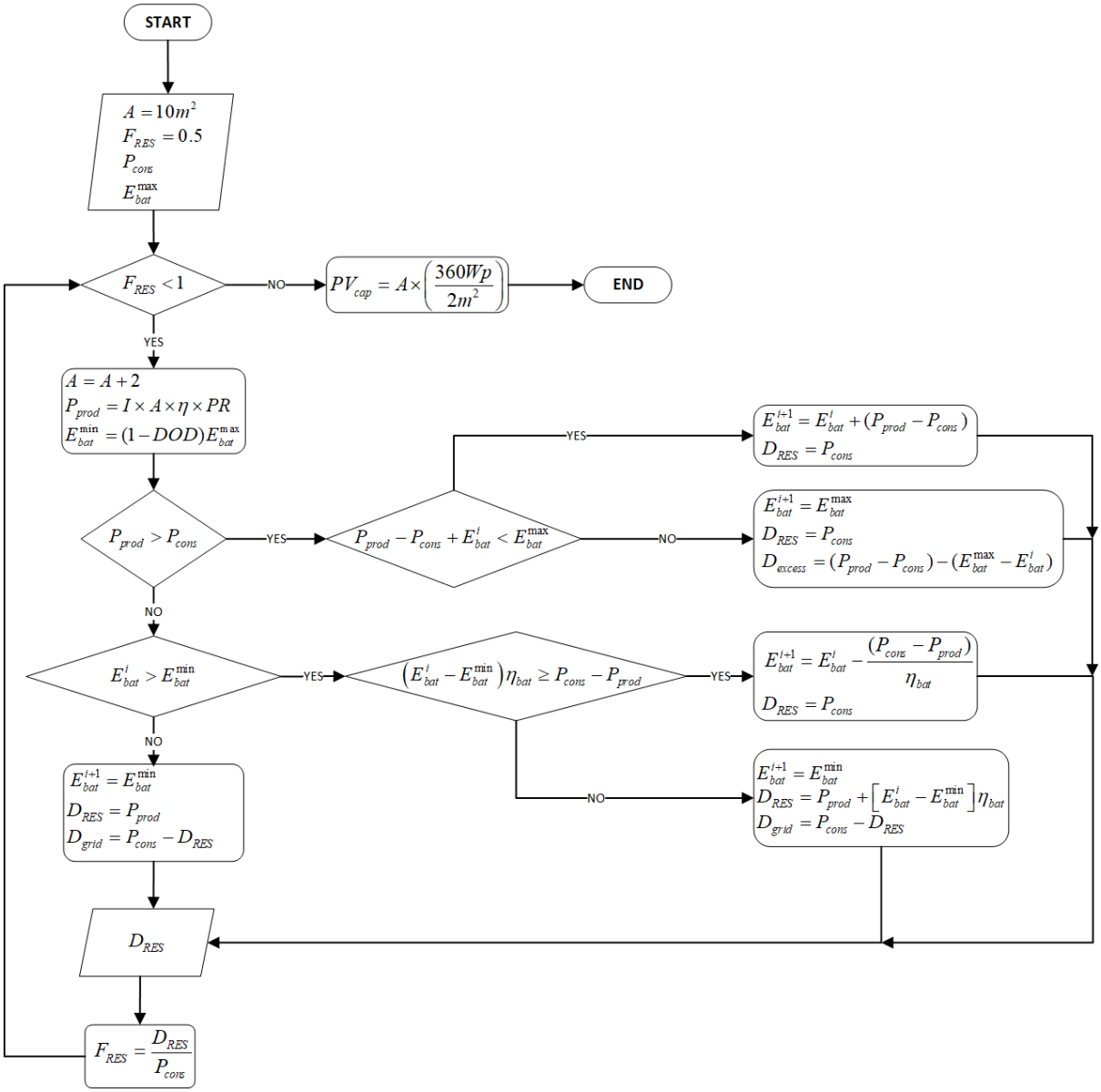

Figure 54. Algorithm of finding the minimum capacity of PV for a given size of battery

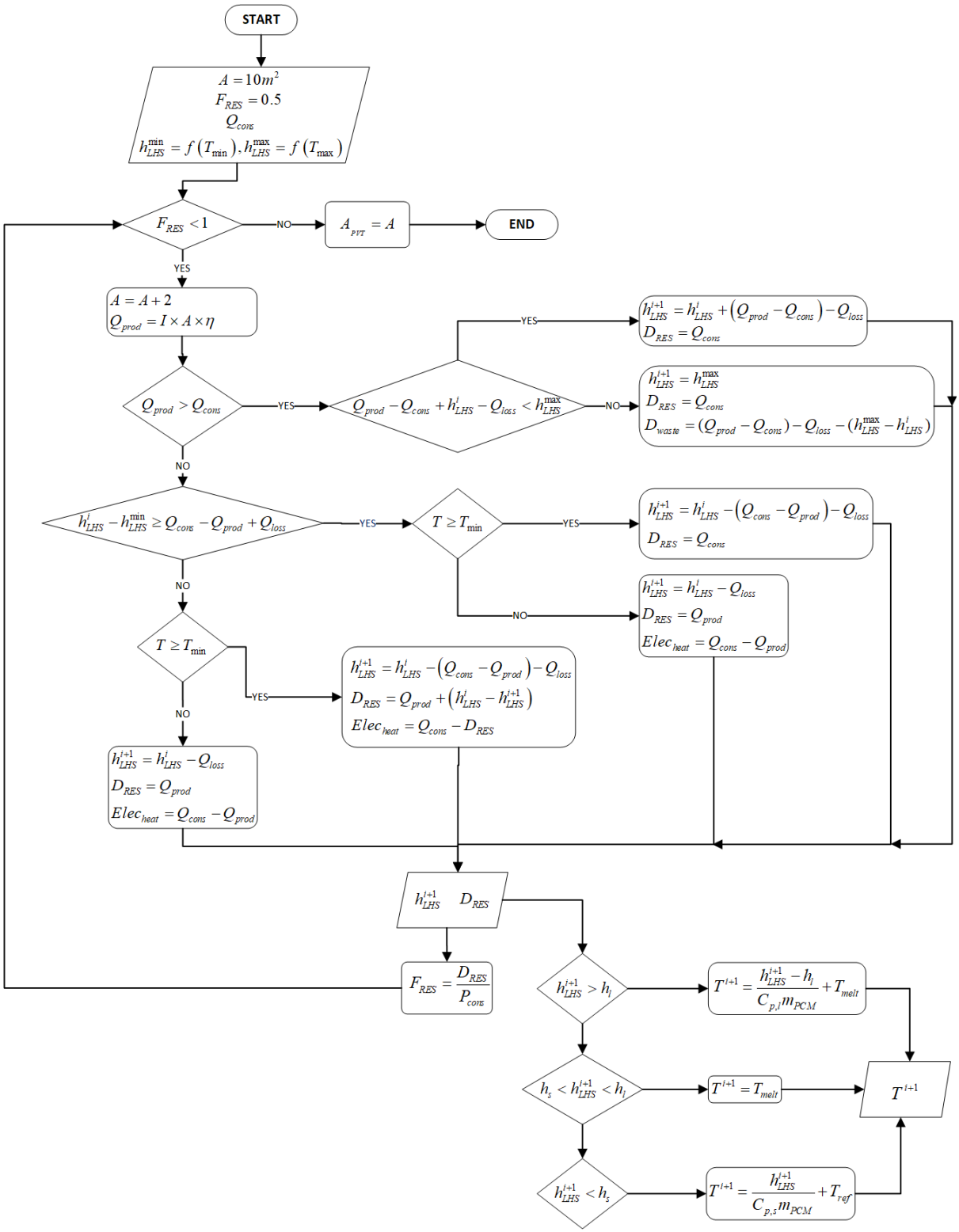

Figure 55. Algorithm of finding the minimum area of PV/T for a given size of heat storage

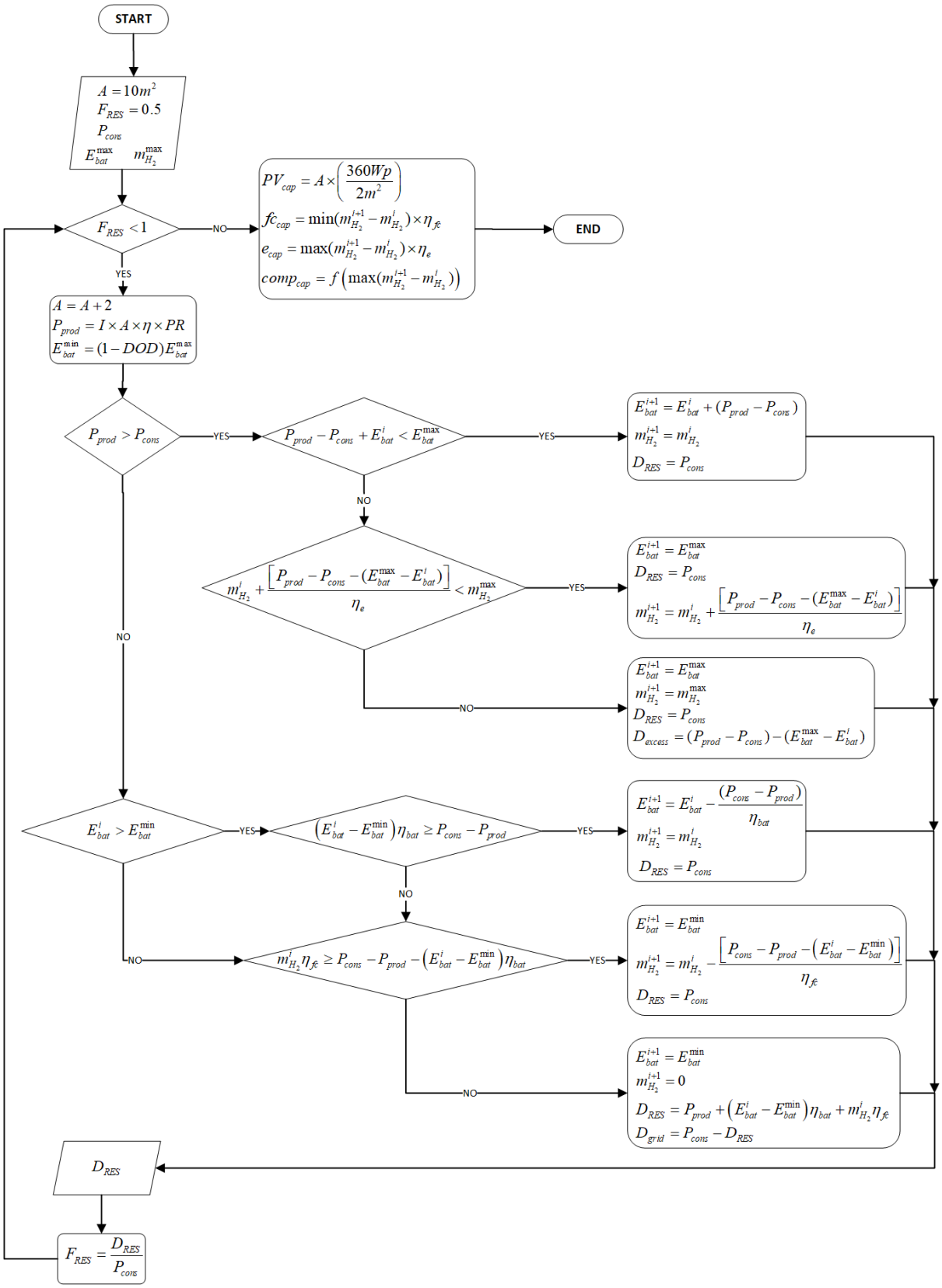

Figure 56. Algorithm of finding the minimum capacity of PV for a given size of battery and hydrogen storage

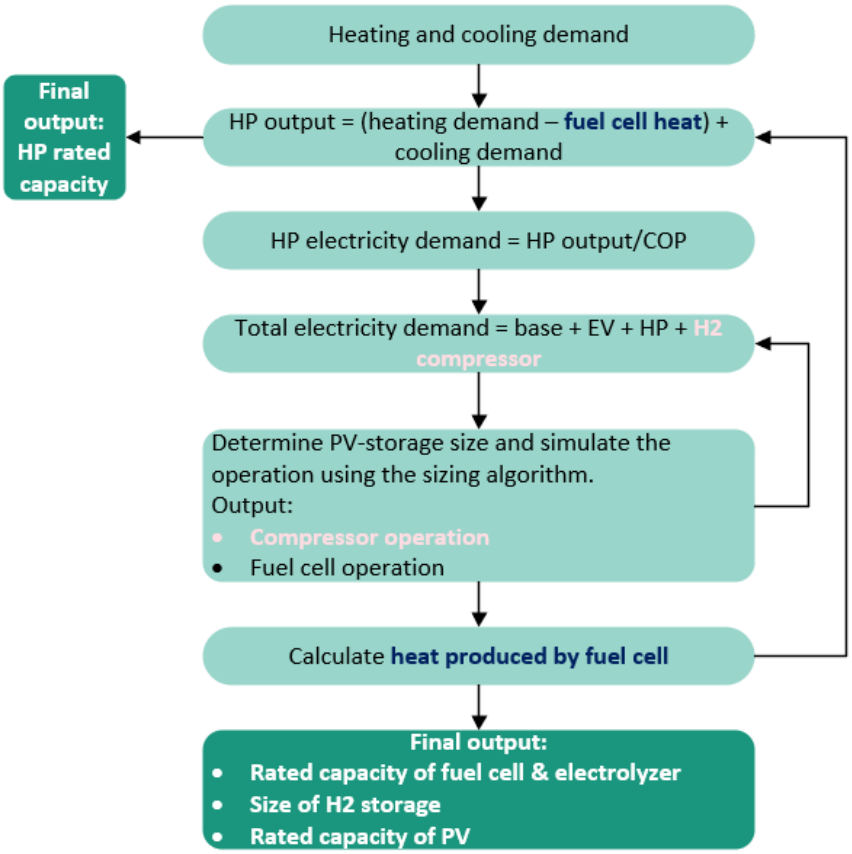

Figure 57. Logic flowchart of energy system with hydrogen storage, with iteration loop for compressor electricity consumption and fuel cell heat supply

A.6 Energy demand

Heat balance of room

Heat flow rate supplied to the house by the heater:

$$\frac{dQ_s}{dt} = (UA)_{rad}(T_h - T_{in}) \tag{26}$$

Transmission heat loss from the house to the outdoors due to temperature difference:

$$\frac{dQ_{trans}}{dt} = ((UA)_{floor} + (UA)_{window} + (UA)_{wall} + (UA)_{roof})(T_{in} - T_{out}) \tag{27}$$

Infiltration heat loss from the house to the outdoors due to ventilation:

$$\frac{dQ_{vent}}{dt} = (1.2\ ACH\ V_{room})(T_{in} - T_{out}) \tag{28}$$

The heat balance of the house is equal to the heat gain subtracted by the heat loss, shown by equation (29). Besides the heater, heat gain is also obtained from solar radiation through glass windows (Q_{rad}) and from person, lighting, and appliances (Q_{pla}). Q_{rad} is a function of the house's orientation, solar irradiance, glass layers, and its surface area. Its detailed calculation is shown in Appendix A.2. Q_{pla} is assumed constant at 67W per person.

$$\left[\frac{dQ_s}{dt} + \frac{dQ_{rad}}{dt} + \frac{dQ_{pla}}{dt}\right] - \left[\frac{dQ_{trans}}{dt} + \frac{dQ_{vent}}{dt}\right] = V_{room}\ \rho_{air}\ Cp_{air}\ \frac{dT_{in}}{dt} \tag{29}$$

Substituting equation (26),(27), and (28) to equation (29), and moving the $\frac{dT_{in}}{dt}$ to the left-hand side of the equation yields equation (10) in section 3.5.1.1.

Heat balance of DHW tank

Heat demand for DHW is based on equation (30). The mains temperature varies every month and is based on the Dutch drinking water temperature data in Blokker and Pieterse-Quirijns' research [98].

$$Q_{DHW} = \dot{m}_{DHW}\, Cp_{water}\, (T_{DHW} - T_{mains}) \tag{30}$$

Heat loss from DHW tank to the environment is based on equation (31). The dimension of DHW tank follows an insulated hot water cylinder by Daikin in the version of EKHWS200(U)-D3V3, which has a volume of 200L, a surface area of 1.8 m^2, and an overall heat loss coefficient of around 0.6 $W/m^2.°C$ [99].

$$Q_{loss} = (UA)_{tank}\, (T_{DHW} - T_{out}) \tag{31}$$

The amount of heat input for DHW tank depends on three aspects. First, the heat to increase water temperature inside tank to 50°C; second, the heat to increase fresh water from mains temperature (about 10°C) to 50°C; and lastly, heat to make-up for the loss from the tank to the environment. Based on this assumption, the heat balance of the DHW tank:

$$Q_{in} - Q_{DHW} - Q_{loss} = V_{tank}\, \rho_{water}\, Cp_{water} \frac{dT_{water}}{dt} \tag{32}$$

Substituting equation (30) and (31) to equation (32) yields equation (11) in section 3.5.1.2.

A.7 Energy density and power density of components

Table 26. Energy density and power density of energy system components

Component	Energy or power density	Source
Li-ion battery	260 Wh/L	[4]
Heat pump	1950 L	[100]
Electrolyzer	3.1 kW/L	(Assumed to be the same as fuel cell)
Hydrogen tank	22,647 L	(See calculation below)
Fuel cell	3.1 kW/L	[101]
Latent heat storage (LHS)	125 Wh/L	(See calculation below)
DHW tank	2x200L	[99]

The energy density of LHS is estimated using the following equation

$$\text{Energy density}_{LHS} = \left[C_{p,s}(T_{melt} - T_{min}) + \lambda + C_{p,l}(T_{max} - T_{melt})\right]\rho_{PCM} \tag{33}$$

To estimate the volume of hydrogen tank, we cannot simply use the ideal gas equation because it does not accurately describe the condition pressure, volume, and temperature for hydrogen. Instead, we use the Beattie-Bridgeman equation [102]. The volume of hydrogen tank is estimated using the following equation. In this study, it is known that the desired hydrogen tank pressure is 200 bar, therefore, we can do iterations to find the volume.

$$P = \frac{n^2 RT}{V^2}\left(1 - \frac{cn}{VT^3}\right)\left[\frac{V}{n} + B_0\left(1 - \frac{bn}{V}\right)\right] - \frac{A_0\left(1 - \frac{an}{V}\right)n^2}{V^2} \quad (34)$$

where

P = pressure of hydrogen in the tank [atm]

V = volume of the hydrogen tank (L)

T = temperature of hydrogen (K)

N = number of moles of hydrogen in the tank (mol)

R = gas constant = 0.08206 L.atm/(mol.K)

A_0 = 0.1975 atm.L^2/mol^2

B_0 = 0.02096 L/mol

a = -0.00506 L/mol

b = -0.04359 L/mol

b = 0.0504 x 104 L.K^3/mol

A.8 Sankey diagram

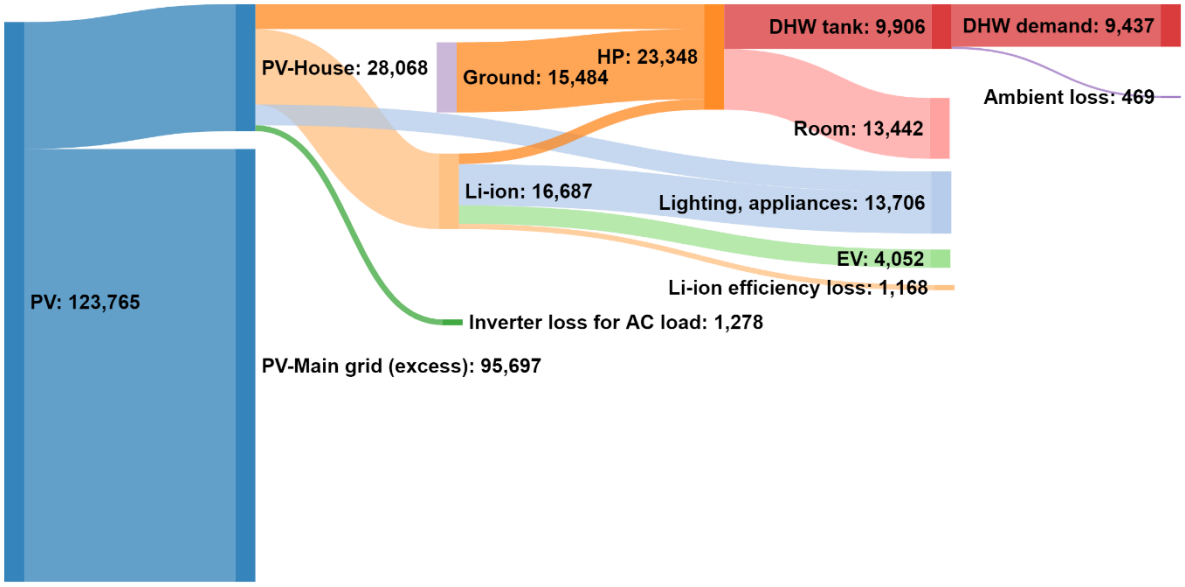

Figure 58. Configuration 1: Sankey diagram (in kWh)

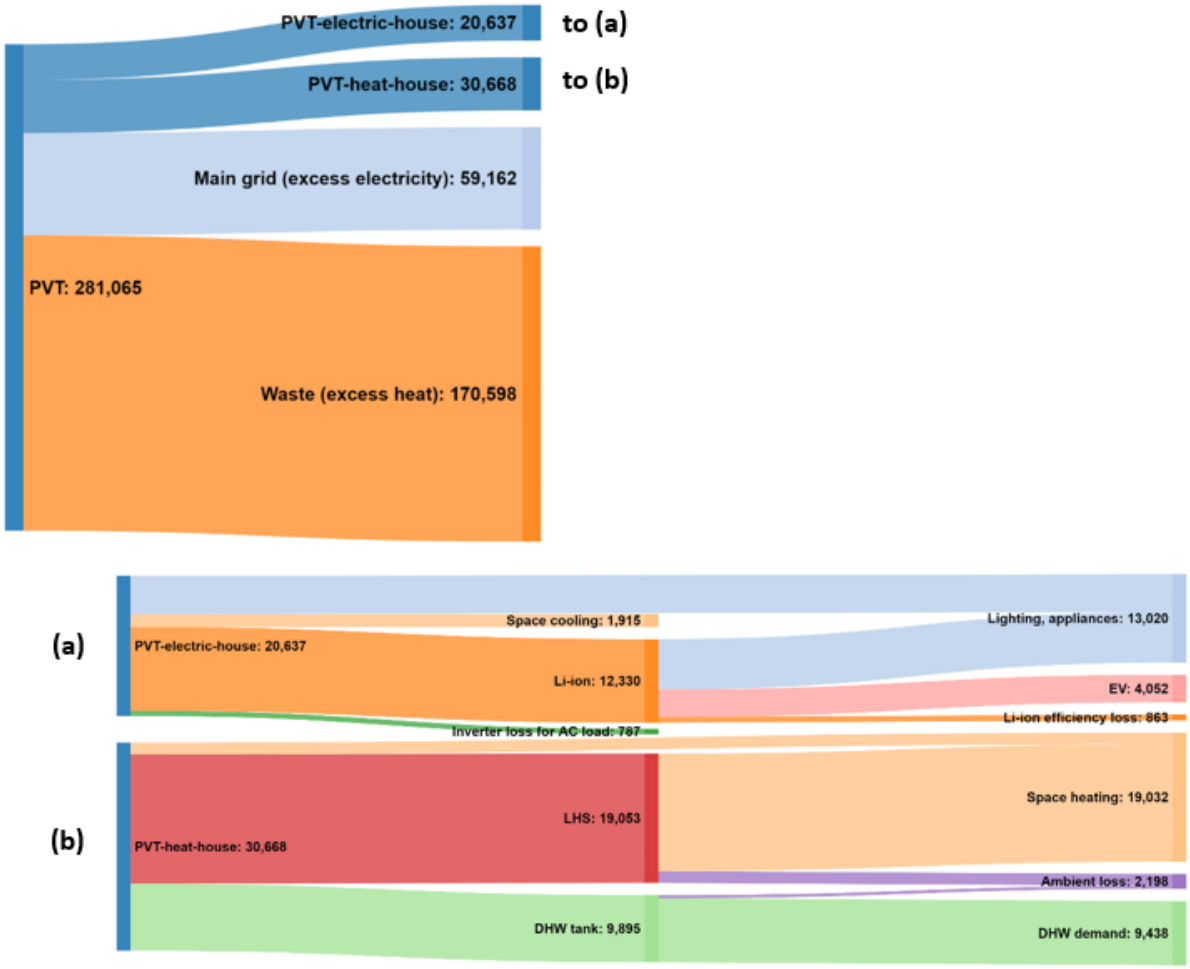

Figure 59. Configuration 2: Sankey diagram (in kWh)

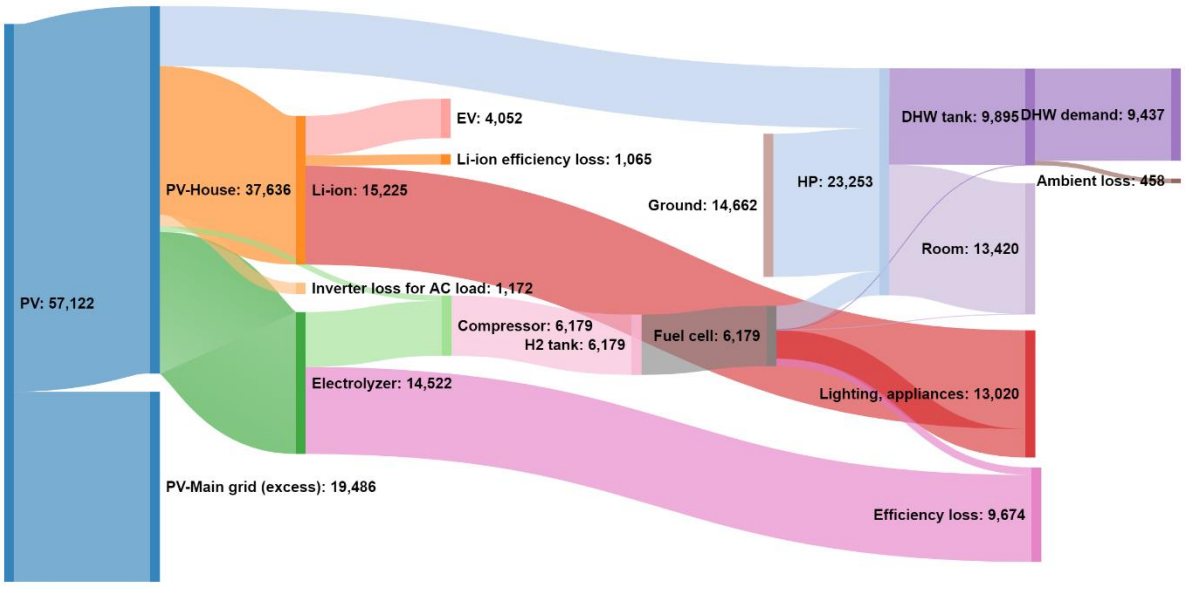

Figure 60. Configuration 3 (chosen option, hydrogen storage minimized): Sankey diagram (in kWh)

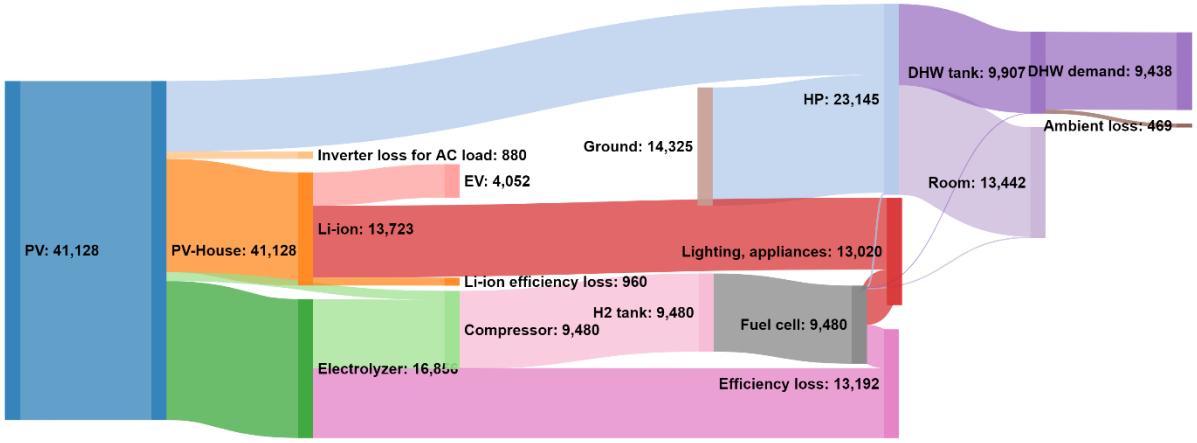

Figure 61. Configuration 3 (example of other option, PV size minimized): Sankey diagram (in kWh)

A.9 Economic analysis

Table 27. Coefficient values used in the formula to determine compression system capital cost [78]

Coefficient	Value
A	100,000
B	300,000
a	0.66
b	0.66
c	0.25
d	0.25

Table 28. Cost of energy system components and their lifetime [11]

Component	Capital cost [€/kW]	Replacement cost [€/kW]	O&M cost [€/kW/yr]	Lifetime [years]
PV	890	667.5	21 [103]	25
PV/T	1920 (or 345.6 €/m^2) [13]	1920 (or 345.6 €/m^2)	2% capital cost per year†	20 [104]
STC	169 €/m^2 [13]	169 €/m^2	2% capital cost per year [104]	20 [105]
Li-ion	400.5 €/kWh [106]	211 €/kWh [107]	0	10 [108]
Electrolyzer	979	757	10	15
Compressor	€36,457*	€36,457	5% capital cost per year [109]	15
Hydrogen tank	890 €/kg	667.5 €/kg	0	25
Fuel cell	3,560	2,670	0.01 €/kW/op.hr	50,000 hours
Heat pump	€14,487 (24 kW) €9,276 (17 kW) [100]	€14,487 (24 kW) €9,276 (17 kW)	160.2 €/yr [110]	15 [111]
Air conditioner	389 €/unit	389 €/unit	75 €/unit/yr [112]	15 [113]
Ground coils	€2,750** [114]	-	0†	-
DHW tank	€1,165 (2x200L) [115]	€1,165	134.4 €/yr [116]	20 [117]
LHS	229 €/kWh [118]	229 €/kWh	0 [119]	40,000 cycles [120]

**obtained from equation (13)*

***assumed to be fixed, regardless of the HP capacity*
†assumption

Table 29. Energy category for LCOE

Component	Category
PV	100% electricity for configuration without heat pump
	30% heat and 70% electricity for configurations with heat pump
PV/T	50% heat and 50% electricity
STC	Heat
Li-ion	Electricity
Electrolyzer	Electricity
Compressor	Electricity
Hydrogen tank	Electricity
Fuel cell	Electricity
Heat pump	Heat
Air conditioner	Heat
Ground coils	Heat
DHW tank	Heat
LHS	Heat

Table 30. Net present cost of all energy system configurations over 20 year-period

Present value	**1st configuration: PV – Li-ion - GSHP**	**2nd configuration: PV/T – Li-ion - LHS**	**3rd configuration: PV - Li-ion - H_2 storage - GSHP**
Capital cost	217,117	263,910	315,682
Replacement cost	41,064	26,169	40,721
O&M cost	27,016	23,175	37,751
Income	-69,968	-41,961	-17,156
Salvage value	-18,384	-18,183	-25,913
Net present value	196,845	253,110	351,085